

**MUTATIONAL ANALYSIS OF UBIQUITIN SHUTTLE RECEPTOR  
DOCKING SITES ON THE 26S PROTEASOME**

Thesis by

Tara Adele Gomez

In Partial Fulfillment of the Requirements

for the Degree of

Doctor of Philosophy

California Institute of Technology

Pasadena California

2011

(Defended May 20, 2011)

© 2011

Tara Adele Gomez

All Rights Reserved

## ACKNOWLEDGMENTS

*“Only love has no limits. In contrast, **our predictions can fail, our communication can fail, and our knowledge can fail.** For our knowledge is patchwork, and our predictive power is limited. But when perfection comes, all patchwork will disappear.”*

(1 Cor. 13:8–10)

I am extremely grateful to have had the chance to work in the lab of Dr. Raymond Deshaies. Ray is one of the smartest people I have ever met. His scientific brilliance is however, matched by his master negotiation skills. I am thankful that I learned not only, how to be a better scientist from Ray, but also, some business savvy! I am grateful for all of the support and help Ray offered me. I feel truly privileged to have received said support and encouragement.

I would also like to thank my thesis committee members: Dr. Judy Campbell, Dr. David Chan, Dr. William Dunphy, and Dr. Angelike Stathopoulos. My committee was immensely supportive and helpful in giving me both excellent suggestions and encouragement.

I am also very indebted to my colleagues in the Deshaies lab. I would like to thank the Deshaies' lab graduate students for continued advice, community, and support. I will miss our monthly “Grad Student Lunches”. I would like to especially thank KJ Chang and Natalie Kolowa for being great colleagues, work-out companions, and friends. In addition, Nathan Pierce, Michael Rome, and Ruzbeh Mosadeg were great inspirations.

I am also very grateful to Rati Verma for sharing with me her 26S knowledge, which helped propel my project forward during its darkest days. Gary Kleiger was also extremely helpful in helping my project during dark days, and helped teach me how to be a better scientific writer. The technical support of Heenam Park and Rob Oania undoubtedly deserve my accolades as well.

I would be remiss to not thank the summer students I worked with during my time in the Deshaies lab. Marvin Gee, a Caltech SURF student, performed an experiment that contributed to my publication. Caitlin Rugani did many experiments that never made it to the paper, but were essential and for which I will be eternally grateful. My 2008 summer high school student volunteer, Derek Tu, would open my centrifuge tubes for me and kept me company during my RY2H screen!

I am thankful for the amazing undergraduate and postbacc research opportunities I was provided with in the lab of Dr. Steven G. Clarke, my undergraduate thesis advisor. His continued support throughout my graduate career allowed us to publish several papers during my tenure here at Caltech, although unfortunately, they were not allowed in my Caltech thesis!

I would also like to acknowledge the following programs, offices and people at Caltech and in the Pasadena area that made what could have become a very mundane five years, a much more balanced five years: Liz Ayala, Gwen Murdock, Denise Nelson-Nash, the YESS program, Caltech Classroom Connection (CCC), Huntington Library and Botanical Gardens, Eye Dreams, Biology Graduate Student Invited Speaker Series, Caltech Public Events Office for letting me host Reel Science and Science Saturdays, MSE/CCD office, Grad Chats, Women's Center, GSC and the Caltech Y.

To my closest friends, and graduate school mentors: Julianne Lyons, Dr. Chris Lyons, Sindhuja Kadambi, Michelle Fontes, Nicole Tetreault, Brianna Williams, Schetema Stevens, Chinney Idigio, Dr. Princess Imoukhuede, Dr. Kelle Cruz, Nneka Williams, Dr. Jennifer Keefe, Dr. Cecilia Zurita-Lopez, Dr. Tanya Porras-Yakushi, and Dr. Melissa Gulmezian, I would like to thank you for advice, companionship, and mentorship throughout the PhD process. I would especially like to thank the Lyons who walked this path with me the closest, and are the absolute best friends one could ever wish for.

I would like to thank my entire family and extended family. To my in-laws, the Hampton clan, you are extraordinary people that have enriched my life and remind me to laugh as much as I can! To my brother Jason Gomez, I think 2011 was a big year for the both of us. I am proud of you. To my sister, Felicia Gomez, I am very blessed to have you as a sister. Your love and support are unwavering and just what I need. Furthermore, I love that we have a shared passion for seeing the world and a similar sense of humor that allows us to share the world together.

And to my biggest supporters in this world, who are undoubtedly my parents and my husband, I realize I am where I am today because of you! This thesis is dedicated to my mother, who swears that I was the "best dancer" in the 2011 Caltech Dance Show, not because this is a fact (it isn't), but because she believes in me more than anyone I have ever met. This thesis is also dedicated to my father who loves me deeply and cultivated my knowledge as a child. When I was a child, he even exchanged landscaping work for tuition fees at my private elementary school to ensure I got an amazing education. This thesis is also dedicated to my husband Tyron Hampton, who honestly thinks that I am capable of anything and puts up with all of my temper tantrums. I don't know how he does it!

Finally, I am most thankful for the grace and guidance of God. Despite sin and imperfection, God offers His grace. I believe I am here today because of the silent and merciful hand that He put out for me to reach hold to. "*The LORD is the stronghold of my life...*" Psalm 27:1.

## ABSTRACT

Protein degradation is essential for many basic cellular functions. Most intracellular protein degradation occurs via the ubiquitin proteasome system. Cellular proteins are marked for degradation by the appendage of an ubiquitin chain. Ubiquitin receptor proteins recognize the ubiquitin chains and play a “garbage man” function in ensuring delivery of the protein trash to the cell’s degradation machinery, the proteasome.

One such class of ubiquitin receptor proteins, known as UBA-UBL proteins, recognizes ubiquitylated substrates and shuttles them to the proteasome. These shuttle receptors include Rad23, Dsk2, and Ddi1. The goal of this dissertation research has been to understand how these UBA-UBL proteins interact with the proteasome. In budding yeast, *Saccharomyces cerevisiae*, Rpn1 has been proposed to be the major docking site for UBL-containing proteins. More recent studies suggested that proteasome subunits Rpn10 and Rpn13, may also bind UBA-UBL proteins. However, no *cis* proteasome mutants existed to address these plausible redundant modes of delivery to the proteasome.

The specific aims of this proposal were to: identify the sites on the proteasome that are necessary for specific UBA-UBL receptor docking, to study the consequence of the deletion of these sites (such as the effects on protein turnover), and to assess if the elimination of these sites is the same as elimination of the receptor proteins themselves.

Here, I describe a two-pronged genetic screen I conducted to identify a specific docking site within Rpn1 for UBA-UBL proteins. I uncover a highly conserved residue, D517A that appears to impinge on the ability for both Ddi1 and—in the absence of Rpn13 or the dual absence of the ubiquitin interaction motifs of Rpn10 and Rpn13—Dsk2 to

interact with the proteasome. However, under no set of genetic conditions does a mutation at Rpn1-D517 have any effect on Rad23 or the UBL-containing ubiquitin isopeptidase Ubp6. Taken together, my observations point to unanticipated diversity and complexity in the mechanisms underlying the recruitment of UBA-UBL proteins to the proteasome.

Hence, I show that docking sites on the proteasome are not completely exclusive, both Ddi1 and Dsk2 share the D517 residue of Rpn1. However, there may be exclusive sites for docking Rad23 and Ubp6. There also appears to be a layer of complexity and redundancy in docking UBA-UBL proteins to the proteasome. Follow-up studies on these proteasome *cis* mutants have also uncovered roles of the proteasome in regulating mitochondrial protein import and the methyl cycle.

## TABLE OF CONTENTS

Title Page	i
Copyright Page	ii
Acknowledgements	iii
Abstract	v
Table of Contents	vii
List of Tables and Figures	x
<b>CHAPTER 1: INTRODUCTION TO SUBSTRATE RECOGNITION BY THE 26S PROTEASOME</b>	<b>1</b>
<b>The 26S proteasome</b>	<b>2</b>
<b>The ubiquitin proteasome system</b>	<b>3</b>
<b>Substrate delivery to the proteasome</b>	<b>4</b>
<b>Rad23, the best-characterized shuttle receptor</b>	<b>5</b>
<b>Dsk2, the next best-characterized UBA-UBL protein</b>	<b>6</b>
<b>Ddi1, the most controversial shuttle receptor</b>	<b>7</b>
<b>Overlapping and distinct roles for the UBA-UBL shuttle receptors</b>	<b>9</b>
<b>Proteins implicated in binding UBA-UBL proteins</b>	<b>11</b>
<b>Research objectives</b>	<b>12</b>
<b>CHAPTER 2: REVERSE-YEAST TWO-HYBRID SCREENING FOR PUTATIVE INTERACTION-DEFECTIVE ALLELES OF RPN1</b>	<b>17</b>
<b>Introduction</b>	<b>18</b>
<b>Methods</b>	<b>20</b>
Cloning RY2H bait and prey proteins	20
<b>Results</b>	<b>25</b>
Optimizing the Rpn1 reverse-yeast two-hybrid interaction	25
Expression of baits on a 2 $\mu$ plasmid enhance positive and false positive signals	26
Isolation of putative Rpn1 IDAs	27
Rpn1 IDAs appear universal in their ability to disrupt binding to UBL proteins	28
Putative Rpn1 IDA alleles have wild-type phenotypes when introduced into Rpn1 null cells	28
Rpn1 mutant proteins assemble into fully intact and active 26S proteasomes	29
RY2H-derived Rpn1 IDA alleles do not impair the interaction between the proteasome and the UBA/UBL proteins <i>in vivo</i>	30

<b>Discussion</b>	<b>31</b>
<b>Figure legends</b>	<b>34</b>
<b>CHAPTER 3: IDENTIFICATION OF A FUNCTIONAL DOCKING SITE IN THE RPN1 LRR DOMAIN FOR THE UBA-UBL DOMAIN PROTEIN DDI1</b>	<b>44</b>
<b>Abstract</b>	<b>45</b>
<b>Methods</b>	<b>50</b>
<b>Results</b>	<b>55</b>
Rpn1 <sup>391-642</sup> interacts with UBL domain proteins	55
Identification of mutations in Rpn1 <sup>391-642</sup> that block binding to UBL domain proteins	55
Mutant <i>rpn1</i> alleles display synthetic growth defects in combination with ubiquitin receptor mutants	56
Recruitment of Ddi1, Dsk2, and ubiquitin conjugates to proteasomes is compromised in <i>rpn1-D517A</i> and <i>rpn1-K484A</i> mutants	58
<i>In vitro</i> confirmation of a Ddi1 binding defect of Rpn13-deficient Rpn1-D517A mutant proteasomes	60
<i>rpn1-D517A</i> mutants exhibit a selective defect in protein degradation	61
<b>Discussion</b>	<b>62</b>
<b>Authors' contributions</b>	<b>65</b>
<b>Acknowledgements</b>	<b>65</b>
<b>Figure legends</b>	<b>66</b>
<b>Supplementary data</b>	<b>75</b>
<b>CHAPTER 4: COMPARATIVE ANALYSIS OF PROTEASOME <i>CIS</i> MUTANTS TO UBA-UBL NULL STRAINS</b>	<b>87</b>
<b>Introduction</b>	<b>88</b>
<b>Methods</b>	<b>90</b>
<b>Results</b>	<b>91</b>
One surface of Rpn1 may be necessary for binding UBA-UBL proteins	91
The <i>rpn1-VKD</i> mutant shows only slightly more dramatic synthetic lethality than <i>rpn1-STN</i> in combination with mutations of intrinsic ubiquitin receptors	92
Only Rpn1 VKD surface mutations stabilize the Ddi1 substrate Ufo1	93
Rpn1-D517A and Ddi1 interact genetically	93
The <i>rpn1-D517A</i> does not mimic a <i>ddi1Δ</i> mutant in steady-state accumulation of <i>HO</i> endonuclease	94
The <i>ddi1Δ dsk2Δ</i> mutant does not have diminished Ub conjugate binding to the proteasome	95
<b>Discussion</b>	<b>96</b>
<b>Figure legends</b>	<b>99</b>

<b>CHAPTER 5: INSIGHTS INTO THE BINDING OF RAD23 AND UBP6 TO THE 26S PROTEASOME</b>	<b>104</b>
<b>Introduction</b>	<b>105</b>
<b>Methods</b>	<b>106</b>
<b>Results</b>	<b>106</b>
Rpn10 and Rpn13 contribute to docking of UBA-UBL receptor proteins	106
A sole deletion of Rpn13 is not sufficient to interrupt binding of any ubiquitin receptor protein to the proteasome	107
Proteasomes from <i>ufd2</i> $\Delta$ are less abundant for Rad23	108
<b>Discussion</b>	<b>108</b>
<b>Figure legends</b>	<b>110</b>
<b>CHAPTER 6: MITOCHONDRIAL IMPORT AND METHIONINE SYNTHESIS PATHWAYS ARE PERTURBED BY INTERFERENCE OF UBA-UBL BINDING TO THE PROTEASOME</b>	<b>119</b>
<b>Introduction</b>	<b>120</b>
<b>Methods</b>	<b>121</b>
<b>Results</b>	<b>124</b>
Rpn1-D517A proteasomes show diminished amounts of specific PIPs	124
Galactose-inducible Aac2 appears to be stabilized in <i>rpn1-D517A</i>	125
Cellular concentrations of Sam2, Cys3, and Fsr1 are shifted in <i>rpn1-D517A</i> mutants	126
Methionine and cysteine biosynthesis pathways appear perturbed in <i>rpn1-D517A</i> cells	127
<i>rpn1-D517A</i> mutants have an abundance of mitochondrial proteins at their proteasomes and respiration defects	128
<i>rpn13</i> $\Delta$ <i>rpn1-D517A</i> mutants accumulate precursor forms of Hsp60	128
<b>Discussion</b>	<b>129</b>
<b>Figure legends</b>	<b>133</b>
<b>CHAPTER 7: FINDINGS, IMPLICATIONS, AND FUTURE DIRECTIONS</b>	<b>154</b>
<b>Summary</b>	<b>155</b>
<b>Future directions</b>	<b>158</b>
<b>BIBLIOGRAPHY</b>	<b>159</b>

## List of Tables and Figures

TABLE 1.1. IDENTIFIED YEAST UBA AND UBL CONTAINING PROTEINS.....	14
TABLE 1.2. UBA-UBL RECEPTORS HAVE VARYING AFFINITIES FOR THE DIFFERENT FORMS OF UBIQUITIN.....	15
FIGURE 1.1. THE EUKARYOTIC PROTEASOME.....	16
TABLE 2.1. RY2H STATISTICS.....	36
TABLE 2.2. POINT MUTATIONS IN RPN1 THAT DISRUPT BINDING TO EITHER RAD23 OR DSK2 IN A RY2H SYSTEM.....	37
TABLE 2.3. 3-AT RESISTANCE OF BAIT/PREY PAIRS.....	38
FIGURE 2.1. FORWARD-YEAST TWO-HYBRID INTERACTIONS BETWEEN RPN1-DB AND PREY PROTEINS.....	39
FIGURE 2.2. MOST PUTATIVE RPN1 IDAS PRODUCE VIABLE YEAST STRAINS.....	40
FIGURE 2.3. MUTANT <i>RPN1</i> ALLELES DO NOT DISPLAY TYPICAL PROTEASOME MUTANT PHENOTYPES.....	41
FIGURE 2.4. MUTANT <i>RPN1</i> ALLELES DO NOT INTERFERE WITH PROTEASOME ASSEMBLY.....	42
FIGURE 2.5. SELECT RY2H SCREEN <i>RPN1</i> ALLELES REDUCE PROTEASOME STABILITY BUT DO NOT IMPINGE ON UBA-UBL BINDING TO THE PROTEASOME.....	43
FIGURE 3.1. A TWO-PRONGED STRATEGY IDENTIFIES 18 RPN1 RESIDUES THAT MAY BE IMPORTANT FOR BINDING UBL DOMAIN PROTEINS.....	69
FIGURE 3.2. MUTANT <i>RPN1</i> ALLELES DISPLAY GENETIC INTERACTIONS WITH MUTATIONS IN GENES THAT ENCODE UBIQUITIN RECEPTORS INTRINSIC TO THE PROTEASOME.....	70
FIGURE 3.3. RECRUITMENT OF DDI1, DSK2, AND UB CONJUGATES TO THE PROTEASOME IS COMPROMISED IN <i>RPN1-D517A</i> AND <i>RPN1-K484A</i> MUTANTS.....	71
FIGURE 3.4. <i>RPN1-D517A</i> REDUCES BINDING OF DDI1 <i>IN VITRO</i> .....	72
FIGURE 3.5. <i>RPN1-D517A</i> MUTANTS EXHIBIT A SELECTIVE DEFECT IN PROTEIN DEGRADATION.....	73
FIGURE 3.6. MODEL FOR UBL PROTEIN INTERFACING WITH THE PROTEASOME.....	74
SUPPLEMENTAL TABLE 3.1. ADDITIONAL RATIONAL RPN1 MUTANTS USED IN THIS STUDY.....	77
SUPPLEMENTAL TABLE 3.2. YEAST STRAINS USED IN THIS STUDY.....	79
SUPPLEMENTAL TABLE 3.3. PLASMIDS USED IN THIS STUDY.....	81
SUPPLEMENTAL TABLE 3.4. ANTIBODIES USED IN THIS STUDY.....	82
FIGURE 3.S1. MUTANT <i>RPN1</i> ALLELES DERIVED FROM BOTH THE RY2H SCREEN AND RATIONAL MUTATIONS DISPLAY GENETIC INTERACTIONS WITH MUTATIONS IN GENES THAT ENCODE UBIQUITIN RECEPTORS INTRINSIC TO THE PROTEASOME.....	83
FIGURE 3.S2. <i>RPN1-D517A</i> , <i>RPN10-UIM RPN1-D517A</i> , AND <i>RPN10-UIM RPN13-KKD RPN1-D517A</i> LIMIT BINDING OF UBA-UBL PROTEINS DDI1 AND DSK2.....	84
FIGURE 3.S3. MUTATIONS AT RPN1 RESIDUES A418, N549, F565, AND G571 RENDER UNSTABLE PROTEASOMES.....	85
FIGURE 3.S4. <i>RPN1-D517A</i> MUTANTS EXHIBIT A SELECTIVE DEFECT IN PROTEIN DEGRADATION.....	86
TABLE 4.1 STRAINS USED IN THIS CHAPTER.....	101
FIGURE 4.1. THE ‘VKD’ SURFACE OF RPN1 MAY BE RESPONSIBLE FOR BINDING UBA-UBL PROTEINS.....	102
FIGURE 4.2. <i>RPN1-D517A</i> AND <i>DDI1A</i> MUTANTS MAY HAVE SOME PARALLEL FUNCTIONS IN PROTEIN TURNOVER.....	103
TABLE 5.1 STRAINS USED IN THIS CHAPTER.....	111
TABLE 5.2. PIPS THAT ARE LESS ABUNDANT IN <i>RPN13Δ</i> PROTEASOMES.....	112
TABLE 5.3. PIPS THAT ARE MORE ABUNDANT IN <i>RPN13Δ</i> PROTEASOMES.....	114
TABLE 5.4. UBIQUITIN RECEPTOR LEVELS ARE UNCHANGED IN <i>RPN13Δ</i> PROTEASOMES.....	116
FIGURE 5.1. RPN10 AND RPN13 CONTRIBUTE TO DOCKING OF UBA-UBL RECEPTOR PROTEINS.....	117
FIGURE 5.2. UFD2 CONTRIBUTES TO RECRUITMENT OF RAD23 TO THE 26S PROTEASOMES.....	118

TABLE 6.2. PLASMIDS USED IN THIS CHAPTER .....	140
TABLE 6.3. PIPS THAT ARE REDUCED IN <i>RPN13Δ RPN1-D517A</i> 26S PROTEASOME PREPARATIONS .....	141
TABLE 6.4. PIPS THAT ARE INCREASED IN <i>RPN13Δ RPN1-D517A</i> 26S PROTEASOME PREPARATIONS .....	143
FIGURE 6.1. SCREENING FOR PUTATIVE <i>RPN1-D517A</i> SUBSTRATES FROM THE SILAC DATA SET .....	145
FIGURE 6.2. GALACTOSE-INDUCIBLE AAC2 IS SLIGHTLY STABILIZED IN AN <i>RPN1-D517A</i> STRAIN. ....	146
FIGURE 6.3. STEADY-STATE CONCENTRATIONS OF MULTIPLE GFP TAGGED ORFS CHANGE IN AN <i>RPN1-D517A</i> MUTANT. ....	147
FIGURE 6.4. STEADY-STATE CONCENTRATIONS OF ORFS FOUND LESS ABUNDANTLY IN <i>RPN13Δ RPN1-D517A</i> PROTEASOMES.....	148
FIGURE 6.5. STEADY-STATE CONCENTRATIONS OF ORFS FOUND MORE ABUNDANT IN <i>RPN13Δ RPN1-D517A</i> PROTEASOMES.....	149
FIGURE 6.6. METHIONINE AND CYSTEINE BIOSYNTHETIC PATHWAYS CONTAIN MULTIPLE ENZYMES THAT ARE PERTURBED IN <i>RPN1-D517A</i> . ....	150
FIGURE 6.7. <i>RPN13Δ RPN1-D517A</i> MUTANTS HAVE MITOCHONDRIAL DEFECTS. ....	151
FIGURE 6.8. <i>RPN13Δ RPN1-D517A</i> MUTANTS ACCUMULATE HSP60 PRECURSOR PROTEINS. ....	152
FIGURE 6.9 TWO HYPOTHESES DESCRIBE HSP60 ACCUMULATION IN PROTEASOME MUTANTS. ....	153

**Chapter 1:**

**Introduction to substrate  
recognition  
by the 26S proteasome**

Individual proteins, pairs of proteins, or small protein complexes, carry out many important cell processes. However, in some cases, very large assemblies of proteins form complicated quaternary structures, resembling nanomolecular machines, and they carry out pivotal jobs in the cell as well. These large protein complexes are enigmatic. Why is such a large complex required to complete the job? Such large protein complexes include the nuclear pore complex (~ 120 mDA), ribosomes (2–10 mDA), the largest known eukaryotic protease, tripeptidyl peptidase II (~ 6 mDa), and the 26S proteasome (~ 2.5 mDa). While we may never truly understand why evolution selected for such complex molecular machines, it appears to be factual that the complexity of the machine itself represents only a small fraction of the complexity found in the biological system it regulates. The 26S proteasome is no exception to this rule.

## **The 26S proteasome**

The 26S proteasome is analogous to a recycling center. Cellular protein trash is delivered to the proteasome and the proteasome proteolyzes the target into small peptides that can be recycled in the cell for the creation of new proteins. The proteasome has ~ 33 unique protein subunits making up a ~ 66-protein subunit complex (Figure 1.1). The proteasome is composed of two main components: A 19S regulatory particle (RP) and the 20S core. The 19S caps one or both ends of the 20S catalytic cylindrical core (CP). The 19S regulatory particle is itself composed of two subcomplexes, the lid that is composed of ~ 11 non-ATPase subunits, and the base that is made up of two non-ATPase subunits, Rpn1 and Rpn2, that act as scaffolding subunits, and six ATPase subunits, Rpt1–6, that

require energy for the unfolding of substrates. The 19S RP recognizes an ubiquitin tag found on protein substrates, unfolds the substrate, and sends it into the channel of the 20S CP. Using three different proteolytic activities, the 20S degrades the substrate into small peptides (Pickart and Cohen, 2004).

## **The ubiquitin proteasome system**

Degradation of cellular proteins is a selective process, that in many cases, is even controlled at a spatial and temporal level (Grabbe et al., 2011). Ubiquitin (Ub) is a small 76-amino acid protein whose conjugation to target proteins precedes degradation, and is the crux of the ubiquitin proteasome system (UPS). Ubiquitin is added to protein substrates through a series of three reactions involving enzymes known as E1s, E2s, and E3s. An E1 enzyme activates a free mono-Ub molecule by forming a covalent thioester bond. This activated ubiquitin is then transferred to an E2 conjugating enzyme and finally to an E3 ubiquitin ligase enzyme. Each E3 enzyme acts only on specific substrates and adds one of many levels of selectivity to the UPS (Hershko and Ciechanover, 1998). Polyubiquitin (polyUb) chains can be built onto substrates through the sequential addition of ubiquitin molecules to one another via the E1, E2, E3 enzymatic steps (Pierce et al., 2009). Ubiquitin molecules form isopeptide linkages with one another through their lysine residues. Ubiquitin has multiple lysine residues through which multiple types of chain linkages can be produced.

Polyubiquitin tags of different linkages play diverse cellular roles. Lys-48 polyubiquitin chain appendages target proteins to the proteasome for degradation. A Lys-48 tetraubiquitin chain has been shown to be the minimal signal necessary for

proteasomal recognition (Thrower et al., 2000). Alternatively, polyubiquitin chains made from Lys-63 or Lys-29 linkages generally have non-proteasomal signaling roles in the cell (Ikeda and Dikic, 2008).

## Substrate delivery to the proteasome

In 1995, the discovery that a human proteasome subunit, S5a, bound polyubiquitin, led to the first insights into how ubiquitylated substrates are recognized by the proteasome (Deveraux et al., 1995a). Homologs of S5a, including the yeast homolog, Rpn10, were also found to bind polyubiquitin and to be necessary for the proper turnover of artificial substrates (van Nocker et al., 1996). Rpn10 is believed to create a hinge between the 19S and 20S (Glickman et al., 1998) and contains an ubiquitin interacting motif (UIM) that was found to be responsible for this recognition of Ub chains (Young et al., 1998) and necessary for the efficient delivery of ubiquitinated targets to the proteasome (Lambertson et al., 1999). However, deletion of *RPN10* did not lead to phenotypes suggestive of large-scale deficits in cellular protein degradation (Saeki et al., 2002a), and only 27% of all UPS substrates are influenced by *RPN10* (Mayor et al., 2007). This all leads to the belief that there are multiple cellular proteins involved in recognizing substrates for degradation at the proteasome.

Such a belief was confirmed shortly. After the discovery of Rpn10 as an intrinsic ubiquitin receptor, receptors known as UBA-UBL (ubiquitin association-ubiquitin-like) proteins—namely, Rad23, Dsk2, and Ddi1—were discovered. These proteins are stoichiometric interactors with the proteasome. They act as shuttles that bind and unbind the proteasome rapidly and transiently (Wang and Huang, 2008). They contain an amino

terminal ubiquitin like domain (UBL) that is responsible for docking to the proteasome and a carboxyl terminal ubiquitin association domain (UBA) that binds ubiquitin chains (Chen et al., 2001; Wilkinson et al., 2001). Binding to ubiquitin chains via the C-terminal and the proteasome via the N-terminal presented a novel mode of translocation for ubiquitylated targets to the proteasome. These UBA-UBL proteins are conserved from yeast to man (Mueller and Feigon, 2002; Zhu et al., 2007), although they are not essential (Díaz-Martínez et al., 2006). The yeast proteasome has an array of proteins containing UBA and/or UBL domains (Table 1.1). However, Rad23, Dsk2, and Ddi1 represent a very small group of proteins that actually contain both domains (Table 1.1). The UBA-UBL proteins have been the focus of my dissertation research and each of them has unique attributes that appear to play a role in their function in substrate delivery to the proteasome.

## **Rad23, the best-characterized shuttle receptor**

Rad23 is a highly conserved from yeast to man (Bertolaet et al., 2001a). It was originally identified as a gene important for cellular resistance to UV stress; specifically it plays a role in nucleotide excision repair (Miller et al., 1982). It was later discovered that the UBL domain of Rad23, which shares 23% identity with ubiquitin (Bertolaet et al., 2001a), binds the proteasome. Rad23 was the first UBA-UBL domain protein of its kind to be invoked in the UPS system, and the discovery of this role made it plausible that other similar proteins behave in the same way (Schauber et al., 1998).

To date, Rad23 is the best-characterized UBA-UBL protein. Distinguishing it from other yeast proteins in its family, Rad23 has two UBA domains, each of which

appears to have different affinities for Lys-48 and Lys-63 chains (Raasi et al., 2005). Nonetheless, as a whole, Rad23 has a greater affinity for binding Lys-48 linked chains than for any other, suggesting that its major cellular role is recognition of proteasome substrates (Raasi et al., 2005).

The roles Rad23 plays in UV stress response and in proteasome substrate delivery are not necessarily individual separable tasks. For instance, *rad23ΔUBL* mutants are sensitive to UV irradiation and other DNA damage responses (Watkins et al., 1993). Additionally, only partial complementation of a *RAD23* mutant can be achieved by transformation with *rad23ΔUBL* (Lambertson et al., 2003). These results may indicate that Rad23 needs to bind the proteasome for full activity in DNA damage responses.

## **Dsk2, the next best-characterized UBA-UBL protein**

Budding yeast Dsk2 was first described as a receptor by Funakoshi and colleagues in 2002, who showed that it preferentially bound Lys-48 chains in comparison to Lys-63 chains (Funakoshi et al., 2002). Like Rad23, Dsk2 also plays multiple roles in the cell. Specifically, it is important for spindle pole body duplication (Biggins et al., 1996). Overexpression of *DSK2* causes accumulation of cellular Ub conjugates and is a lethal event (Funakoshi et al., 2002). Multiple papers show that Dsk2 and its homologs bind the proteasome (Chandra et al., 2010; Fatimababy et al., 2010; Saeki et al., 2002b; Wilkinson et al., 2001). The UBA domain of Dsk2 has been proposed to bind monoUb and Lys-48, Lys-63, and Lys-29 chains with similarly strong affinities (Raasi et al., 2005). Another recent study also suggests that Dsk2 binds Lys-63 linkages more tightly than any of the other UBA-UBL proteins (Fatimababy et al., 2010). However, structural models of the

Dsk2 UBA domain agree with the original Funakoshi paper in that it would actually selectively bind Lys-48 chains over any other linkage (Lowe et al., 2006). Nonetheless, it has been found to be necessary for the proper proteolytic turnover of several endogenous cellular proteins and model substrates (Barbin et al., 2010; Liu et al., 2009; Medicherla et al., 2004; Richly et al., 2005).

## **Ddi1, the most controversial shuttle receptor**

Before its role in the UPS was uncovered, Ddi1 was identified as a DNA damage-inducible gene, and was studied for its role in binding v-SNARE proteins (Liu and Xiao, 1997; Lustgarten and Gerst, 1999). Ddi1 is expressed in the nucleus and the cytoplasm and has a high level of sequence conservation and representation throughout all eukaryotic genomes (Gabriely et al., 2008; Krylov and Koonin, 2001). Interestingly, Ddi1 appears to be the most divergent of the UBA-UBL protein family. Its UBL domain only shares 16% identity to ubiquitin (Bertolaet et al., 2001a) and such a distinction is the key element that differentiates the proteolytic functions of Rad23 and Ddi1 (Kim et al., 2004). The *S. pombe* homolog of Ddi1, Mud1, was first linked to the UPS when it was identified as a suppressor of the temperature-sensitive phenotype for a Rpn1/Mts4 mutant (Wilkinson et al., 2001).

The role of Ddi1 in substrate delivery has been harder to understand. Supporting a role for Ddi1 in targeting substrates to the proteasome are observations such as the fact that its UBA domain binds longer Ub chains better than shorter chains (Trempe et al., 2005; Wilkinson et al., 2001), albeit to much less of an extent than Rad23 and Dsk2 (Kaplan et al., 2005; Saeki et al., 2002b). It is noteworthy that the expression of

proteasomes is also mainly nuclear and cytoplasmic and that the localization of Ddi1 to these regions is dependent on presence of UBA and UBL (Gabriely et al., 2008; Peters et al., 1994). However, there are at least three publications that cast doubt on the role of Ddi1 as a shuttle receptor. Some researchers have not been able to detect binding of Ddi1 or its homologs to the proteasome or subunits of the proteasome (Chandra et al., 2010; Fatimababy et al., 2010; Kim et al., 2004). Despite this controversy, Ddi1 is necessary for turnover of some proteins (Ivantsiv et al., 2006; Kaplun et al., 2005). Furthermore, a *ddi1ΔUBL* mutant does not properly turnover the Ddi1 substrate, HO. This result suggests that the interaction of Ddi1 with the proteasome is necessary for HO degradation (Ivantsiv et al., 2006).

It should also be noted that conflicting data regarding the role of both Rad23 and Rpn10 in acting as ubiquitin receptors had also been raised. For instance, over-expression experiments of *RAD23* suggested that it might actually antagonize the turnover of endogenous and model substrates instead of enhancing it (Ortolan et al., 2000). Rpn10 was also cast into doubt when a published report failed to see it bind polyubiquitin in the context of an intact proteasome and when the *Arabidopsis thaliana* ortholog was seen to inhibit proteolysis (Deveraux et al., 1995b; Lam et al., 2002). However, currently in the field, these doubts have subsided (Elsasser et al., 2004; Verma et al., 2004).

Controversy aside, the role of Ddi1 in the UPS is further confounded by the knowledge that Ddi1 and its orthologs share a conserved retroviral aspartyl protease sequence signature, D[S/T]G (Krylov and Koonin, 2001). Based on the fold of this aspartyl protease domain, Ddi1 is predicted to be proteolytically active (Sirkis et al., 2006). However, there are no published reports showing definitive proof that the protease

domain of Ddi1 has cellular activity. The presence of this protease domain may even suggest that Ddi1 may play a novel deubiquitinating enzymatic role, although this is an unproven hypothesis (Krylov and Koonin, 2001). One might also ask if any of the identified Ddi1 substrates are solely dependent on Ddi1 acting as a receptor, or solely or dually dependent on its aspartyl protease activity.

However, the closest the field is to understanding if the aspartyl protease domain of Ddi1 has any biological implications comes from the study of Pds1, an important cell cycle checkpoint factor that must be degraded to promote anaphase progression (Ciosk et al., 1998). The aspartyl protease domain is necessary for Ddi1 homodimerization and for suppression of the temperature sensitivity phenotype of a *pds 1-128* mutant (Clarke et al., 2001; Gabriely et al., 2008). This result is intriguing because the deletion of the UBA or the UBL domain of Ddi1 is also required for suppression of the *pds1-128* temperature-sensitive phenotype (Gabriely et al., 2008). This phenotype suppression may be due to the ability of Ddi1 to regulate the stability of cellular levels of Pds1. Supporting this is the fact that over expression of *RAD23* has also been implicated in *pds1-128* suppression (Clarke et al., 2001).

## **Overlapping and distinct roles for the UBA-UBL shuttle receptors**

An outstanding question has been: How do these UBA-UBL proteins work together, if they do at all, for delivery of substrates to the proteasome? It is suggested that Dsk2 delivers polyUb substrates to the proteasome cooperatively with other UBA-containing proteins (Lowe et al., 2006). Additionally, UBA-UBL proteins have been

shown to form heterodimers with one another, and tetraubiquitin can simultaneously bind two different ubiquitin receptor proteins (Kang et al., 2006). In conflict with this idea are studies which conclude that UBA-UBL proteins do not bind Ub as dimers (Bertolaet et al., 2001a). Another study concluded that the conflict may be resolved by structural studies that imply that the UBA domain may interact with Ub as well as with other proteins in more than one way while utilizing the same binding surface (Mueller et al., 2004).

Cooperation of the UBA-UBL proteins is still rather uncertain. The overlapping roles of these proteins in the cell cycle seem to further confound their independent cellular contributions (Díaz-Martínez et al., 2006). Further, none of the UBA-UBL proteins are essential for cell viability. Even the full deletion of all three UBA-UBL proteins in budding yeast is not lethal, although it does cause cell cycle delay at high temperatures (Díaz-Martínez et al., 2006; Kim et al., 2004).

The UBA-UBL shuttle receptors are generally believed to specifically bind Lys-48 polyUb chains with a high affinity (Raasi et al., 2005; Rao and Sastry, 2002; Wilkinson et al., 2001). However, they each do so with varying affinities for multi-ubiquitin chains (Table 1.2), and they have been shown to each have a unique repertoire of substrates whose degradation they promote (Verma et al., 2004). Their ability to bind the proteasome also appears to be a disparity between them (Saeki et al., 2002b), although there may be some cooperativity between the UBA-UBL receptors, such as in the case where two or more UBA-UBL proteins are necessary for substrate turnover (Medicherla et al., 2004). In agreement with this, *rad23Δdsk2Δ* mutant proteasomes have drastically reduced levels of Ub conjugates (Elsasser et al., 2004). However, there are

also undoubtedly some individual roles they each play in substrate turnover as well, as many substrates have been identified that are specifically regulated by only one UBA-UBL protein.

In addition to there being potential redundancy between the UBA-UBL proteins, there may also be redundancy and/or cooperation between them and the intrinsic receptor Rpn10. Rad23 and Rpn10 have some overlapping and redundant functions. For instance, delivery of Ub conjugates by Rad23 to the proteasome is largely unaffected by loss of the UIM domain of Rpn10 (Elsasser et al., 2004; Fatimababy et al., 2010). However, Rpn10 can rescue the turnover defects of *rad23Δ* proteasomes (Verma et al., 2004).

## **Proteins implicated in binding UBA-UBL proteins**

When this dissertation research began, the UBA-UBL proteins had been implicated in binding the leucine-rich repeat region one (LRR1) of Rpn1 (a base component of the proteasome) (Elsasser et al., 2002; Seeger et al., 2003). LRR regions are horseshoe-shaped motifs thought to be important in protein-protein interactions. The LRR domains of Rpn1 have been defined. Rpn1 is made up of 9 repeat segments that are composed of 35–40 residues each (Lupas et al., 1997). The first five repeat segments constitute LRR1. A 134-acidic amino acid stretch separates LRR1 and LRR2, which encompass the last four repeat segments (Elsasser et al., 2002; Lupas et al., 1997). Through a combination of yeast two-hybrid and GST pull-down assays, it was determined that the minimal region sufficient for Rad23 binding to Rpn1 is limited to amino acids 417–628, which is comprised of LRR1 and a 21-acidic amino acid stretch adjacent with the region (Elsasser et al., 2002).

While the current dissertation research was underway, several insights were additionally made in understanding recruitment of UBA-UBL proteins to the proteasome. For instance, a proteasome subunit, Rpn13, was discovered to be an intrinsic ubiquitin receptor (Husnjak et al., 2008). Rpn13 is conserved from yeast to man, binds ubiquitin, and is important in turnover of model substrates (Husnjak et al., 2008; Verma et al., 2000). Additionally, Dsk2 was found to bind both Rpn10 and Rpn13 and Rad23 was found to bind a proteasome ATPase subunit, Rpt6, and Rpn10 (Fatimababy et al., 2010; Matiuhin et al., 2008b; Zhang et al., 2009).

The exact mechanism by which UBA-UBL receptors deliver targets to this wide array of proteasome subunits, Rpn1 and intrinsic receptors, Rpn10 and Rpn13, is a mystery. For instance, do UBA-UBL proteins utilize all of these binding surfaces simultaneously? Does docking at specific subunits at the proteasome regulate degradation of only specific substrates?

## **Research objectives**

With the current tools available, addressing the separate contributions of Rad23, Dsk2, and Ddi1 to protein turnover has been difficult to resolve. This enigma leaves a multitude of questions, such as: Is the fate of a proteasome substrate dependent on the receptor by which it is delivered (Elsasser et al., 2002)?

This dissertation addresses three gaps in the existing knowledge:

- 1) Where do Ub receptors dock the proteasome? This is discussed extensively in Chapter 3, which comes from an article published in *BMC Biology*. Chapter 2 describes optimizing the screen I used in Chapter 3.
- 2) What is the consequence of the elimination of these *cis* binding sites? I will discuss the quantitative mass spectrometry technique I used to discover consequences in Chapter 6.
- 3) Is elimination of these sites equivalent to the elimination of the receptors themselves? In Chapter 4 I delve into this topic and show that the physiology of a proteasome *cis* mutant has some unanticipated surprises.

I have discovered that the binding landscape at the proteasome for UBA-UBL proteins is rather complex. A single mutation in Rpn1 at residue D517 is able to reduce the binding of Ddi1 to the proteasome. However, such is not the case for any other UBL-containing protein. Dsk2 is seen to interact less with the proteasome only when there are multiple simultaneous mutations present in Rpn1, Rpn13, and Rpn10. It will be interesting for future research to follow up on how the substrate repertoire of these UBA-UBL proteins depends, if at all, on which subunit of the proteasome they dock to.

**Table 1.1. Identified Yeast UBA and UBL containing Proteins <sup>a</sup>**

ORF Name	UBL/ UBX	UBA	Intrxn Rpn1	Interacts with				
				Rpn2	Rpn10	Cdc48	Rpn13	Ufd2
Ede1	--	✓						
Ubx1/Shp1	✓	✓		✓ <sup>b</sup>		✓		✓
Atg8	✓	--						
Ubp14	--	✓						
Atg12	✓	--	✓		✓			
Ubx7	✓					✓		
Ste50	✓	--						
Ubx3	✓	--				✓		
Rub1	✓	--						
Ubc1	--	✓						
Don1	--	✓						
Swa2	--	✓	✓					
Ubx5	✓	✓				✓		
Esc2	✓	--						
Smt3	✓	--	✓			✓		
Pac2	✓	--	✓					
Ddi1	✓	✓	✓					
Ubp6	✓	--	✓	✓	✓		✓	
Cue3	--	✓						
Gts1	--	✓						
Egd2	--	✓						
Rpl40a	✓	--						
Ubx6	✓	--						
Cue2	--	✓						
Rpl40b	✓	--						
Ubi4	✓	--			✓	✓		✓
Dcn1	--	✓						
Rps31	✓	--				✓		
Ylr419w	--	✓						
Ubx2	✓	✓				✓		
Usa1	✓	--				✓		
Vps9	--	✓						
Ubx4	✓	--						
Dsk2	✓	✓	✓ <sup>b</sup>		✓			✓
Hub1	✓	--						
Mdy2	✓	--						
Cue5	--	✓						
Rup1	--	✓						
Mex67								
Atg11	✓	--						
Rad23	✓	✓	✓	✓	✓	✓		✓

<sup>a</sup> This list was composed using [www.yeastgenome.org](http://www.yeastgenome.org)

<sup>b</sup> genetic interaction. All other noted interactions are via Affinity Capture MS or Y2H

**Table 1.2. UBA-UBL receptors have varying affinities for the different forms of ubiquitin.**

Ub Type (Reference)	$K_d$ (or relative binding affinity) <sup>a</sup>		
	Rad23	Dsk2	Ddi1
<b>monoUB</b>			
(Trempe et al., 2005)	nd	nd	390 $\mu\text{M}^*$
(Bertolaet et al., 2001a)	8 $\mu\text{M}$	nd	10 $\mu\text{M}$
(Raasi et al., 2005)	nd	15 $\mu\text{M}$	nd
(Lowe et al., 2006)	nd	8 $\mu\text{M}$	nd
(Hobeika et al., 2007)	19 $\mu\text{M}$	nd	nd
(Ohno et al., 2005)	12.9 $\mu\text{M}^2$	nd	nd
	nd	14.8 $\mu\text{M}$	nd
<b>Lys-48 diUB</b>			
(Trempe et al., 2005)	nd	nd	3 $\mu\text{M}^*$
<b>Lys-48 <math>\geq</math>tetra-UB</b>			
(Fatimababy et al., 2010)	+++	+++	+
(Raasi et al., 2005)	++/+ <sup>1</sup>	+++	++
(Wilkinson et al., 2001)	nd	nd	30 nM <sup>*</sup>
(Hobeika et al., 2007)	7.8 $\mu\text{M}$	nd	nd
	6.1 $\mu\text{M}^2$	nd	nd
<b>Lys-63 diUB</b>			
(Trempe et al., 2005)	nd	nd	140 $\mu\text{M}^*$
<b>Lys-63 <math>\geq</math>tetra-UB</b>			
(Fatimababy et al., 2010)	+	++	+
(Raasi et al., 2005)	+/+++ <sup>1</sup>	+++	++

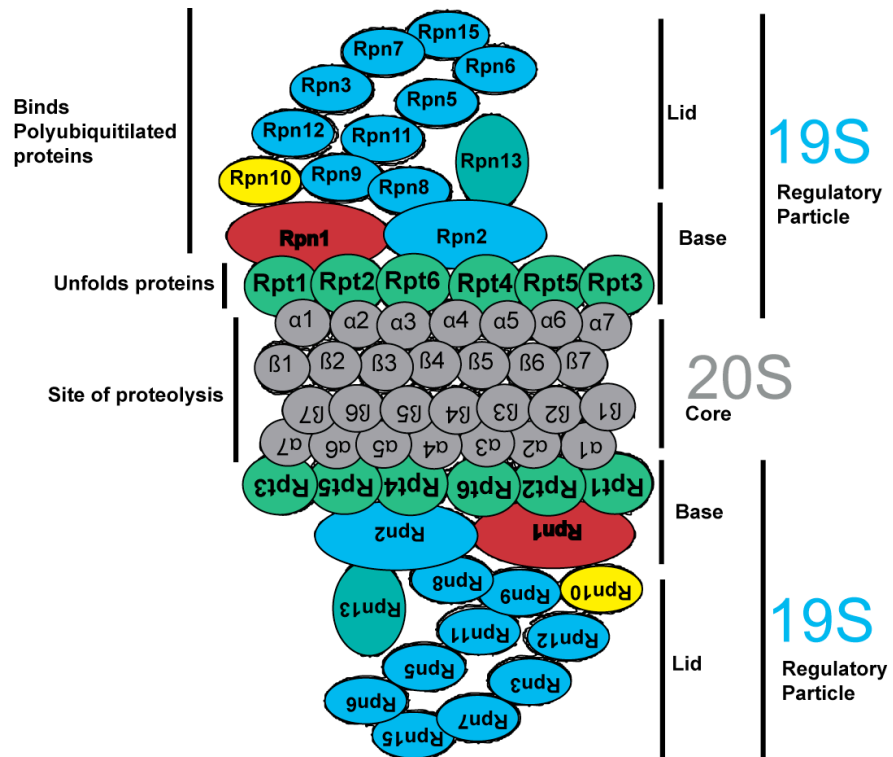
<sup>a</sup>In some publications, no  $K_d$  was provided, instead a “+” system is used, where more pluses means there is better binding.

<sup>\*</sup> Mud1, the *S. pombe* homolog of Ddi1 was used for these measurements.

<sup>1</sup> Rad23 has two UBA domains; the affinities for UBA1 and UBA2 were measured separately.

<sup>2</sup> Two separate measurements of the Rad23 UBA2 domain were made in this study.

Figure 1.1. The eukaryotic proteasome



## **Chapter 2:**

# **Reverse-yeast two-hybrid screening for putative interaction-defective alleles of Rpn1**

## Introduction

The ubiquitin proteasome system (UPS) is conserved throughout the eukaryotic branches of life. Recent studies have even found a prokaryotic ubiquitin-like degradation system in myobacteria (Burns et al., 2009; Pearce et al., 2008). The proteasome is a large multi-subunit catalytic machine that selectively degrades proteins that have been marked for destruction with an ubiquitin appendage. Ubiquitylated substrates are also selectively delivered to the proteasome by ubiquitin receptors, as extensively reviewed (Finley, 2009).

Shuttle ubiquitin receptors, such as the UBA-UBL proteins Rad23 and Dsk2, have been speculated to act as “*trans*” targeting activators of degradation. Their ubiquitin association domain (UBA) brings the degradation initiation sites of their substrates in close proximity to the proteasome (Prakash et al., 2008; Schaubert et al., 1998). They are able to deliver their cargo by binding to the proteasome with their ubiquitin-like domain (UBL), without becoming substrates themselves (Heessen et al., 2005). Such a role, allows UBA-UBL proteins to regulate the degradation of many important cellular proteins, some of which may be involved in intricate complexes that require the selective degradation of a single subunit—for example, Sic1 must be degraded while in complex with cyclin-CDK (Verma et al., 2001).

Each of these UBA-UBL shuttle receptors delivers a specific subset of cellular proteins to the proteasome (Verma et al., 2004). However, there are not a sufficient number of genetic and biochemical tools available to understand the individual contribution each one of these UBA-UBL receptors has in the selective degradation of the majority of the cell’s proteome (Rock et al., 1994). Such an understanding of the

specific repertoire of each shuttle receptor could lead to better understanding of how the UPS system is regulated and possibly even to future medical advances. For instance, human Rad23 (hHR23) has been implicated in the stability of p53, a tumor suppressor (Glockzin et al., 2003).

Hence, I aimed to create a proteasome *cis* mutant that would be unable to bind UBA-UBL proteins Rad23 and Dsk2. At the inception of my dissertation project, it was believed that Rad23 and Dsk2 primarily bound Rpn1, and some crosslinking data suggested it possibly bound Rpn2 (Elsasser et al., 2002; Saeki et al., 2002b; Seeger et al., 2003). The first step in the creation of a proteasome *cis* mutant would be to identify amino acids on Rpn1 necessary for binding UBA-UBL proteins. I employed the use of a reverse-yeast two-hybrid system to screen for these putative amino acid residues.

Reverse-yeast two-hybrid (RY2H) systems allow for identification of interaction-defective alleles (IDAs). One of the major faults of traditional reverse-yeast two-hybrid screens is the large number of false positives, due to truncated proteins. To alleviate this error, Gray and colleagues created an *in vitro* library assembly protocol, in which the bait of interest is inserted in frame with a gene responsible for kanamycin resistance in *E. coli*. Hence, a selection for full-length clones is created. This approach also allows for creation of a high-coverage allele library that will subsequently be transformed into yeast (Gray et al., 2007).

I report here, that Rpn1 has relatively weak yeast two-hybrid interactions with UBA-UBL proteins. This weak affinity may be a consequence of these proteins being in non-endogenous chimera states, or may be a consequence of a physiologically relevant weak affinity that allows them to transiently interact with one another for the disposal of

ubiquitylated proteins. Further, despite the advantages offered by this new RY2H system, of the 11 unique amino acid substitutions that were identified in this screen, none of them yielded IDA phenotypes in the context of fully intact proteasomes. The IDA phenotype exhibited in the RY2H screen was not transferable in a physiologically relevant environment. However, some of the identified residues appeared to destabilize proteasome stability, underlining potential causative reasons for why such alleles appeared in this screen.

## Methods

### Cloning RY2H bait and prey proteins

The entire ORF of Rpn1 was PCR amplified from RDB2078 with oligos TG36 and TG37. The PCR product was BP cloned into pDONR-EXP, thus creating pENTR-*RPNI* (RDB2167). pEXP-DB-*RPNI* (RDB 2169) was created by LR cloning pENTR-*RPNI* with pDEST-DB (a gift from the Marc Vidal lab). *RAD23*, *DSK2*, and *RPNI0* were similarly PCR amplified and cloned into pDONR-Express and LR cloned into pDEST-AD.

### ***RPNI*<sup>391-640</sup> allele library construction**

Described in detail in Chapter 3.

## **2 $\mu$ activation-domain yeast two-hybrid vector construction**

pDEST-AD, a kind gift from the Marc Vidal lab, was used as template for amplification of the ADH1 promoter, the NLS, the GAL4 Activation Domain, the gateway cloning sites attR1, the chloramphenicol resistance marker, the ccdB gene, the attR2 site, and the ADH1TT terminator. This entire 4.1 kb fragment was amplified with forward and reverse primers, respectively, TG43 5'-

GCGCATCGATGGATCGAAGAAATGATGGTA-3' and TG42 5'-

GCGCACTAGTTCGGCATGCCGGTAGAGGTG-3' and cloned into the *Spe1/Cla1*

sites of pRS424, which is a high copy 2 $\mu$  vector. The resultant vector, pRS424-

GAL4pAD (RDB 2178) was created. pENTR-clones were LR cloned into this vector.

## **Yeast two-hybrid interaction assay**

Plasmids were transformed into the reporter strain MaV203 (*MAT $\alpha$* ; *leu2-3,112*; *trp1-901*; *his3 $\Delta$ 200*; *ade2-101*; *cyh2R*; *can1R*; *gal4 $\Delta$* ; *gal80 $\Delta$* ; *GAL1::lacZ*;

*HIS3UASGAL1::HIS3@LYS2*; *SPAL10 UASGAL1::URA3*). Transformants were plated

onto synthetic medium prepared with 2% dextrose and lacking tryptophan and leucine

with or without 3-AT and 5FOA. After 3 d incubation at 30°C, the plates were analyzed

for growth.

## **Reverse-yeast two-hybrid screen**

The reverse-yeast two-hybrid assay was performed as described (Gray et al., 2007).

Briefly, pEXP-DB-Rpn1 allele library was cotransformed with pEXP-AD-Rad23 or

pEXP-AD-Dsk2 into the reporter strain *MaV203* using lithium acetate transformation

procedures. The transformation was plated onto SC-Leu-Trp + 0.2% 5FOA. Plates were grown for about 1 week, and putative 5FOA<sup>R</sup> colonies were picked and screened for reporter phenotypes. Interaction-defective alleles were tested for absence of activation on *GAL1::lacZ*, failure of growth on *SC-HIS*+3-amino-1,2,4-triazole (3-AT). Mild interaction-defective alleles showed some growth on 3-AT. pEXP-DB Rpn1 allele library plasmids were either purified or PCR amplified from yeast colonies that displayed 5FOAR phenotypes, and sequenced using primer 5'-GGC TTC AGT GGA GAC TGA TAT GCC TC-3' (Li et al., 2004). Clones containing mutations were then retransformed into *MaV203* and retested for proper reporter phenotypes.

### **LacZ reporter assay**

Yeast colonies were frosted onto a hybrid nylon membrane atop YPD agarose media. After ~2–3 days of growth at 30°C, the membranes were submerged into liquid nitrogen and freeze thawed two times. After allowing the membrane to completely thaw, it was placed atop Whatman filters soaked in ~6 ml of buffer (60 mM Na<sub>2</sub>HPO<sub>4</sub>, 40 mM NaH<sub>2</sub>PO<sub>4</sub>, 10 mM KCl, 1 mM MgSO<sub>4</sub>, 0.7 M 2-mercaptoethanol, 21 mM X-gal). The soaked membranes were sealed in an airtight bag and placed at 37°C for 4–24 h.

### **Putative Rpn1 IDA insert sequencing**

Direct PCR amplification of the pEXP-DB-Rpn1 insert was done as described in Li and Vidal. Briefly, yeast colonies were resuspended in 15 µl lysis buffer (50 units zymolase in 0.1 M Na-Phosphate buffer pH 7.4) and incubated for 15 min at 37°C and 10 min at 95°C. For PCR reactions, 0.3 µl of the lysed cells were used as template and amplified

using primers 5'-GGCTTCAGTGGAGACTGATATGCCTC and 5'-GGAGACTTGACCAAACCTCTGGCG.

### ***RPN1* mutant strain construction**

*RPN1* was replaced by *Kanmx6* using a one-step PCR-mediated technique (Longtine et al., 1998). *Kanmx6* with *RPN1* 5' and 3' UTR homology was amplified from the pFA6a-KanMX6 vector (Longtine et al., 1998) by PCR using oligonucleotides TG20 (GGTCTACATAAGGTGCGATTCGTATAAATTTGGAAGACAATTGCAAGAAACGGATCCCCGGGTTAATTAA) and TG21 (GGTTTTGAATTTTTCTATTCTGGTTGATATTGCCCAAAGCTATTCAGTGAA TTCGAGCTCGTTTAAAC). The PCR product was transformed into a diploid W303 strain (RJD381) creating strain RJD4166 which lacks the entire *RPN1* ORF. This diploid strain was transformed with a CEN/ARS *URA3* plasmid, pRS316-*RPN1* (RDB--), sporulated, and used to select for haploid strains resistant to G418 and able to grow on SD-Ura. The resultant strain, RJD4189 was used for plasmid shuffling.

### **Construction of putative Rpn1 IDA plasmids**

The *RPN1* locus, including 200 bp regions upstream and downstream of the gene, were PCR amplified from purified *S. cerevisiae* genomic DNA using primers TG18 (GGGCGCCTCGAGGTTGACTATTTACAGCTCATC) and TG19 (GCGCCCGAGCTCAGCGCATCCATATTTACT). The resulting PCR product, containing *XhoI/SacI* restriction sites, was digested and ligated into pRS315 and pRS316 CEN/ARS vectors. Silent mutations via a single nucleotide change resulted in an *AvrII*

restriction site at bp 1174 (amino acid 392) and an *EagI* site at bp 1920 (640). The mutations were engineered into the wild-type *RPNI* locus using the Multisite Directed Mutagenesis Kit (Stratagene) and oligonucleotides TG12 (5' GTCATTTGTCAACGGGTTCTTAAACCTAGGTTATTGTAACGATAAATTAAT 3') and TG14 (5' GCAGATGAAGAAGAAACGGCCGAAGGACAGACTA 3'). Mutations identified on pEXP-DB-Rpn1 plasmids in the reverse two-hybrid screen were introduced into this construct by double digestion and ligation into the *AvrII* and *EagI* sites.

### **Growth assays**

For plating assays, strains were grown overnight in YPD and diluted to an OD<sub>600</sub> of 0.3 in YP. Five-fold dilutions were prepared in YP and spotted onto YPD plates supplemented with various additives as described in the text. Plates were incubated at 30°C or 37°C for 2–3 days.

### **Small-scale yeast extract preparation for native gels**

Extracts were prepared as described (Elsasser et al., 2005). Briefly, 50 mLs of saturated culture grown overnight to late log phase was harvested by centrifugation and the pellet was weighed. Pellets were resuspended in 1.5 mL of lysis buffer (50 mM Tris-HCl [pH 8.0], 1 mM EDTA, 5 mM MgCl<sub>2</sub>, and 1 mM ATP, 1X ATP Regeneration System) per gram of wet weight. An equal volume of glass beads was added and cells were lysed in a fastprep machine (ThermoSavant, Holbrook, NY) for 60 s at a speed of 6.5. Extracts are cleared by centrifugation at 20,000 g at 4°C for 30 minutes. Cleared extracts were then filtered through a milipore spin column.

## **26S native gel analysis**

Described in detail in Chapter 3.

## **Native immunoprecipitation of proteasomes**

Described in detail in Chapter 3.

# **Results**

## **Optimizing the Rpn1 reverse-yeast two-hybrid interaction**

My goal was to create an Rpn1 *cis* mutant that would be unable to bind UBA-UBL proteins through the use of a genetic reverse-yeast two-hybrid screen. The first step in accomplishing this goal was to confirm and optimize forward yeast two-hybrid interactions between Rpn1 and prey proteins of interest. The RY2H system we employed to assay interactions between Rpn1 and various PIPs has several reporter genes that can be simultaneously assayed. Positive interactions result in growth in the absence of uracil, in the presence of the drug 3-AT (with strong interactors being resistant to higher concentrations of 3-AT), and induction of *lacZ*. The RY2H system has the additional advantage of allowing for the selection of non-interacting bait and prey pairs. Growth in the presence of the drug 5FOA, which normally causes toxicity in the presence of the *URA3* protein product, signals non-productive Y2H interactions. Since it had been shown that a region encompassed by amino acids 391–642 of Rpn1 was necessary for interaction with UBA-UBL proteins (Elsasser et al., 2002; Seeger et al., 2003), the

interaction between Rpn1<sup>391-642</sup>-DB was assayed with multiple baits including: Rad23-AD, Rad23ΔUBL-AD, Ubp6, Ubp6ΔUBL-AD, Dsk2-AD and Rpn10-AD. A full-length Rpn1-DB bait was also tested for interactions with these prey. Unexpectedly, in all tested combinations, growth was not seen on medium lacking uracil and induction of *lacZ* was only detected after several hours. However, growth on 50 mM 3-AT for Rad23-AD and Dsk2-AD in combination with Rpn1<sup>391-642</sup>-DB was observed (Figure 2.1). However, when the polarity of this interaction was reversed so that Rpn1<sup>391-642</sup>-AD was tested for interaction with prey, no productive interactions were detectable (data not shown). Taken together, these results are consistent with a very weak interaction occurring between Rpn1-DB, both the full-length and truncated forms, and the tested prey proteins.

### **Expression of baits on a 2μ plasmid enhance positive and false-positive signals**

We postulated that interaction between Rpn1-DB and its prey might be improved by over expression of one of the interacting partners. It is possible that Rpn1-DB and Rad23-AD are interacting with endogenous proteins, and we might detect an increased reporter gene signal if we increase the pool of prey or bait proteins. To query this hypothesis, a high copy number 2μ Y2H pAD vector was created. In testing the strength of the interactions with this clone, several observations were made. Firstly, the importance of the polarity of the interaction was again observed, positive interactions were detected between Rpn1-DB pairs and activation-domain-carrying baits and not vice versa (data not shown).

Furthermore, there is an increase in putative negative interacting partners. Unexpectedly, pAD-2μ vectors cause growth on 5FOA, in most tested cases. For instance, pAD-2μ-

Rad23 grows on uracil whereas its CEN/ARS plasmid counterpart does not, but it also grows on 5FOA (Figure 2.1). Hence, the pAD-2 $\mu$  vectors appear to create false positive and negative signals and would not be optimal for use in a RY2H screen.

### **Isolation of putative Rpn1 IDAs**

Using the strongest forward-yeast two-hybrid interactions we could detect (those between Rpn1<sup>391-642</sup>-DB and Dsk2 and Rad23 *CEN/ARS* baits, we proceeded with the RY2H screen. The Rpn1<sup>391-642</sup>-DB allele library, containing over 500,000 individual clones, was co-transformed with either Rad23-AD or Dsk2-AD. Transformations were plated directly onto medium containing 5FOA and incubated at 30°C until putative IDAs grew. A total of 964 5FOA<sup>R</sup> colonies appeared and were screened in a Rad23/Rpn1 assay. For the Dsk2/Rpn1 assay, a total of 322 colonies were screened. Of those, 90 Rpn1-Rad23 IDAs and 22 Rpn1-Dsk2 IDAs appeared positive when screened for the proper reporter phenotypes and were subsequently sequenced. For the Rpn1-Rad23 screen, 22% of all putative positives contained a mutation, either silent (2.2%), a truncation or frameshift (3.3%), or a single or double mutation (16.7%). For the Dsk2-Rpn1 screen, again, roughly 22% of all putative positives contained a mutation of some sort, with 18.2% of these clones containing single or double mutations (Table 2.1). When these putative positive Rpn1 IDAs were retransformed with either Rad23 or Dsk2, only 10% of Rad23/Rpn1 IDAs retested as positives and 75% of Dsk2 clones. The mutations identified in this screen are shown (Table 2.2).

## **Rpn1 IDAs appear universal in their ability to disrupt binding to UBL proteins**

The Rpn1 IDAs identified in the Rad23 and Dsk2 screens were tested for their ability to interact with other UBLs, including Rad23, Dsk2, and the deubiquitinase UBL-containing enzyme, Ubp6. It was found that in all tested cases, every Rpn1 IDA hampered to some degree the interaction with any tested UBL in comparison to the wild-type interaction. Additionally, similar levels of 3-AT were found necessary for inhibition of growth (Table 2.3).

## **Putative Rpn1 IDA alleles have wild-type phenotypes when introduced into Rpn1 null cells**

To assess the physiological consequences of the putative Rpn1 IDAs I identified in the RY2H screen, mutant *LEU2* plasmids were plasmid shuffled into *rpn1* $\Delta$  haploid cells sustained by a low copy *URA3* plasmid containing *RPNI*. Transformants were plated onto 5FOA to evict the wild-type *RPNI* plasmid, and clones sustained by the mutagenized plasmid were sought. All alleles of *rpn1* were viable with the exception of *rpn1*-F534S (Figure 2.2).

To identify mutants that exhibited broad defects in the ubiquitin–proteasome system, we tested these alleles for growth defects. Proteasome mutants often show growth defects under conditions that induce protein misfolding, such as in a variety of proteasome assembly mutants (Saeki et al., 2009). Strains lacking multiple ubiquitin receptors, such as the double and triple UBA-UBL strains, *rad23* $\Delta$ *dsk2* and *rad23* $\Delta$ *dsk2* $\Delta$ *ddi1* $\Delta$ , are also sensitive to protein misfolding, salt, and ethanol stress

(Husnjak et al., 2008; Kim et al., 2004; Lambertson et al., 1999). I postulated that if any of the identified Rpn1 IDAs diminished binding of UBA-UBL proteins *in vivo*, they would show sensitivity to stress conditions. Two *rpn1-1* mutant isolates were also used in this assay as positive controls. The *rpn1-1* strain is an unmapped mutation within *RPN1* that was identified in a genetic screen for mutants that accumulate 3-hydroxy-3-methylglutaryl-CoA reductase (Hampton et al., 1996). The *rpn1* mutants were tested for their ability to grow on YPD medium at 30°C and 37°C. In addition, their ability to grow in the presence of ethanol (EtOH) and the proline analog AZC (L-azetidine-2-carboxylic acid) was also tested. Proteasome mutants exhibit stress when grown on AZC, as it promotes misfolding in proteins and presumably overloads the proteasome (Fowden and Richmond, 1963). Surprisingly, all of the *rpn1* mutant strains show similar viability in comparison to wild type under all tested conditions (Figure 2.3). As expected, the *rpn1-1* strains show sensitivity to elevated temperature and AZC.

The *rpn1* mutants were also tested for ubiquitin conjugate accumulation by Western blotting cell extracts. All of the mutants seemed to show wild-type levels of Ub conjugate accumulation (data not shown).

### **Rpn1 mutant proteins assemble into fully intact and active 26S proteasomes**

Cell extracts were resolved in non-denaturing gels in the presence of ATP and MgCl<sub>2</sub> and visualized with the fluorogenic substrate SUC-LLVY-AMC. Rpn1 IDA mutants contained wild-type ratios of double-capped 26S proteasomes, single-capped 26S proteasomes, and 20S core particles (Figure 2.4A). Thus, we conclude that there are no

assembly defects. Additionally, using a fluorogenic chymotrypsin activity assay, mutant proteasomes were found to have wild-type levels of chymotrypic activity (Figure 2.4B).

### **RY2H derived Rpn1 IDA alleles do not impair the interaction between the proteasome and the UBA/UBL proteins *in vivo***

Despite the *rpn1* mutants showing no other physiological signs that they may have impaired delivery of ubiquitinated substrates to the proteasome, I performed immunoprecipitation experiments to examine recruitment of UBA-UBL proteins to mutant proteasomes. To determine which UBA-UBL proteins were able to interact with 26S proteasome complexes from wild type and *rpn1* mutants, I subjected strains expressing Pre1-Myc to native immunoprecipitation. In wild-type cells, Rad23, Dsk2, and Ubp6 were detected (Figure 2.5A). These UBA/UBL proteins were also detected in *rpn1* mutants V447H, D503G, L506S, A531T, N539D, and I546T (Figure 2.5A and data not shown). Notably, *rpn1* mutants A418V, N549D, F565V, and G571S seemed to destabilize proteasomes during the IP procedure, as they showed reduced levels of the UBA-UBL proteins Rad23, Dsk2, and Ubp6, but also of proteasome subunits Rpn10 (base), Rpt6 (base), and Rpn11 (lid), indicating that the proteasome subcomplexes were disassociated during the immunoprecipitation (Figure 2.5A). Because the presence of the proteasome inhibitor MG262 has been shown to increase proteasome stability (Kleijnen et al., 2007), the *rpn1* mutants that showed proteasome instability were reassayed with exogenous 2  $\mu$ M MG262 added to the extracts and under milder native buffer IP conditions (75 mM NaCl and 0.1% NP40). Under these conditions, all mutants that had showed instability in the prior assay now remained assembled, with the exception of

*rpn1-A418V*. In addition, none of these mutants interfered with the proteasomes' ability to co-immunoprecipitate with Rad23 or Dsk2 (Figure 2.5B and data not shown).

## Discussion

Approximately 250 of the residues that had previously been determined to be necessary for binding UBA-UBL proteins were included in the aforementioned RY2H screen (Elsasser et al., 2002; Seeger et al., 2003). A ~150 residue span was identified within this ~250 amino acid fragment, containing 11 residues that perturbed Rad23 and/or Dsk2 binding to Rpn1 within the context of a yeast two-hybrid interaction. However, when these mutations were used to replace endogenous Rpn1 within a yeast cell and probed for their ability to bind UBA-UBL proteins, unexpectedly, binding was not diminished.

It is hard to ascertain why such a discrepancy in binding occurred between the results of the genetic screen and the results of following full-length physiologically relevant protein interactions.

Considering the large number of IDAs identified that decreased proteasome stability (4 IDAs out of 11 total IDAs), it is plausible that the RY2H screen selected for residues that enhanced misfolding of Rpn1, which in turn eliminated binding of UBA-UBL proteins. Since a truncated version of Rpn1 was used in the screen, misfolding events are conceivable. Supporting this claim is an electron microscopy study of Rpn1 which shows that truncated forms of Rpn1 do not fold correctly (Effantin et al., 2009). Interestingly, one residue uncovered in the RY2H screen caused lethality. Since Rpn1 is the largest subunit of the proteasome, misfolding events that lead to improper scaffolding

of adjacent subunits could very well be a lethal event. It may be interesting to do *in vitro* studies with mutant Rpn1-F534S protein to determine if this residue causes severe misfolding of Rpn1 that impinges on proteasome function.

Another reason true IDAs were not identified in the RY2H screen may be due to the inherent nature of the proteasome to interact with *GAL1-10* promoter *in vivo* through binding the activation domain of (AD) of Gal4. Gal4-AD interacts with proteasome subunits, Sug1/Rpt6, Sug2/Rpt4, and Rpn1, Rpn2 (Gonzalez et al., 2002). This may have allowed Rpn1-DB to naturally interact with Gal4-AD containing proteins. Admittedly, since all forward Y2H interactions were quite weak (Figure 2.1) this may be the weakest argument. However, the possibility exists that this natural tendency for endogenous proteasome subunits to interact with Gal4-AD may have compounded other intrinsic problems with this genetic screen.

It is also possible that in the context of the RY2H screen the interactions between Rpn1 are truly impaired with UBA-UBL proteins. However, *in vivo*, a lot of binding redundancy exists that precludes the exhibition of phenotypes from a single residue mutation in Rpn1. This hypothesis was examined and will be the focus of a subsequent chapter (Chapter 3).

At the time this work was completed, there were two *rpn1* allele mutations that had been crudely defined in the literature, *rpn1-1* and *rpn1-821*. The *rpn1-1* mutation was identified in a genetic screen for mutations that stabilized cellular HMG-CoR levels (Hampton et al., 1996). In my hands, I saw that this mutant was sensitive to temperature and AZC stress, so I was attracted to follow up on its possible role in UBA-UBL protein binding. However, after extensive sequencing analysis of the *RPNI* from this strain, I

found no apparent mutation in the ORF, or within at least 200 bp of the 5' or 3' UTR of this gene. Hence, I believe the mutation was improperly mapped to *RPNI* and stopped pursuing it as a potential *RPNI* allele of interest. The *rpn1-821* mutation was identified in a screen for mutants that suppressed the *Dsk2* over-expression lethality (Funakoshi et al., 2002). However, this allele was not of interest to follow up as it was determined to have assembly defects (Funakoshi et al., 2009).

While these studies were largely unsuccessful, there may be insights into proteasome stability, Rpn1 structure, and still, possibly even UBA-UBL protein interactions that may become apparent in future lines of research.

## Figure legends

### Figure 2.1. **Forward-yeast two-hybrid interactions between Rpn1-DB and prey proteins.**

Positive interactions (growth on –URA and 3-AT) and negative interactions (growth on 5FOA) of prey proteins can be observed with either a truncated form of Rpn1<sup>391-642</sup> or full-length Rpn1 with various prey proteins. Yeast cells were co-transformed with plasmids expressing Gal4-DBD fused to Rpn1 and Gal4-AD fused to either Rad23, Dsk2 expressed on *CEN/ARS* plasmids or Rad23, Rad23ΔUBL, or Rpn10 expressed on 2μ high expression plasmids. Protein-protein interaction is indicated by growth on 50 mM 3-AT and lack of growth on 0.2% 5FOA.

### Figure 2.2. **Most putative Rpn1 IDAs produce viable yeast strains.**

Mutant *rpn1* alleles identified in the RY2H screen were reconstructed into full-length pRS315-*RPNI-LEU2* vectors and plasmid shuffled into an *rpn1Δ* pRS316-*RPNI-URA3* yeast strain. *RPNI* alleles that produce viable strains were able to evict the wild-type *URA3* plasmid and sustain growth on 5FOA. Empty pRS315 vector is used as a negative control.

### Figure 2.3. **Mutant *rpn1* alleles do not display typical proteasome mutant phenotypes.**

Five-fold serial dilutions of cells were plated onto the indicated media. The *rpn1* mutants (*rpn1\**) were grown at either 30°C or 37°C, with 5 mM AZC (a proline analog), or on

12% ethanol. Two isolates of a *rpn1-1* mutant were used as control. Some of the mutants shown in the figure will be discussed in Chapter 3.

**Figure 2.4. Mutant *rpn1* alleles do not interfere with proteasome assembly.**

(A) Proteasomes isolated from *rpn1* mutants are intact. Cell lysates from the indicated *rpn1* mutant were run on non-denaturing gels. The native gel was incubated with Suc-LLVY-AMC in the presence of ATP and 0.05% SDS to visualize RP and CP activity. (B) Chymotryptic activity of cell lysates was quantitatively measured using Suc-LLVY-AMC in the presence and absence of SDS.

**Figure 2.5. Select RY2H screen *rpn1* alleles reduce proteasome stability but do not impinge on UBA-UBL binding to the proteasome.**

(A) Affinity-purified *rpn1* mutant proteasomes do not contain reduced levels of UBA-UBL proteins. However, some *rpn1* mutant proteasomes disassociate during the course of affinity purification. Reduced levels of Rpn10 (base), Rpt6 (base), and Rpn11 (lid) are seen in *rpn1*-A418V, N549D, F565V, and G571S mutants. (B) *rpn1* mutants that showed proteasome stability defects were purified under more gentle immunoprecipitation conditions: low salt, gentle detergent, and in the presence of proteasome inhibitor MG262. All tested mutants, with the exception of *rpn1*-A418V were stable under these conditions. Association with Rad23 is observed with these mutant proteasomes under these conditions.

**Table 2.1. RY2H statistics**

	<b>Rad23/Rpn1</b>	<b>Dsk2/Rpn1</b>
	# (%)	# (%)
Total Colonies Screened	964	322
Total Colonies Sequenced <sup>a</sup>	90	22
<b>Clones containing mutations</b>	20 (22.2%)	5 (22.9%)
Truncated or Frameshifted Clones	3 (3.3%)	1 (4.7%)
Silent Mutation Clones	2 (2.2%)	0 (0%)
Single or Double Mutant Clones	15 (16.7%)	4 (18.2%)
Positive Clones Post Retransformation <sup>b</sup>	9 (10%)	3 (75%)

<sup>a</sup> Of the total colonies that grew on 5FOA after the RY2H transformation, only those that retested for 5FOAR and showed proper reporter phenotypes were selected for sequencing.

<sup>b</sup> This number is shown as a percentage only of single/double mutant clone isolates from the above column.

**Table 2.2. Point mutations in Rpn1 that disrupt binding to either Rad23 or Dsk2 in a RY2H system.**

<b>Position</b>	<b>AA Change WT →Mutant</b>	<b>Hits<sup>b</sup></b>	<b>Identified in pEXP-AD-X Screen</b>
418	A→V	1	Rad23
447	V→H	2	Dsk2
	V→D		Dsk2
503	D→G	1	Rad23
506	L→S	1	Rad23
531	A→T	1	Rad23
534	F→S	1	Rad23
539	N→D	1	Rad23
546	I→T	1	Rad23
549	N→D	1	Rad23
565	F→V	1	Rad23
571	G→S	1	Dsk2

<sup>a</sup> Position indicates the amino acid residue identified

<sup>b</sup> Only hits that tested positive after retransformation are shown.

**Table 2.3. 3-AT resistance of bait/prey pairs**

Allele	3-AT phenotype (mM) <sup>a</sup>		
	Rad23	Dsk2	Ubp6
A 418 A	100	nd	nd
V 447 H	>100	>100	nd
V 447 D	>100	>100	nd
D 503 G	100	nd	nd
L 506 S	100	nd	nd
A 531 T	100	100	100
F 534 S	50	50	50
N 539 D	100	>100	nd
I 546 T	50	50	50
N 549 D	50	50	nd
F 565 V	50	nd	nd
G 571 S	100	>100	nd

<sup>a</sup> The (3-AT) listed is the concentration required to inhibit growth under histidine selection.

**Figure 2.1. Forward-yeast two-hybrid interactions between Rpn1-DB and prey proteins**

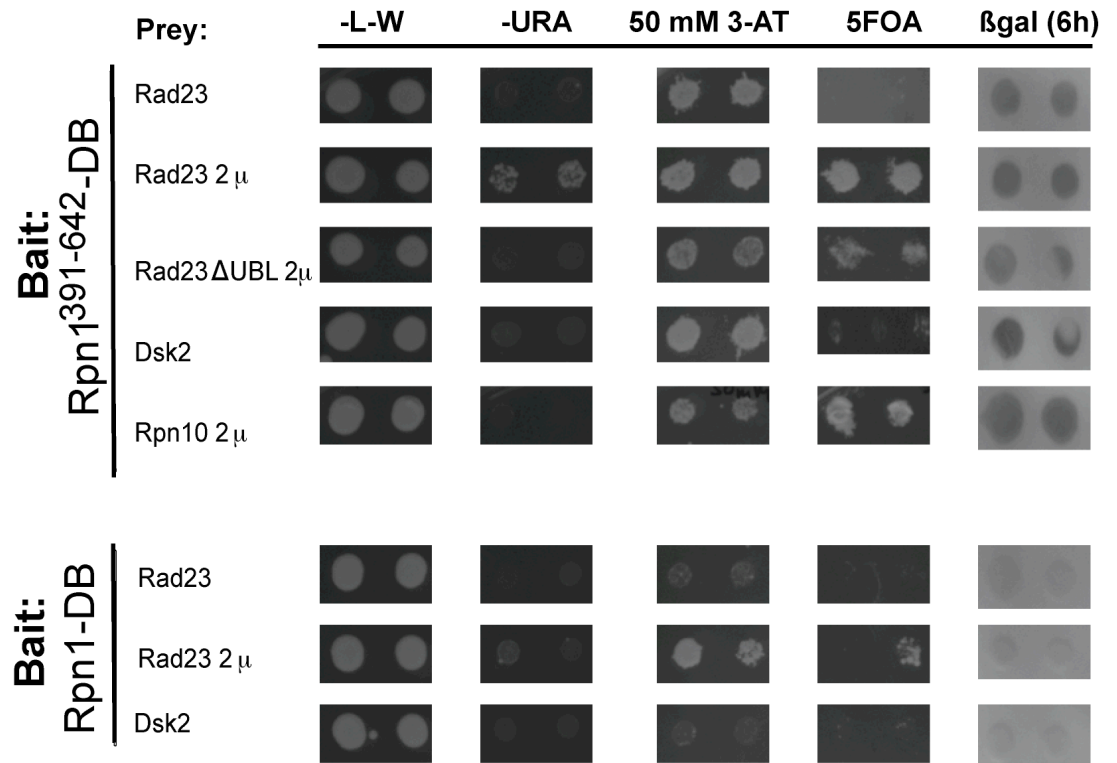
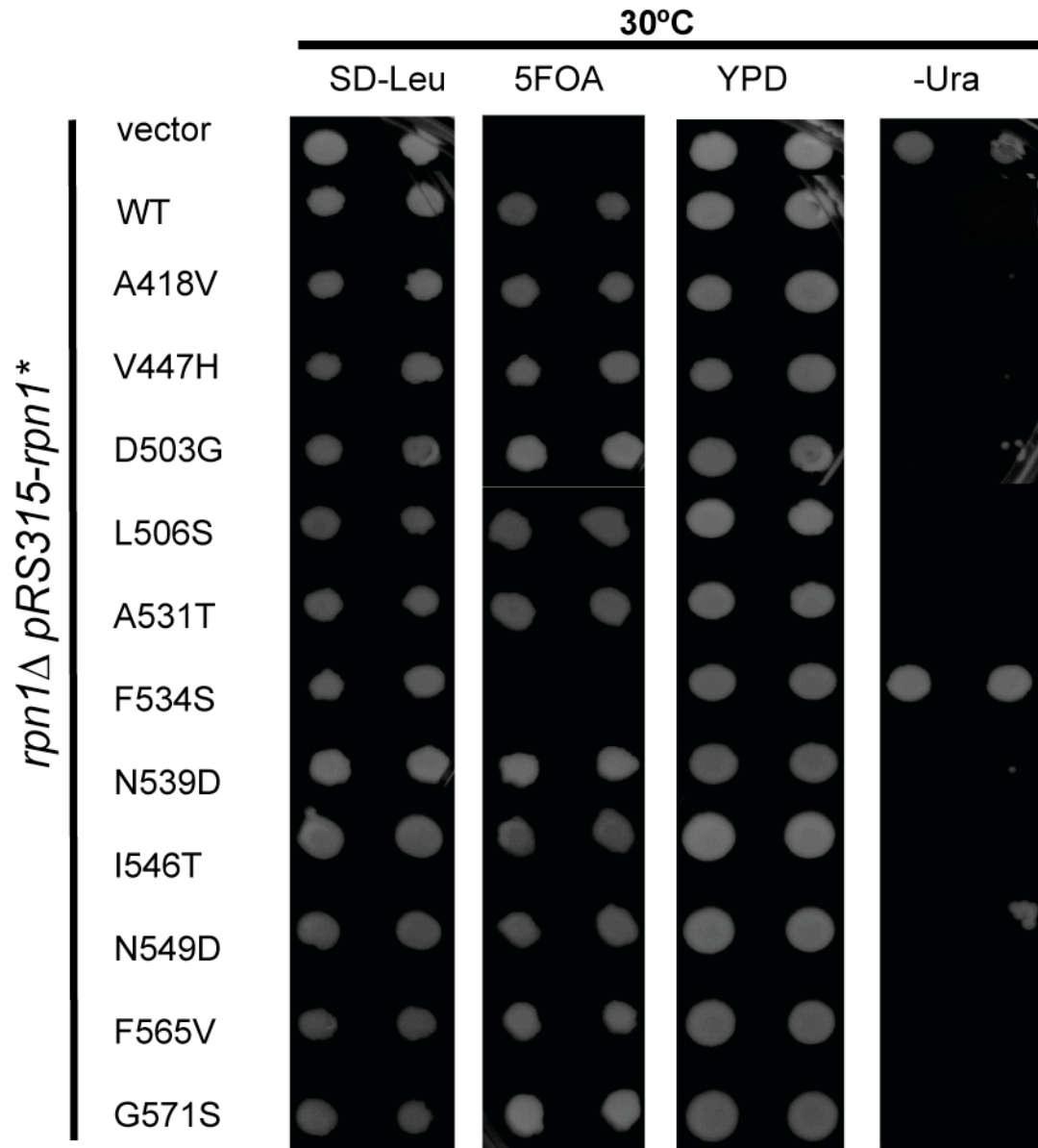


Figure 2.2. Most putative Rpn1 IDAs produce viable yeast strains.



**Figure 2.3. Mutant *rpn1* alleles do not display typical proteasome mutant phenotypes.**

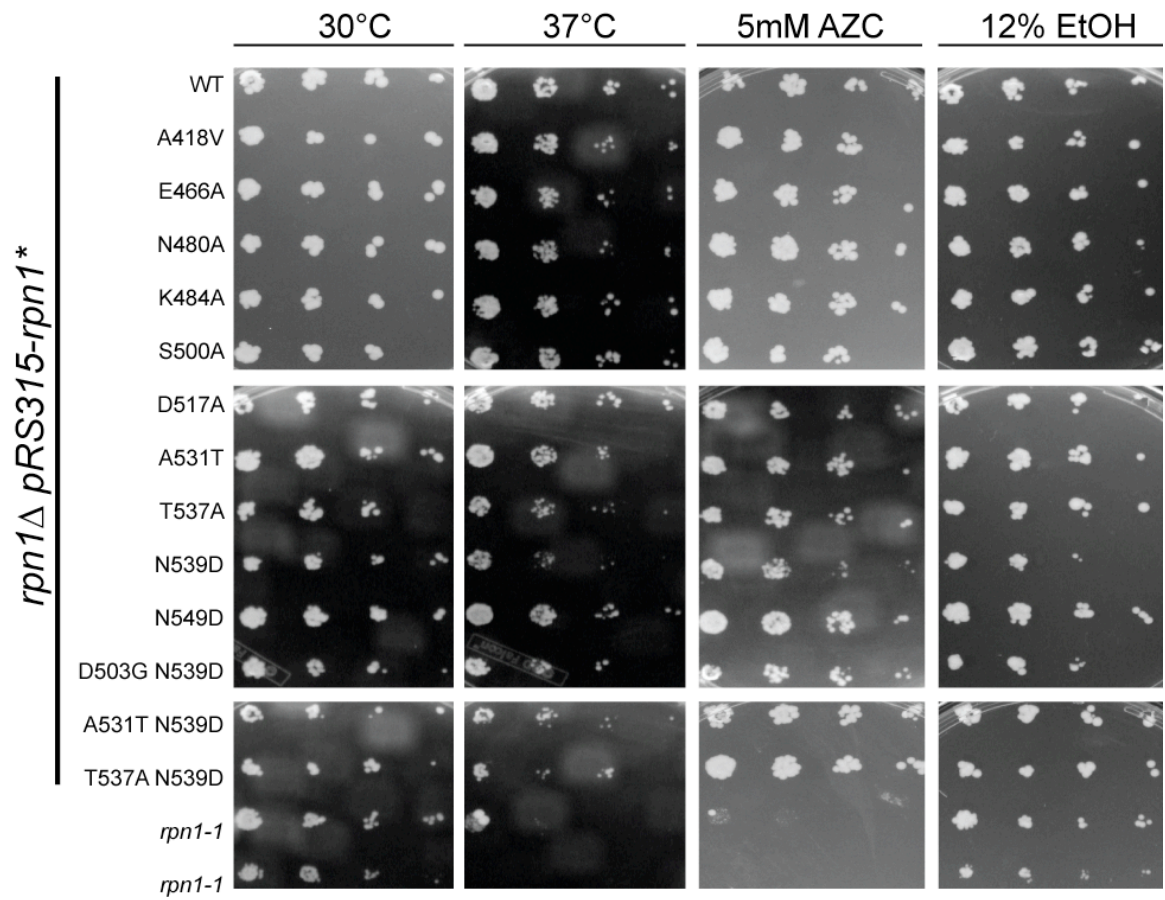
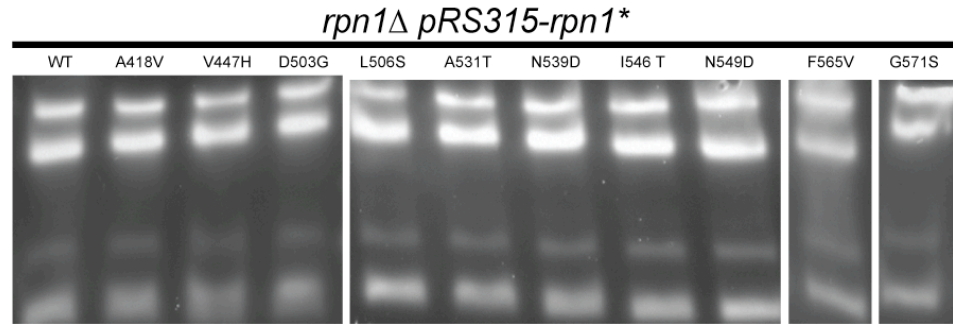
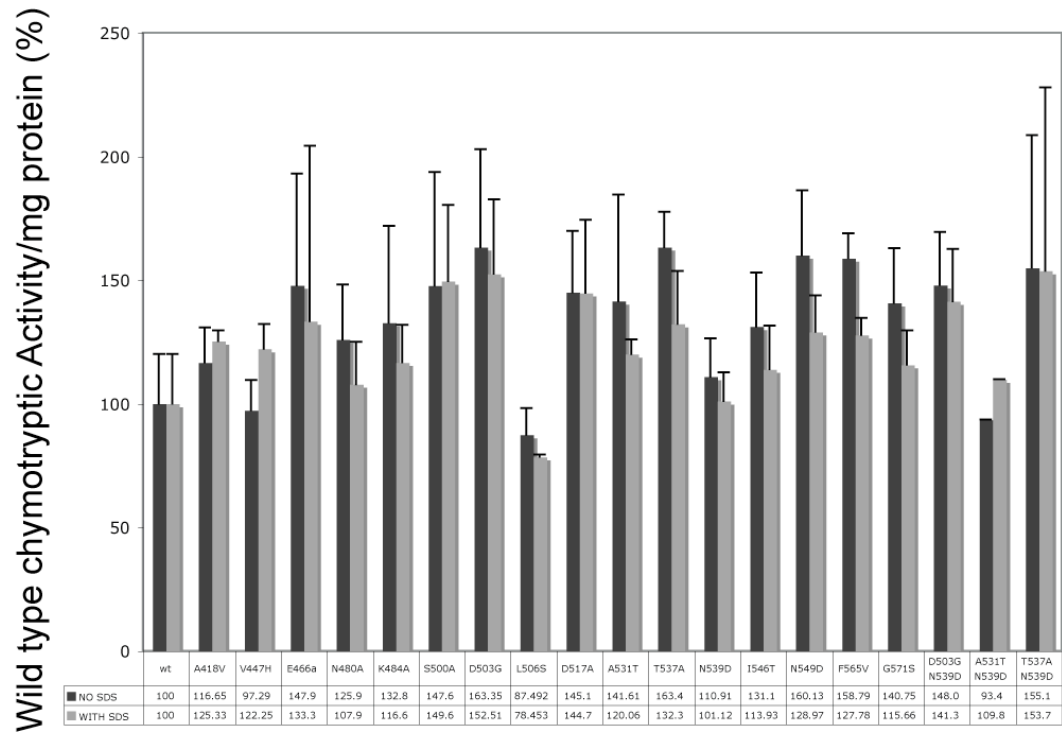
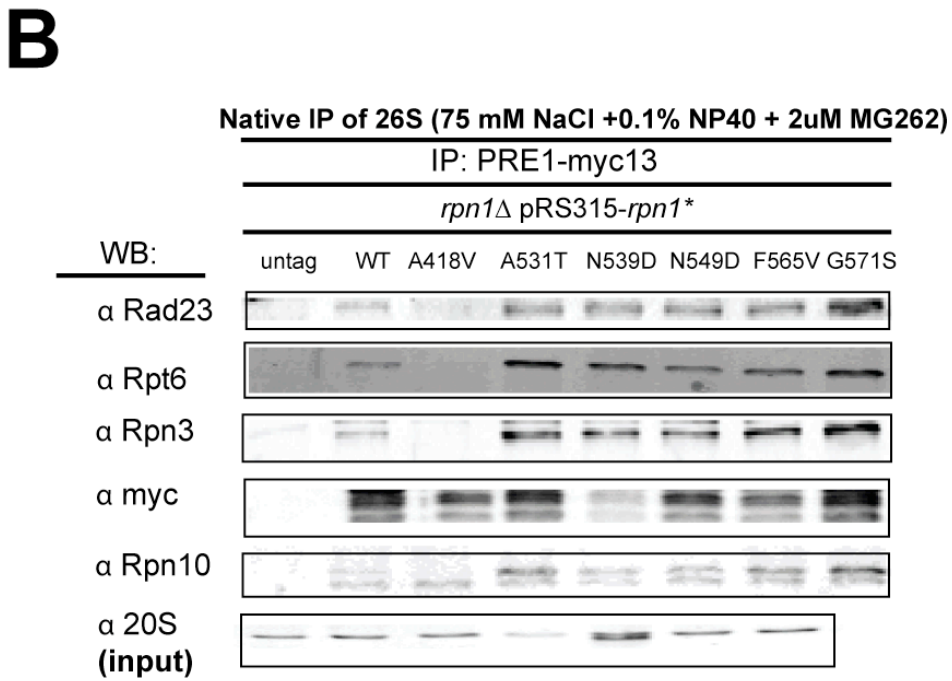
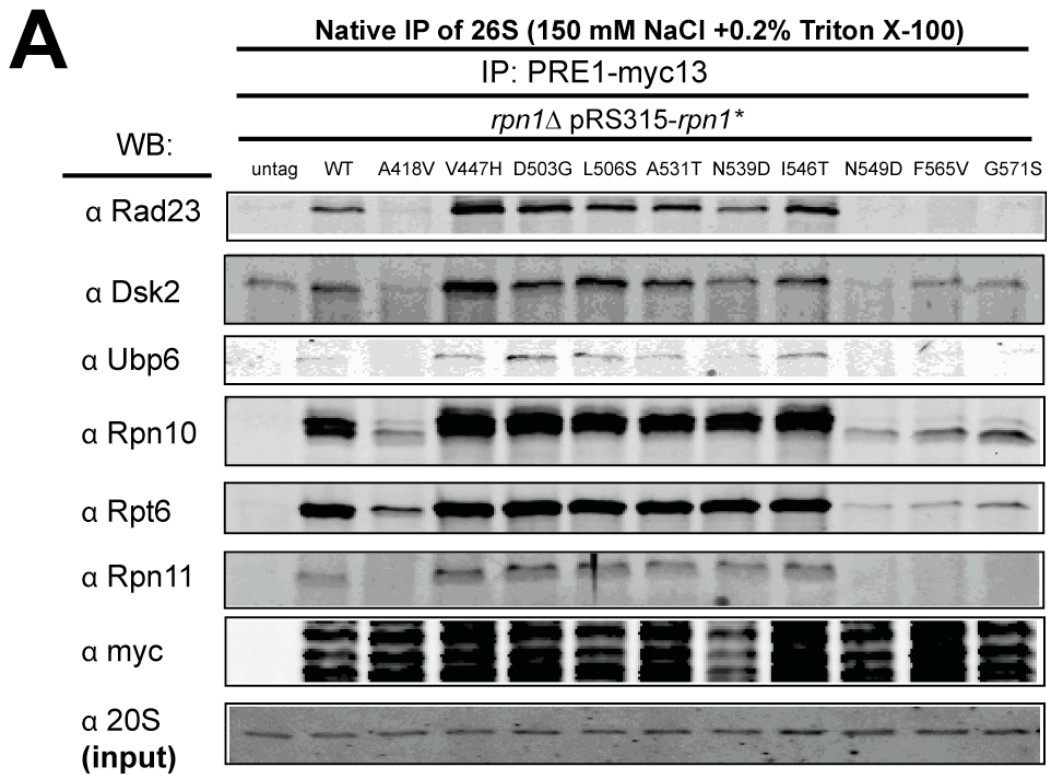


Figure 2.4. Mutant *rpn1* alleles do not interfere with proteasome assembly**A****B**

**Figure 2.5. Select RY2H screen *rpn1* alleles reduce proteasome stability but do not impinge on UBA-UBL binding to the proteasome.**



# **Chapter 3:**

## **Identification of a functional docking site in the Rpn1 LRR domain for the UBA–UBL domain protein Ddi1**

\*\*This chapter was accepted for publication by *BMC Biology*. The authors for this chapter are: Tara A. Gomez, Natalie Kolawa, Marvin Gee, Michael J. Sweredoski, and Raymond J. Deshaies.

## Abstract

### Background

The proteasome is a multi-subunit protein machine that is the final destination for cellular proteins that have been marked for degradation via an ubiquitin (Ub) chain appendage. These ubiquitylated proteins either bind directly to the intrinsic proteasome ubiquitin chain receptors Rpn10, Rpn13, or Rpt5, or are shuttled to the proteasome by Rad23, Dsk2, or Ddi1. The latter proteins share an Ub association domain (UBA) for binding poly-Ub chains and an Ub-like-domain (UBL) for binding to the proteasome. It has been proposed that shuttling receptors dock on the proteasome via Rpn1, but the precise nature of the docking site remains poorly defined.

### Results

To shed light on the recruitment of shuttling receptors to the proteasome, we performed both site-directed mutagenesis and genetic screening to identify mutations in Rpn1 that disrupt its binding to UBA–UBL proteins. Here we demonstrate that delivery of Ub conjugates and docking of Ddi1 (and to a lesser extent Dsk2) to the proteasome are strongly impaired by an aspartic acid to alanine point mutation in the highly-conserved D517 residue of Rpn1. Moreover, degradation of the Ddi1-dependent proteasome substrate, Ufo1, is blocked in *rpn1-D517A* yeast cells. By contrast, Rad23 recruitment to the proteasome is not affected by *rpn1-D517A*.

### Conclusions

These studies provide insight into the mechanism by which the UBA–UBL protein Ddi1 is recruited to the proteasome to enable Ub-dependent degradation of its ligands. Our studies suggest that different UBA–UBL proteins are recruited to the proteasome by distinct mechanisms.

## Background

Protein degradation via the ubiquitin proteasome system (UPS) is one of the cell's tools for selective negative regulation of intracellular proteins. Degradation via the UPS has roles in maintaining protein quality control, signaling, and cell cycle progression (Hershko, 1997; Vembar and Brodsky, 2008). Ubiquitin is a small protein that is highly conserved in eukaryotes and is the crux of the UPS system. The UPS system is built upon three classes of enzymes—E1, E2, and E3—that act sequentially to build ubiquitin chains on protein substrates. Once a protein substrate has been modified by a chain of at least 4 ubiquitins, it is then degraded by the 26S proteasome in an ATP-dependent manner (Pierce et al., 2009; Thrower et al., 2000).

The proteasome is a 33-subunit protein complex that is responsible for degrading a minimum of 20% of the yeast proteome (SCUD; <http://scud.kaist.ac.kr/index.html>). Other lines of evidence suggest that the vast majority of cytoplasmic protein turnover is mediated by the proteasome (Rock et al., 1994). The proteasome is composed of two main components: A 20S catalytic core particle (CP) and a 19S regulatory particle (RP). The 19S regulatory particle can be dissected into two sub-complexes, the lid and the base. The base sub-complex is composed of two non-ATPase subunits, Rpn1 and Rpn2, as well as six ATPase subunits (Rpt1–6) that feed unfolded substrate into the CP.

How ubiquitylated substrates converge onto the proteasome is an active area of research that has been studied with the greatest depth in *Saccharomyces cerevisiae*. So far, at least two independent mechanisms have been discovered. In the first case, the yeast proteasome contains two intrinsic receptors, Rpn10 and Rpn13, that contain defined ubiquitin binding domains (Husnjak et al., 2008; van Nocker et al., 1996). Mammalian proteasomes contain a third intrinsic receptor, Rpt5 (Lam et al., 2002). Rpn10 contains a highly conserved ubiquitin interaction motif (UIM), whereas Rpn13 binds ubiquitin via a pleckstrin motif that was not previously known to interact with ubiquitin (Husnjak et al., 2008; van Nocker et al., 1996). Although neither Rpn10 nor Rpn13 is essential, *rpn10Δ* and *rpn13Δ* mutants exhibit phenotypes consistent with a role for these proteins in docking of substrates to the proteasome. Rpt5 can be cross-linked to ubiquitin chains, but the means by which it binds ubiquitin and the genetic significance of this activity remain

to be determined. Substrates may be able to bind the proteasome directly via these three intrinsic receptors.

In the second mode of delivery to the proteasome, a class of receptors encompassing the budding yeast Rad23, Dsk2, and Ddi1 proteins contain an N-terminal ubiquitin like domain (UBL) that binds to the proteasome and a C-terminal ubiquitin association domain (UBA) that binds to ubiquitin chains (Bertolaet et al., 2001a; Chen et al., 2001; Funakoshi et al., 2002; Wilkinson et al., 2001). Unlike Rpn10 and Rpn13, these proteins are not stoichiometric subunits of the proteasome. Instead, it is thought that this class of proteins rapidly cycles on and off the proteasome (Wang and Huang, 2008), serving as ‘shuttle’ receptors that bind substrates in the cytoplasm and nucleus and deliver them to the proteasome. The UBA–UBL proteins dock at the proteasome by binding the largest subunit of the proteasome, Rpn1 (Elsasser et al., 2002; Funakoshi et al., 2002; Kaplun et al., 2005), although recent evidence suggests that the UBA–UBL proteins also bind other subunits within the proteasome. For example, multiple lines of evidence suggest that in yeast Dsk2 may also be able to interact with Rpn10 and Rpn13, and yeast Rad23 may also bind Rpt6 (Fu et al., 2010; Husnjak et al., 2008; Matiuhin et al., 2008b; Zhang et al., 2009). Human Rad23 is also able to bind both human Rpn10 and Rpn13 (Husnjak et al., 2008) and in an NMR experiment, binding of yeast Rad23 to Rpn10 was observed (Zhang et al., 2009).

While it is clear that substrates can use two different mechanisms to engage the proteasome, we still do not understand how each pathway controls the fate of each substrate of the proteasome. While there is evidence that some protein substrates utilize both the intrinsic and shuttling receptors (Kang et al., 2006), some proteasomal substrates are entirely dependent on either Rpn10 or Rad23 (Verma et al., 2004). Moreover, although Rpn10 and Rpn13 are undoubtedly important receptors, electron microscopy and quantitative mass spectrometry data suggest that there are two populations of proteasomes—those containing and those not containing the intrinsic receptors (Bohn et al., 2010; Fôrster et al., 2010; Nickell et al., 2009b). Furthermore, deletion of *RPN10* or *RPN13* does not lead to profound deficits in cellular protein degradation (Husnjak et al., 2008; Saeki et al., 2002a; van Nocker et al., 1996). Finally, while highly conserved (Mueller and Feigon, 2003), the UBA–UBL proteins are not essential for yeast cell

growth (Díaz-Martínez et al., 2006; Kim et al., 2004; Saeki et al., 2002a). Thus, although the proteasome itself is essential, none of the receptors that link substrates to the proteasome (with the exception of Rpt5) is essential. This has led to the assumption that targeting of substrates to the proteasome occurs by multiple, partially redundant mechanisms. Obtaining a clear understanding of how each pathway contributes to substrate recognition by the proteasome is of considerable importance given the central role of the UPS in regulatory biology and the clinical significance of the proteasome as a target for cancer therapy (Fisher et al., 2006; Richardson et al., 2005).

Rpn1, the largest subunit of the proteasome, is composed of 9 repeat segments, known as leucine rich repeats (LRR), which adopt horseshoe-shaped structures that are thought to be generally important for protein–protein interactions (Kobe and Kajava, 2001). The LRR portions of Rpn1 are thought to form a slightly open monomeric  $\alpha$ -solenoid (Effantin et al., 2009; Kajava, 2002). The first five contiguous repeat segments constitute LRR1, whereas the next four contiguous LRR repeats form LRR2. A 134-acidic amino acid stretch links LRR1 and LRR2 (Elsasser et al., 2002; Lupas et al., 1997). The minimal region sufficient for Rad23 binding to Rpn1 has been mapped to residues 417–628, which comprise LRR1 and an adjacent 21-residue acidic stretch on the C-terminal side. The UBL domains of Dsk2 and Ddi1 have also been shown to interact with the LRR domain of Rpn1 (Elsasser et al., 2002; Kaplun et al., 2005; Leggett et al., 2002; Saeki et al., 2002b; Seeger et al., 2003).

To gain a better understanding of how substrate delivery to the proteasome is controlled, we sought to identify an Rpn1 mutant that is defective in binding the UBA–UBL receptor proteins. We identified two mutations that disrupted binding of the UBA–UBL protein Ddi1 to the proteasome. Docking of Dsk2 to the proteasome was also moderately affected by these mutations in *rpn13 $\Delta$*  and *rpn10-uim rpn13-KKD* strain backgrounds. The delivery of ubiquitin conjugates to the proteasome is diminished in an *rpn1-D517A* single and even more so in an *rpn13 $\Delta$  rpn1-D517A* double mutant. Lastly, we show that an *rpn1-D517A* mutant stabilizes the Ddi1 substrate, Ufo1.

## Methods

### Yeast strains and growth conditions

Strains used in this study are listed in Supplemental Table 3.2. Listed strains are derivatives of the wild-type strain RJD 360 (W303 background). Standard yeast genetic techniques were used. Unless otherwise stated, strains were grown at 30°C and cultured on YPD.

### Plasmids

The *RPNI* locus including 200 bp upstream and downstream of the ORF was amplified by polymerase chain reaction (PCR) from purified *S. cerevisiae* genomic DNA using primers TG18 (5' GGGCGCCTCGAGGTTGACTATTTACAGCTCATC 3') and TG19 (5' GCGCCCGAGCTCAGCGCATCCATATTTACT 3'). The resulting PCR product containing flanking *XhoI* and *SacI* restriction sites was digested with these enzymes and ligated into pRS315 and pRS316 CEN/ARS vectors. Silent mutations introduced by site-directed mutagenesis with oligonucleotides TG12 (5' GTCATTTGTCAACGGGTTCTTAAACCTAGGTTATTGTAACGATAAATTAAT 3') and TG14 (5' GCAGATGAAGAAGAAACGGCCGAAGGACAGACTA 3') resulted in an *AvrII* restriction site at bp 1174 (amino acid 392) and an *EagI* site at bp 1920 (amino acid 640). Rpn1 mutations identified in the reverse two-hybrid screen or generated by the 'rational' approach were introduced into this construct by double digestion and ligation into the *AvrII* and *EagI* sites or by site mutagenesis. pEXP-Rpn1<sup>391-640</sup> was created by PCR amplification with primers TG1 (5' GGGGACA AGT TTG TAC AAA AAA GCA GGC TCTATGATGAACCTAGGTTATTGTAACGATAAA 3') and TG2 (5' GGG GAC CAC TTT GTA CAA GAA AGC TGG GTT TTCGGCCGTTTCTTCTTCATCTGCATC 3') and cloned using BP Gateway into pDONR-Express (Invitrogen) and LR-cloned into pDEST-AD. *RAD23*, *DSK2*, *DDI1*, *UBP6*, and *RPN2* were amplified by PCR and cloned into pDONR-Express and subsequently LR-cloned into pDEST-AD. All plasmids used in this study are listed in Supplemental Table 3.3.

### ***RPN1*<sup>391-640</sup> allele library construction**

*Rpn1* amino acids 391-640 were chosen as the target area to test for forward and reverse-yeast two-hybrid interactions. The pEXP-*Rpn1*<sup>391-642</sup> clone was used as a template for the allele library generation. Using attB primers TG4 (GGGGACA AGT TTG TAC AAA AAA GCA G) and TG5 (GGGGAC CAC TTT GTA CAA GAA AGCT), bp 1174–1926 were amplified by 25 cycles of PCR in 48 independent reactions, concentrated, and gel purified. Approximately 150 ng of gel-purified product was BP-cloned into pDONR-Express and transformed via electroporation into TOP10 Electro-comp cells (Invitrogen). Plasmid DNA was collected from bacterial clones containing functional pENTR-*Rpn1*<sup>391-642</sup> clones. A yield of 500,000 clones was desired for good library coverage and this number was exceeded. Approximately 250 ng of purified pENTR-*Rpn1* allele library DNA was LR-cloned into pDEST-DB and transformed via electroporation into *E. coli*. Again, over 500,000 colonies were pooled and the resulting pEXP-*Rpn1* allele library DNA was purified.

### **Forward and reverse-yeast two-hybrid screen**

The reverse yeast two hybrid assay was performed as described (Li et al., 2004). Briefly, pEXP-DB-*Rpn1* allele library was cotransformed with pEXP-AD-Rad23 or pEXP-AD-Dsk2 into the reporter strain *MaV203* using the lithium acetate procedure. The transformation reactions were plated onto SC-Leu-Trp + 0.2% 5FOA. Plates were grown for ~ 1 week, and putative 5FOA<sup>R</sup> colonies were picked and screened for reporter phenotypes. Interaction-defective alleles were tested for lack of activation of *GAL1-lacZ* and failure to grow on SC-*HIS*+3-amino-1,2,4-triazole (3-AT). Mild interaction-defective alleles showed some growth on 3-AT. pEXP-DB *Rpn1* allele library plasmids were either purified or amplified by PCR from yeasts colonies that displayed 5FOA<sup>R</sup> phenotypes and sequenced using primer 5'-GGC TTC AGT GGA GAC TGA TAT GCC TC-3'. Clones containing mutations were then retransformed into *MaV203* and retested for proper reporter phenotypes. Direct PCR amplification of their pEXP-DB-*Rpn1* insert was done as described (Li et al., 2004). Forward interactions were tested by assaying for growth on

50 mM or 100 mM 3AT and 0.1% or 0.2% 5FOA. The plates were scored between 24–72 hours.

### **Plasmid shuffling of *rpn1* alleles**

*RPNI* was replaced by *Kanmx6* (Longtine et al., 1998) by amplifying a cassette from pFA6a-KanMX6 using oligonucleotides TG20 (5' GGTCTACATAAGGTGCGATTTCGTATAAAATTTGGAAGACAATTGCAAGAAACG GATCCCCGGGTTAATTAA 3') and TG21 (5' GGTTTTGAATTTTTTCCTATTCTGGTTGATATTGCCCAAAGCTATTCAGTGAA TTCGAGCTCGTTTAAAC 3'). The PCR product was transformed into a diploid W303 strain (RJD381) creating strain RJD4166. This diploid strain was transformed with pRS316-RPN1 (RDB 2090), sporulated, and haploid segregants were selected for growth on G418 and SD-Ura. The resultant strain, RJD 4189, was used for plasmid shuffling. Plasmids were transformed into RJD 4189 and then transformants were selected for growth on 5FOA-containing media.

### **26S proteasome native gel analysis**

Native gels were prepared and run as described (Kleijnen et al., 2007). Briefly, 2 mL of 5X native buffer (450 mM Tris base, 450 mM boric acid, 25 mM MgCl<sub>2</sub>, 2.5 mM EDTA [pH 8]), 0.9 ml 40% acrylamide/Bis solution (37.5:1), 7 ml H<sub>2</sub>O, 10 μl 0.5 M ATP, 90 μl 10% APS, and 9 μl TEMED) were combined and allowed to set using the BioRad Mini-Protean Tetra gel system. About 90–300 μg of protein supplemented with xylene cyanol and glycerol, was loaded per lane. Either purified proteasomes or cell extracts were run on native gels. Extracts were prepared as described (Elsasser et al., 2005). Gels were run at 100 V for 3.5–4 hours with 1X native buffer supplemented with 1 mM ATP. The gels were then soaked in 25 mL of developing buffer (50 mM Tris pH 7.5, 5 mM MgCl<sub>2</sub>, 1 mM ATP) followed by a 15 minute incubation at 30°C in substrate solution (50 mM Tris pH 7.5, 5 mM MgCl<sub>2</sub>, 1 mM ATP, 20 μM SVC LLVY AMC, 0.02% SDS). Cleavage of the fluorogenic substrate was visualized by exposure to UV light using an alphascreen.

### **Native immunoprecipitation of proteasomes for probing associated UBA–UBL proteins**

Native immunoprecipitations were carried out as described (Verma et al., 2011). Briefly, yeast cultures were grown to an OD<sub>600</sub> between 1–2 in YPD and harvested by centrifugation. Pellets were washed in ice cold water and then flash-frozen in liquid nitrogen. Thawed pellets were resuspended in 1 mL of lysis buffer (composition described below) per 100 O.D. units. One milliliter of this lysate was mixed with an equivalent volume of glass beads and cells were disrupted by vortexing using the FastPrep-24 at a setting of 6.5 for 60 s, cooling on ice, and then repeating. Lysates were clarified by centrifugation at 14,000 rpm at 4°C for 15 min. Clarified supernatants were bound to anti-epitope beads for 1.5 hours at 4°C. The beads were washed 4 times with lysis buffer containing detergent (50 mM Tris, pH 7.5, 150 mM NaCl, 15% glycerol, 0.2% Triton X-100, 25 mM b-glycerophosphate, 25 mM NEM, 1X Protease Inhibitor tablet (minus EDTA), 0.5 mM AEBSF, 2 mM ATP, 5 mM MgCl<sub>2</sub>), and 2 times with buffer B (25 mM Tris pH 7.5, 10 mM MgCl<sub>2</sub>, 2 mM ATP). An equal bead volume of 2X SDS buffer was added prior to boiling for 3 mins. Samples were resolved on 10% or 12.5% SDS-PAGE gels, transferred to nitrocellulose and immunoblotted. Antibodies used in this study are listed in Supplemental Table 3.4.

### **Purification of 26S proteasomes for immunoblotting**

26S proteasomes were purified as described (Verma and Deshaies, 2005). Briefly, Pre1-Flag (20S subunit) or Rpn11-Flag tag containing strains were grown as large-scale cultures (2 L), and lysed by grinding with a mortar in pestle in the presence of liquid nitrogen. Lysates were thawed in buffer A (50 mM Tris pH 7.5, 150 mM NaCl, 10% glycerol, 5 mM MgCl<sub>2</sub>, 5 mM ATP), bound to anti-Flag resin (Sigma), washed three times with buffer A supplemented with 0.2% Triton X-100, then washed two times with buffer B (25 mM Tris pH 7.5, 10 mM MgCl<sub>2</sub>, 2 mM ATP) prior to elution with Flag Peptide (Sigma).

### Turnover of CPY\*HA and GST-Ufo1

For CPY\*HA turnover, pCPY\*HA/*URA3*-containing yeast strains were grown to an  $OD_{600} \sim 0.5$ , shifted to 37°C for one hour, and then treated with 100 µg/ml cycloheximide, at which point a chase was initiated. Turnover of galactose-inducible Ufo1 was carried out as described (Ivantsiv et al., 2006). Briefly, cells containing pEGH-Ufo1 (Open Biosystems) were grown overnight in SRaffinose-URA medium and diluted the next day to an  $OD_{600}$  0.2. At an  $OD_{600} \sim 1$ , 2% galactose was added. Induction was for 14 hours. Cells were filtered and washed in YP and then resuspended in YP containing 2% dextrose. Samples were taken at intervals post dextrose addition, centrifuged, and flash frozen. Protein was extracted using boiling SDS-PAGE sample buffer, resolved by SDS-PAGE, transferred to nitrocellulose and immunoblotted. Blots were quantified by LI-COR Odyssey with IR dye-linked secondary antibodies (Invitrogen).

### Growth assays

For plating assays strains were grown overnight in YPD or SRaffinose-URA and diluted to an  $OD_{600}$  of 0.3 in water. Serial five-fold dilutions were prepared in water and spotted onto either YPD or minimal plates supplemented with various additives as described in the text. Plates were incubated at 30°C for 2–3 days.

### SILAC analysis of purified proteasomes

*RPN11<sup>FLAG</sup>* yeast strains auxotrophic for lysine and arginine, were grown in either CSM with 2% dextrose containing 20 mg/L lysine and arginine or in “heavy” medium with 20 mg/L  $^{13}C_6^{15}N_2$ -lysine and  $^{13}C_6$ -arginine. Cells were grown to an  $OD_{600}$  of 2, harvested, and flash frozen before grinding in liquid nitrogen. Equivalent amounts of heavy and light cells were mixed 1:1 before proceeding with a proteasome affinity purification.

Proteasomes were eluted in 8 M urea. After purification, Lys-C (Wako Chemicals) was added for a 4-hour digestion, followed by an overnight tryptic digestion in 2 M urea. The tryptic peptides were desalted on a C18 macrotrap (Michrom Bioresources) and concentrated in a speedvac. Dried samples were resuspended and subject to StageTip-based strong anionic exchange (SAX) as previously described (Wisniewski et al., 2009). Samples were eluted, concentrated, and then acidified with 0.2% formic acid prior to

mass spectrometric analysis. All mass spectrometry experiments were performed on an EASY-nLC (Thermo Scientific) connected to a hybrid LTQ-Orbitrap Classic (Thermo Scientific) with a nanoelectrospray ion source (Thermo Scientific). Peptides were resolved using a 240-minute gradient from 4% to 25% acetonitrile in 0.2% formic acid at a flow rate of 350 nl per minute. The mass spectrometer was operated in data-dependent mode to automatically switch between full-scan MS and tandem MS acquisition. All settings were as previously described (Lee et al., 2010). Raw data files were analyzed by MaxQuant (v 1.0.13.13) (Cox and Mann, 2008) and searched against the *Saccharomyces* Genome Database. The search parameters included tryptic digestion, a maximum of two missed cleavages, fixed carboxyamidomethyl modifications of cysteine, variable oxidation modifications of methionine, variable protein N-terminus acetylations, and a variable Gly-Gly tag on lysine residues with a 1% FDR thresholds for both peptides and proteins. At least two peptides were required for protein identification and at least two different scanning events were required for protein quantification.

### ***In vitro* UBA–UBL proteasome binding assays**

GST proteins were purified using standard methods and dialyzed into 50 mM Tris pH 7.5, 50 mM NaCl, 1 mM DTT, 10% glycerol. For co-immunoprecipitation experiments with UBA–UBL proteins and purified 26S proteasomes, 1  $\mu$ M of GST or GST-fusion protein was mixed with 0.2 nM of 26S proteasome in the presence of IP buffer (50 mM Tris-HCl at pH 7.5, 150 mM NaCl, 1 mM EDTA, 1mM DTT, 0.2% triton X-100, 10% glycerol, 10 mM MgCl<sub>2</sub>, and 5 mM ATP). The reaction was incubated with rotation for 1 hour at 4°C, after which point 30  $\mu$ l of glutathione-sepharose beads were added to each reaction and reactions were incubated for another hour at 4°C. Beads were washed with 1 mL of IP buffer 3 times. Each sample was boiled in 2X SDS and loaded onto a 10% tris-glycine gel. Gels were both commassie stained and immunoblotted.

## Results

### **Rpn1<sup>391-642</sup> interacts with UBL domain proteins.**

To screen for mutations in Rpn1 that disrupt binding to UBA–UBL proteins, we engineered a reverse-yeast two-hybrid system that reports on association between a fragment of Rpn1 (amino acids 391–642), a fragment including regions previously shown to be necessary and sufficient for UBA–UBL binding, and four distinct UBL-containing proteins (Rad23, Dsk2, Ddi1, and the deubiquitinase Ubp6) known to interact with the proteasome (Elsasser et al., 2002; Leggett et al., 2002; Seeger et al., 2003; Stone et al., 2004; Verma et al., 2000). Productive binding between Rpn1<sup>391-642</sup> and UBL proteins was expected to drive expression of *HIS3* and *URA3*, resulting in growth on 3-aminotriazole (3-AT) and inability to grow on 5-fluororotic acid (5FOA)(Figure 3.1A). Growth assays revealed that Rpn1<sup>391-642</sup> was capable of binding to Rad23, Dsk2, Ddi1, and Ubp6 in yeast cells, whereas a Ddi1 fragment lacking its UBL domain, and Rpn2, a proteasomal subunit, were unable to bind Rpn1<sup>391-642</sup> (Figure 3.1B).

### **Identification of mutations in Rpn1<sup>391-642</sup> that block binding to UBL domain proteins**

Using growth on 5FOA as a positive selection for loss of interaction between Rpn1<sup>391-642</sup> and UBL proteins, we screened a PCR-mutagenized allele library containing over 500,000 individual clones coding for Rpn1<sup>391-642</sup> and selected for mutants that could no longer interact with Rad23 (964 colonies were isolated) or Dsk2 (322 colonies). We screened these 1,286 transformants for their ability to reproduce their 5FOA<sup>R</sup> phenotype. One hundred and ninety colonies that again tested 5FOA<sup>R</sup> were sequenced. Forty-two of the sequenced 5FOA<sup>R</sup> clones contained a mutation; single amino acid substitutions were identified in thirty-two clones, while silent mutations (4), and truncation or frameshift events (6) made up the remainder. Plasmids containing single Rpn1 mutations were then retransformed and assayed for their ability to reproduce the 5FOA<sup>R</sup> phenotype. Twelve amino acid substitutions in 11 different residues of Rpn1 were identified as testing positive after being retransformed into our RY2H system (Figures 3.1C and 3.1D). Given

that a structural model of the LRR region of Rpn1 exists (Kajava, 2002), we also generated a panel of 6 ‘rational’ mutations that perturb residues predicted to be on the outside surface of the LRR domain (Figure 3.1D). The relative positions of the mutations discovered in the ‘reverse-yeast two-hybrid’ screen and the rational mutations are shown on the model structure of the Rpn1 LRR domain (Figure 3.1E).

### **Mutant *rpn1* alleles display synthetic growth defects in combination with ubiquitin receptor mutants.**

To evaluate whether any of the mutations in our panel of 18 substitutions had an effect on proteasome function, we reconstructed them into full-length *RPNI* and performed a ‘plasmid shuffle’ to replace the essential *RPNI* gene with each of our mutant alleles. A yeast *rpn1Δ* strain sustained by wild-type *RPNI* on a *URA3* plasmid was individually transformed with a *LEU2* plasmid bearing each mutant *rpn1* allele and the cells were plated on 5FOA to identify clones from which the *URA3* plasmid was evicted. We recovered 5FOA-resistant colonies from all transformants with the exception of *rpn1*<sup>F534S</sup>, indicating that 17 of our alleles retained at least partial *RPNI* function. To evaluate the impact of our Rpn1 mutations on proteasome function, we plated cells on medium supplemented with the proline analog 1-azetidine-2-carboxylic acid (AZC). Cells with defective proteasome function are sensitive to AZC (Fowden and Richmond, 1963; Saeki et al., 2009), presumably because its incorporation into proteins causes misfolding, thereby placing an elevated demand on cellular quality-control pathways. As shown in Figure 3.2A (and more RY2H-derived alleles are shown in Figure 3.S1A), none of our mutants was hyper-sensitive to AZC.

Multiple receptors dock ubiquitinated substrates to the proteasome, including not only the UBL domain proteins but also Rpn10 and Rpn13 (Husnjak et al., 2008; Verma et al., 2004). Unlike the other subunits of the proteasome, Rpn10 and Rpn13 are not essential. Therefore, we sought to test whether mutations in these receptors might sensitize cells to our *rpn1* alleles. Deletion of *RPNI3* by itself did not cause sensitivity to AZC (compare top rows of Figures 3.2A and 3.2B). However, a subset of our *rpn1* mutants (both rational and RY2H-derived) exhibited striking sensitivity to AZC when

combined with *rpn13Δ* (Figure 3.2B and Figure 3.S1B). To test whether this synthetic defect was due to the role of Rpn13 as an Ub receptor, the five *rpn1* mutants showing the most striking phenotypes were introduced by plasmid shuffle into an *rpn13-KKD* strain that contains a triple-point mutation that inactivates the ubiquitin binding domain (Husnjak et al., 2008). Four of the five tested *rpn1* alleles showed a similar synthetic growth defect in the *rpn13-KKD* mutant background (Figure 3.2C). These data indicate that our Rpn1 mutant proteins sensitized cells to loss of an intrinsic proteasome ubiquitin receptor.

Given the synthetic effects seen with *RPN13* alleles, we sought to test whether our *rpn1* mutants exhibited genetic interaction with *RPN10*. Rpn10 contains two domains—a VWA domain that appears to play a structural role and an ubiquitin-binding UIM domain. We used plasmid shuffle to introduce *rpn1* alleles into a mutant, *rpn10-uim*, in which the UIM domain is inactivated by a cluster of point mutations (Elsasser et al., 2004; Fu et al., 1998). Whereas neither the individual *rpn1* mutants (Figure 3.2A) nor *rpn10-uim* (Figure 3.2D) was hypersensitive to AZC, the double mutants exhibited striking sensitivity (Figure 3.2D). Similarly, we also found that most of our *rpn1* mutants in a *rpn13-KKD rpn10-uim* double mutant background were slightly more sensitive than the *rpn13-KKD rpn10-uim* strain (Figure 3.2E).

As a test for specificity, we introduced the same set of *rpn1* mutations into an *rpn4Δ* background. Rpn4 is a transcription factor that promotes proteasome gene expression, and *rpn4Δ* mutants have reduced proteasome levels and show synthetic phenotypes with a number of mutations that impinge on proteasome function (Ju et al., 2004; Xie and Varshavsky, 2001). In contrast to the results seen with *rpn13Δ*, *rpn13-KKD*, and *rpn10-uim*, none of the five *rpn1* mutants tested exhibited a synthetic AZC-sensitive phenotype when combined with *rpn4Δ* (Figure 3.2F). Taken together, these data suggest that the *rpn1* mutant alleles impinge specifically on compromised receptor function, and do not cause general proteasome impairment.

**Recruitment of Ddi1, Dsk2, and ubiquitin conjugates to proteasomes is compromised in *rpn1-D517A* and *rpn1-K484A* mutants.**

We next aimed to determine if any of the *rpn1* mutations that showed genetic interactions with *rpn10-uim* and *rpn13-KKD* led to defects in recruitment of UBL-containing proteins to the proteasome. To address this question, we first tagged *RPN11* with sequences encoding the Flag epitope in a selection of *rpn13Δ rpn1* mutants. We included *rpn13Δ* in this analysis due to potential redundancy between Rpn13 and Rpn1 for binding UBL domains. Proteasomes were immunoprecipitated from these strains and immunoblotted for the presence of UBL proteins. All double mutant proteasomes that were analyzed contained equivalent levels of associated Rad23, Dsk2, and Rpn10, except for *rpn1-D517A* and *rpn1-K484A*, both of which exhibited reduced levels of bound Dsk2 (Figure 3.3A). None of our *rpn1* single mutants by themselves or in the *rpn10-uim* background showed reduced levels of Dsk2 (see, for example, the *rpn1-D517A* mutant in Figure 3.S2A and 3.S2B; additional data not shown). To see if we could identify additional binding-defective *rpn1* mutations, we generated an additional set of ‘rational’ *rpn1* alleles and tested them by using plasmid shuffle to introduce the alleles into an *RPN11<sup>FLAG</sup> rpn1Δ rpn13Δ* background, followed by immunoprecipitation of the proteasomes and immunoblotting for UBL proteins. None of these mutants, which are listed in Table 3.S1, exhibited a greater UBL binding defect than the D517A or K484A alleles and so they were not pursued further.

Based on the proteasome association studies, we focused our attention on the K484A and D517A mutants. To evaluate the association of UBL proteins in greater depth, we retrieved proteasomes from both mutants (in an *rpn13Δ* background) and immunoblotted the immunoprecipitates to determine their content of Rad23, Dsk2, Ddi1, Ubp6, and total ubiquitin conjugates. The immunoblots are shown in the left panels of Figure 3.3B and densitometric quantification of the results is presented in the right panel. Proteasomes from both *rpn1 rpn13Δ* mutants contain normal or near-normal levels of the UBL proteins Ubp6 and Rad23. In this experiment the levels of Dsk2 were higher than those observed in Figure 3.3A, possibly because the immunoprecipitation was done under less stringent conditions. Interestingly, proteasomes recovered from *rpn13Δ rpn1-D517A*

cells contained reduced levels of Ddi1 and total ubiquitin conjugates compared to proteasomes retrieved from either wild-type or *rpn13Δ rpn1-K484A* cells. Similar results were obtained with proteasomes from *rpn1-D517A* and *rpn10-uim rpn1-D517A* cells (Figure 3.S2A and 3.S2B). These results indicate that mutation of the D517 residue of Rpn1 by itself was sufficient to destabilize Ddi1 docking, and, in combination with loss of Rpn13, modestly destabilized Dsk2 binding.

We were intrigued by the mild defect in recruitment we observed for Dsk2 in *rpn13Δrpn1-D517A* proteasomes and questioned if proteasomes retrieved from strains containing mutations in both intrinsic Ub receptors and containing the *rpn1-D517A* mutation might yield a stronger defect in recruitment of Dsk2 since interaction of the UBL proteins has been observed with Rpn10 and Rpn13 (Matiuhin et al., 2008b; Zhang et al., 2009). We retrieved proteasomes from both a double *rpn10-uim rpn13-KKD* and a triple *rpn10-uim rpn13-KKD rpn1-D517A* mutant and immunoblotted the immunoprecipitates to determine their content of Dsk2 and Ddi1. As expected, the *rpn10-uim rpn13-KKD rpn1-D517A* immunoprecipitated fewer Ub conjugates in comparison to an isogenic strain containing wild-type Rpn1 (Figure 3.S2C). Additionally, we quantified the change in the binding of Ddi1 and Dsk2 and again observed a defect in the recruitment of Ddi1 and Dsk2 in the presence of the Rpn1-D517A mutation (Figure 3.S2C, right panel). This led us to investigate the effect of the Rpn1-D517A mutation in greater detail.

To determine whether Rpn1-D517A proteasomes were generally defective, we characterized them biochemically and found them to be completely normal by multiple methods. Purified Rpn1-D517A proteasomes exhibited a normal subunit composition when evaluated by SDS-PAGE (Figure 3.3C, left panel). Moreover, native nondenaturing gel electrophoresis verified that these proteasomes (Figure 3.3C, right panel) and those of all of the other strains indicated in Figure 3.1D (data not shown) were properly assembled and had normal chymotryptic activity. In fact, although we were manipulating the largest scaffolding subunit of the proteasome, only a small number of the mutations we studied had any negative consequences on proteasome stability (Figure 3.1D and 3.S3). To characterize in detail the impact of the Rpn1-D517A mutation on proteasome composition, we performed a quantitative mass spectrometry technique, SILAC (stable

isotope labeling with amino acid in cell culture). For this experiment, *rpn13Δ* cells were grown in medium supplemented with heavy isotopes of lysine and arginine while *rpn13Δ rpn1-D517A* cells were grown in medium with 'light' lysine and arginine. The two cultures were mixed immediately prior to lysis and proteasomes were purified by affinity chromatography on an anti-Flag resin. The purified sample was then analyzed by multidimensional mass spectrometry and the heavy/light ratios for peptides derived from proteasome subunits were determined (Figure 3.3D). This sensitive analysis confirmed that *rpn1-D517A* does not cause any apparent physical change in the proteasome.

While we did measure a slightly reduced level of Rad23 in *rpn13Δ rpn1-D517A* proteasomes by immunoblotting, our SILAC data indicated that the levels of Rad23 and Ubp6 were largely unaffected in *rpn13Δ rpn1-D517A* proteasomes, as they had heavy-to-light (H/L) ratios of 0.9 and 0.98, respectively. This is not unexpected, since it was reported in a prior SILAC study that the free and proteasome-bound pools of human Rad23 rapidly equilibrate in cell lysate (Wang and Huang, 2008). Unfortunately, Ddi1 and Dsk2 peptides were not seen in our SILAC experiment. Capturing the association of all three UBA–UBL receptor proteins with proteasomes in native preparations is challenging, likely because these proteins interact very dynamically with the proteasome (Wang and Huang, 2008). For instance, the association of Dsk2 with the proteasome has been reported to be difficult to capture (Matiuhin et al., 2008a). Additionally, only one published mass spectrometry study has been able to simultaneously capture Rad23, Dsk2, and Ddi1 with the proteasome, and that study relied on chemical cross-linking to stabilize the association of dynamically-bound proteasome interactors (Guerrero et al., 2008).

### ***In vitro* confirmation of a Ddi1 binding defect of Rpn13-deficient Rpn1-D517A mutant proteasomes**

Due to the challenge in capturing all of the UBL-containing proteins at the proteasome in one experiment, we sought to perform an *in vitro* binding assay that would confirm our analysis of proteasomes purified from mutant cells. Proteasomes were affinity purified from cells expressing Flag-tagged Rpn11 and incubated with recombinant GST–UBA–UBL proteins. Proteasomes affinity purified from *rpn13Δ* cells were successfully pulled-

down by all three baits. However, Rpn13-deficient Rpn1-V447H K484A D517A (VKD) proteasomes exhibited strongly diminished binding capacity for Ddi1 (Figure 3.4). It should be noted that Rpn13-deficient Rpn1-V447H K484A D517A proteasome mutants behaved just as Rpn13-deficient Rpn1-D517A mutant proteasomes in native immunoprecipitation experiments (Table 3.S1 and data not shown). However, it was surprising that we did not see a loss of Dsk2 interaction with proteasomes isolated from an *rpn13Δrpn1-VKD* strain as we did in our native immunoprecipitations (Table 3.S1). Our native immunoprecipitation experiments may be more demanding than our *in vitro* binding assay. For instance, the binding of mutant *rpn1* proteasomes to Dsk2 may have been driven by the high level of bait used in this experiment.

### ***rpn1-D517A* mutants exhibit a selective defect in protein degradation.**

It is thought that UBA–UBL proteins exhibit some degree of selectivity in targeting specific substrates to the proteasome (Verma et al., 2004). We hypothesized that the decrease of Ddi1 binding to proteasomes in an *rpn1-D517A* mutant might therefore result in turnover defects of substrates that are particularly reliant on Ddi1. In agreement with the normal binding of Rad23 and Dsk2 to the proteasome in an *rpn1-D517A* single mutant, no defect was seen in turnover of the Rad23/Dsk2-dependent substrate, CPY\* (Figure 3.5A, and a replicate experiment is shown in Figure 3.S4B) (Medicherla et al., 2004), nor the Dsk2 substrate Kre22 (Figure 3.S4A) (Chang et al.). However, when we tested the Ddi1-dependent substrate, Ufo1 (Ivantsiv et al., 2006), we saw nearly complete stabilization in comparison to a wild-type strain (Figure 3.5B). Note that the steady-state levels here for the *rpn1-D517A* are higher than for the *ddi1Δ* mutant. In two of three replicate experiments, this higher level of expression was seen. We do not know if there is any physiological relevance to the higher level of expression or if this is simply due to the stochastic expression due to using plasmids for expression. A replicate of this experiment is also shown (Figure 3.S4C). In agreement with the turnover data, we observed that over-expression of Ufo1 was toxic to *ddi1Δ* and *rpn1-D517A* cells but not to wild-type cells (Figure 5C). This effect was exquisitely specific—neither *rpn13Δ* (Figure 3.5C) nor any other mutation in *rpn1* that we tested (Figure 3.5D) conferred sensitivity to over-expression of Ufo1.

## Discussion

Of the three UBA–UBL shuttle receptors linked to the proteasome, Ddi1 is the least studied and perhaps the most controversial. Prior data have established that Ddi1 binds polyubiquitin, albeit with lower affinity than Rad23 and Dsk2 (Bertolaet et al., 2001b; Fu et al., 2010; Kang et al., 2006; Saeki et al., 2002a). However, while some studies report a physical interaction of Ddi1 with Rpn1 or the intact proteasome (Kaplan et al., 2005; Saeki et al., 2002a), there are a few reports that question the capacity for Ddi1 to bind the proteasome or Rpn1 (Chandra et al., 2010; Fu et al., 2010; Kim et al., 2004). The disparity in these reports may be due to the qualitative nature of immunoprecipitation experiments and the rapid dynamics of UBL binding to and dissociation from the proteasome (Wang and Huang, 2008). Ddi1 has the most divergent UBL domain among the known UBA–UBL proteins, and hence, may have the weakest affinity interaction with the proteasome (Kim et al., 2004). We have shown that Ddi1 is recovered with proteasomes immunoprecipitated from yeast cells, binds Rpn1 in a yeast two-hybrid assay, and binds to the proteasome in an *in vitro* pull-down assay. We have further validated these results by identifying an Rpn1 mutation that is selectively defective in binding Ddi1 and stabilizes the Ddi1-dependent proteasome substrate Ufo1. Hence, we conclude that Ddi1 does indeed interact with the proteasome in a specific and functionally-relevant manner. If Ddi1 binds the proteasome more weakly than other UBA–UBL proteins, which seems likely, it would explain why the D517A and K484A mutations reported here selectively disrupt interaction of Ddi1 with the proteasome.

Our study highlights the layered complexity of the interaction of shuttle proteins with the proteasome. With a single alanine substitution in the highly conserved D517 residue of Rpn1 we were able to significantly reduce the binding of Ddi1 to the proteasome. However, the interaction of other UBA–UBL proteins with the proteasome appears to be more complex. Recovery of Dsk2 with proteasomes was only mildly diminished in an *rpn1-D517A* mutant that also lacked *RPN13* or the ubiquitin interaction motifs of both *RPN10* and *RPN13*. Meanwhile, recovery of Rad23 was not affected appreciably by any mutation in Rpn1 analyzed during the course of this work. There are

two possible explanations of these results. On the one hand, it is possible that the UBL domains of these proteins have a gradient of affinity for Rpn1, with Ddi1 being the weakest binder and Rad23 the strongest. In this scenario, Rpn1-D517A may be a hypomorph that only modestly perturbs the UBL docking site, such that only the weakest binder (Ddi1) is excluded. We attempted to test this hypothesis by making numerous combinatorial mutations, (including a V447H K484A D517A triple mutant), none of which exhibited a substantially greater UBL binding defect than the D517A or K484A alleles (Supplemental Table 3.1). Thus, we do not favor the hypothesis that it is possible to disrupt recruitment of Rad23 and Dsk2 by mutating a single binding patch on Rpn1.

On the other hand, our model for UBL docking to the proteasome suggests that it is possible that Ddi1 uses only a single mechanism to bind the proteasome (direct binding to the LRR1 domain of Rpn1), whereas, in line with published reports (Matiuhin et al., 2008b; Zhang et al., 2009), Rad23 and Dsk2 may use multiple mechanisms and thus are more resistant to mutation. Additionally, it does not appear that the the K484 or D517 residues of Rpn1 have any bearing on Rad23 nor Ubp6 association with the proteasome; the binding mode for these UBL proteins may be completely distinct (Figure 3.6). Our observation that reduction of Dsk2 binding was only seen in an *rpn1-D517A rpn13Δ* double mutant and more strikingly in a *rpn1-D517A rpn13Δ rpn10-uim* supports the idea that Dsk2 may be tethered to the proteasome by either Rpn1, Rpn13, or Rpn10 (Figure 3.6). The failure to see a significant reduction in binding of Rad23 in any single or double mutant may be due to there being multiple independent docking sites for Rad23 on the proteasome, although it should be noted that all of these docking sites appear to rely on the UBL domain (Fatimababy et al., 2010; Kaplun et al., 2005; Verma et al., 2004; Wilkinson et al., 2001). Other studies have shown that Ubp6 may bind proteasome lid proteins while Rad23 may also bind Rpt6 (Fatimababy et al., 2010; Leggett et al., 2002), and that even Ub chains bound to Rad23 may contribute to its proteasome binding (Ghaboosi and Deshaies, 2007). Biochemical data suggest that human Rad23 is recruited to the proteasome by the UIM domain of Rpn10 (Hiyama et al., 1999; Walters et al., 2002), and that even yeast Rad23 can bind Rpn10 (Zhang et al., 2009), but it should be noted that this hypothesis had not been tested by genetic manipulation of Rpn10 in cells. Thus, the data we present here is the strongest evidence indicating that the intrinsic

receptors play a role in recruitment of Rad23 and Dsk2 to the proteasome. Clearly, more work is needed to unravel the mechanisms underlying recruitment of Rad23 and Dsk2 and the deubiquitinase, Ubp6, to the proteasome.

## **Conclusions**

The current study identifies residues in the LRR1 domain of Rpn1 that contribute to shuttle receptor docking. We validate Ddi1 as a proteasomal shuttle receptor whose stable binding to the proteasome depends on Rpn1 residue D517. Consistent with this, D517 is also important for the degradation of a Ddi1-dependent substrate. We also show that in the absence of Rpn13, or the dual absence of the ubiquitin binding domains of Rpn13 and Rpn10, mutation at the D517 and K484 residues reduces the association of Dsk2 with the proteasome.

## List of abbreviations

3-AT (3-Amino-1,2,4-triazole), 5FOA (5-fluororotic acid), AZC (Azetidine-2-carboxylic Acid), Ub (ubiquitin), UBA (ubiquitin association domain), UBL (ubiquitin-like domain), UIM (ubiquitin interaction domain), RY2H (reverse-yeast two-hybrid)

## Authors' contributions

R.J.D. and T.A.G designed and interpreted all of the experiments and wrote the paper. T.A.G also carried out all of the experiments. N.K performed the mass spectrometry. M.J.S analyzed the mass spectrometry data. M.G designed and performed the first repetition of the experiment in Figure 3.4.

## Acknowledgements

For reagents, we thank M. Vidal, H. Rao, D. Finley, W. Tansey, H. Yokosawa, M. Funakoshi, H. Fu, R. Baker, D. Raveh, J. Gerst, C. Gordon, M. Glickman, K. Tanaka, and K. Madura. We thank the Caltech Proteome Exploration Laboratory for mass spectrometry expertise. We are grateful to Caitlin Rugani and Derek Tu for technical assistance. We thank all members of the Deshaies lab, especially K.J. Chang, G. Kleiger, J.E. Lee, and R. Verma for valuable comments and reagents. T.A.G. was supported with funding from the Gordon Ross Medical Foundation and an NSF pre-doctoral fellowship. R.J.D. is an investigator of the HHMI, which supported this study.

## Figure legends

### Figure 3.1. A two-pronged strategy identifies 18 Rpn1 residues that may be important for binding UBL domain proteins.

(A) The utilized yeast two hybrid system allows for both positive (growth on -HIS, -URA, +3-AT) and negative counter selection (growth on 5FOA) of UBL– Rpn1<sup>391-642</sup> interaction. (B) Rpn1<sup>391-642</sup> was sufficient for binding UBA–UBL proteins in a yeast two-hybrid system. Yeast cells were co-transformed with plasmids expressing Gal4-DBD fused to Rpn1<sup>391-642</sup> (Rpn1<sup>391-642</sup>DB) and Gal4-AD fused to either Rad23, Dsk2, Ddi1, Upb6, Ddi1ΔUBL, or Rpn2. Protein-protein interaction is indicated by growth on 100 mM 3-AT and lack of growth on 0.2% 5FOA. (C) Representative *rpn1* alleles found in the RY2H screen did not interact with Rad23 in the context of an Y2H experiment. (D) Sequence and secondary structure prediction alignments of yeast Rpn1 with mouse Rpn1 were made with MultiAlin (<http://multalin.toulouse.inra.fr/multalin/multalin.html>) using the model structure of Rpn1 (Kajava, 2002). Identical residues (black) and similar residues (gray) are indicated. Mutations identified in the RY2H that disrupt the interaction of Rpn1<sup>391-642</sup> with Rad23 and Dsk2 are indicated in red and rationally designed mutations are indicated in blue. Mutant *rpn1* alleles were plasmid shuffled into an *rpn1Δ* yeast strain and assayed for viability and proper 26S assembly. The positions of the identified mutations are indicated in the figure. A (-) indicates that assembly and viability were like wild type, a (+) indicates that we observed defects in proteasome stability (Figure 3.S3), and (nd) indicates the strain was inviable. (E) The relative position of residues of interest from the RY2H screen and the rational sites chosen in (D) are shown on a model structure of Rpn1. Residue A418 is not included in the model. The colors represent the residues indicated in the key.

### Figure 3.2. Mutant *rpn1* alleles display genetic interactions with mutations in genes that encode ubiquitin receptors intrinsic to the proteasome.

Five-fold serial dilutions of cells were plated onto the indicated media. The *rpn1* mutants (*rpn1\**) were plasmid shuffled into an *rpn1Δ* strain containing (from top to bottom) either no additional mutations or *rpn13Δ* (B), *rpn13-KKD* (C), *rpn10-uim* (D), *rpn13-KKD*

*rpn10-uim* (E), or *rpn4Δ* (F). AZC refers to 5 mM of the proline analog 1-azetidine-2-carboxylic acid (AZC).

**Figure 3.3. Recruitment of Ddi1, Dsk2, and Ub conjugates to the proteasome is compromised in *rpn1-D517A* and *rpn1-K484A* mutants.**

(A) Affinity-purified *rpn13Δ rpn1-K484A* and *rpn13Δ rpn1-D517A* proteasomes contain reduced levels of Dsk2. Detergent was present during the binding step of the immunoprecipitation as described in the Methods section. (B) Affinity-purified *rpn13Δ rpn1-D517A* proteasomes contain reduced levels of Ddi1 and Ub conjugates. Levels of UBA–UBL proteins, the lid subunit Rpn12, and polyubiquitin are shown for affinity purified proteasomes (IP) and in the whole cell extract input (WCE). The purification shown here was performed in the absence of detergent. Densitometric quantification of the blot is shown (right panel). The amount of UBL protein was normalized to Rpn11<sup>FLAG</sup> and wild-type levels were set at 100%. (C) Proteasomes isolated from *rpn1-D517A* are intact. SDS-PAGE and native gel analysis of affinity purified 26S proteasomes from Rpn11-Flag tagged strains. The native gel was incubated with Suc-LLVY-AMC in the presence of ATP and 0.05% SDS to visualize RP and CP activity. The isoforms of the 26S proteasome are indicated. (D) Quantitative SILAC isotopic ratios are shown for all subunits of the proteasome isolated from an *rpn13Δ* strain (labeled with heavy isotopes; “H”) in comparison to proteasomes isolated from an *rpn13Δ rpn1-D517A* strain (labeled with light isotopes; “L”).

**Figure 3.4. Rpn1-D517A reduces binding of Ddi1 *in vitro*.**

GST-fused Rad23, Dsk2, Ddi1, and GST alone (as a negative control) were incubated with either proteasomes affinity purified from *rpn13Δ* or *rpn13Δ rpn1-V447H K484A D517A* (VKD) cells. The binding reactions were immobilized on glutathione resin, which was then washed and extracted with SDS-PAGE sample buffer. An Rpt5 immunoblot (upper panel) and a commassie stain to confirm equivalent recovery of the GST fusion proteins (middle panel) is shown. Inputs were immunoblotted with anti-Rpt5 and are also shown (lower panel).

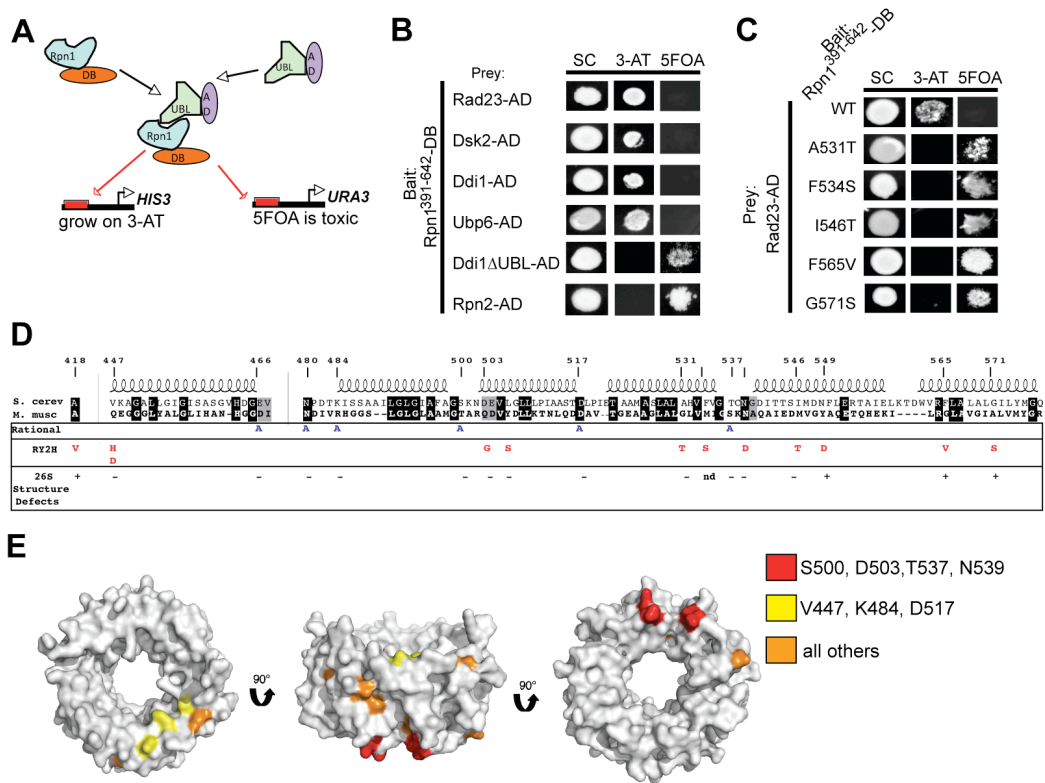
**Figure 3.5. *rpn1-D517A* mutants exhibit a selective defect in protein degradation.**

(A) Mutant *rpn1-D517A* cells degrade the Ufd1/Rad23/Dsk2 substrate CPY\* with normal kinetics in a cycloheximide chase. Equal loading of extracts was confirmed by blotting with an anti-tubulin antibody (lower panel). The quantification of these blots is shown. (B) Ufo1 is stabilized in *rpn1-D517A* and *ddi1Δ* mutants. Wild-type and mutant cells carrying a plasmid that expressed GST-Ufo1 from the GAL1 promoter were grown in raffinose medium and then induced with 2% galactose for 14 h. Dextrose was added at T<sub>0</sub> to extinguish expression and samples were taken at the indicated time points. Quantification is shown. (C) *rpn1-D517A* and *ddi1Δ* do not tolerate over expression of Ufo1. The indicated strains containing a plasmid that expresses GST-Ufo1 under the control of a galactose-inducible promoter were grown on medium containing either glucose (SD, expression OFF) or galactose (SGalactose, expression ON). After 2–3 days, the plates were scored for growth. (D) Sensitivity of *rpn1-D517A* to GST-Ufo1 over-expression is specific and was not shown by other *rpn1* alleles.

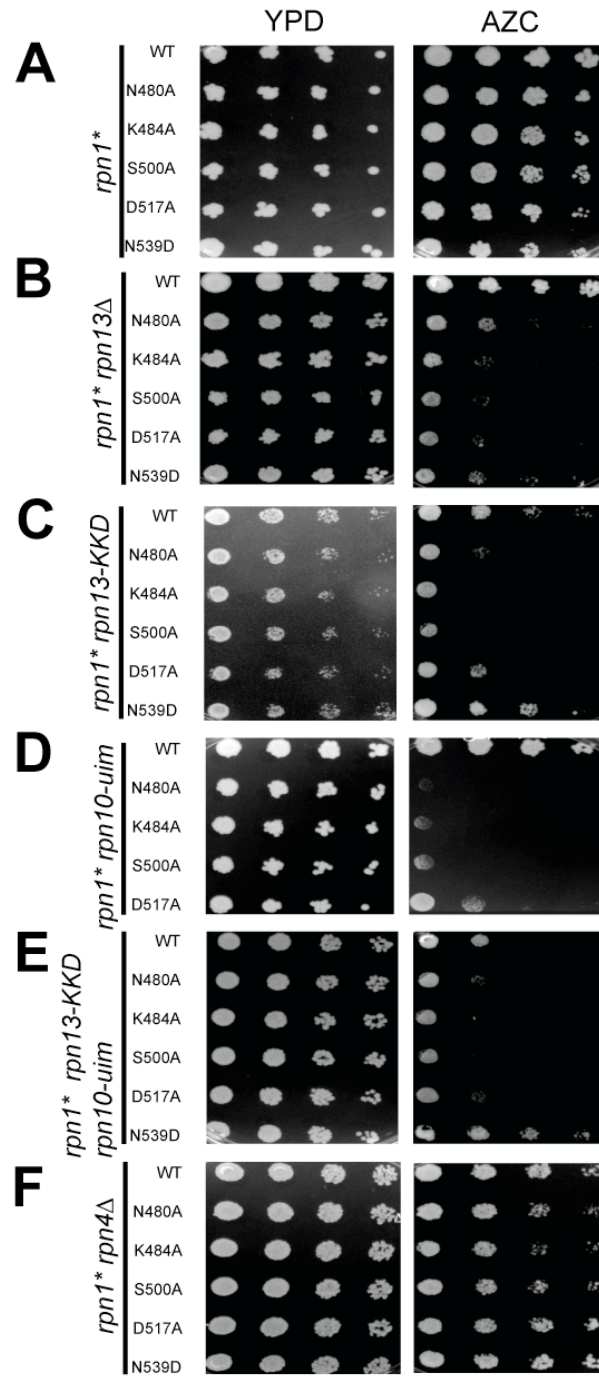
**Figure 3.6. Model for UBL protein interfacing with the proteasome**

Ddi1 shows a large dependence on the D517 residue of Rpn1 for binding with the proteasome. Additionally, deleting the intrinsic receptor Rpn13, or jointly the ubiquitin binding domains of Rpn13 and Rpn10, results in decreased binding of Dsk2 to the proteasome and reveals a role for the Rpn1-K484 residue in binding UBL proteins. However, Rad23 and the deubiquitinase Ubp6 did not show a dependence on residues D517 nor K484 of Rpn1. It is possible that Rad23 and Ubp6 interaction with the proteasome is stabilized by their interactions with other proteasomal subunits and/or other unidentified residues on Rpn1.

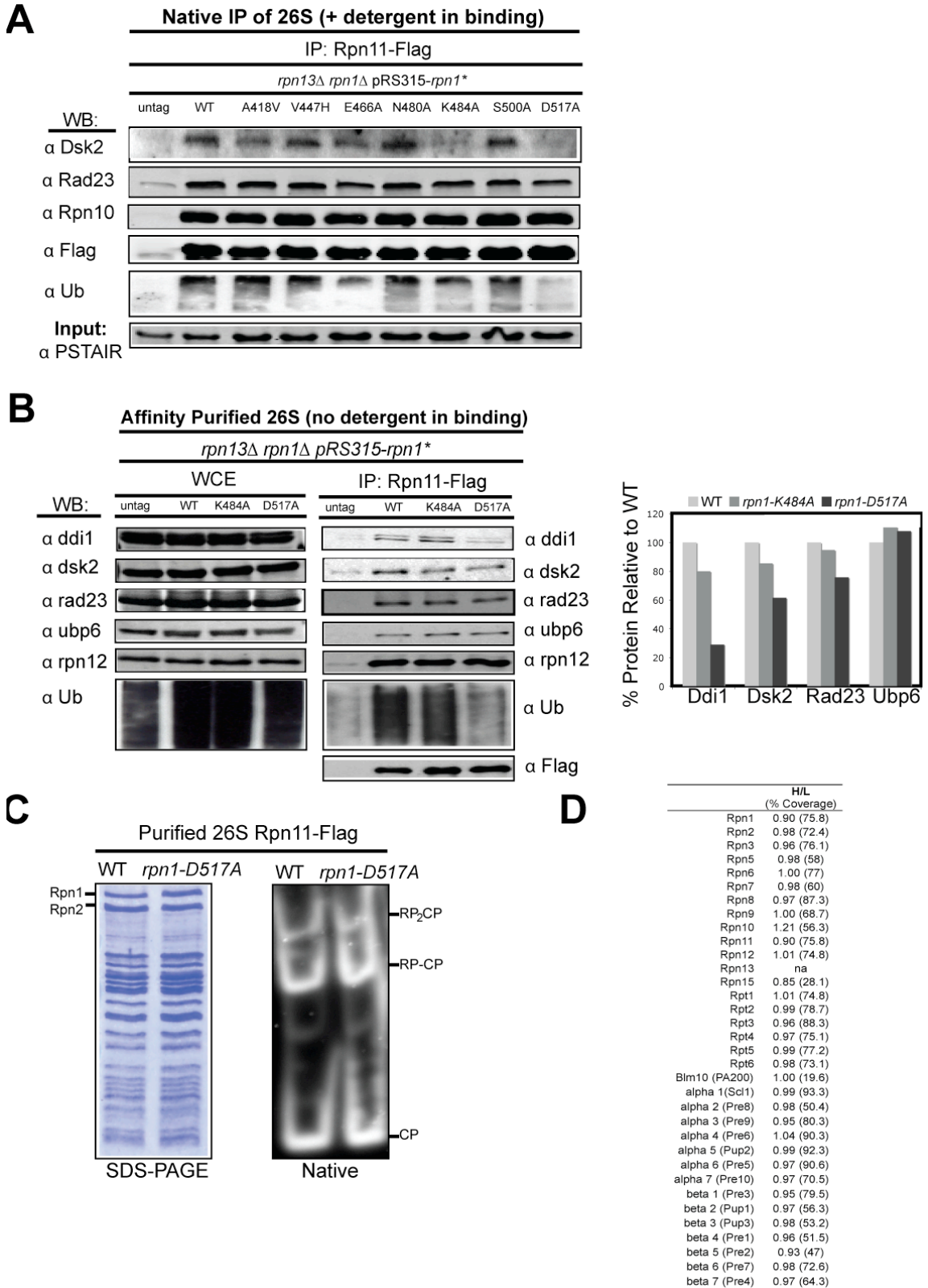
**Figure 3.1. A two-pronged strategy identifies 18 Rpn1 residues that may be important for binding UBL domain proteins.**

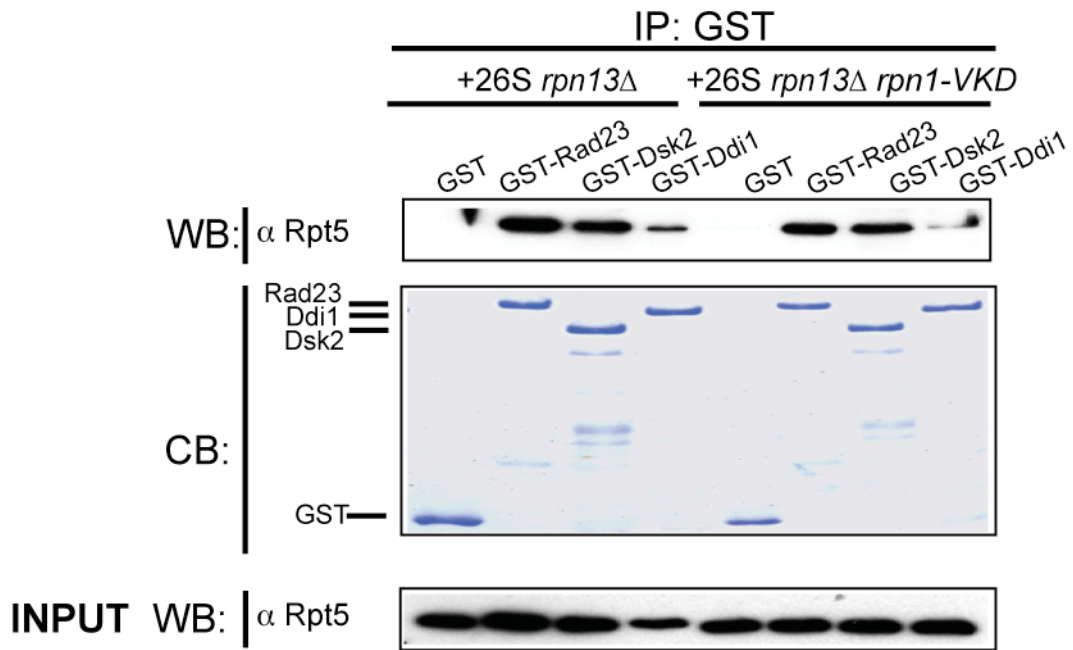


**Figure 3.2. Mutant *rpn1* alleles display genetic interactions with mutations in genes that encode ubiquitin receptors intrinsic to the proteasome.**



**Figure 3.3. Recruitment of Ddi1, Dsk2, and Ub conjugates to the proteasome is compromised in *rpn1-D517A* and *rpn1-K484A* mutants.**



**Figure 3.4. Rpn1-D517A reduces binding of Ddi1 *in vitro*.**

**Figure 3.5. *rpn1-D517A* mutants exhibit a selective defect in protein degradation.**

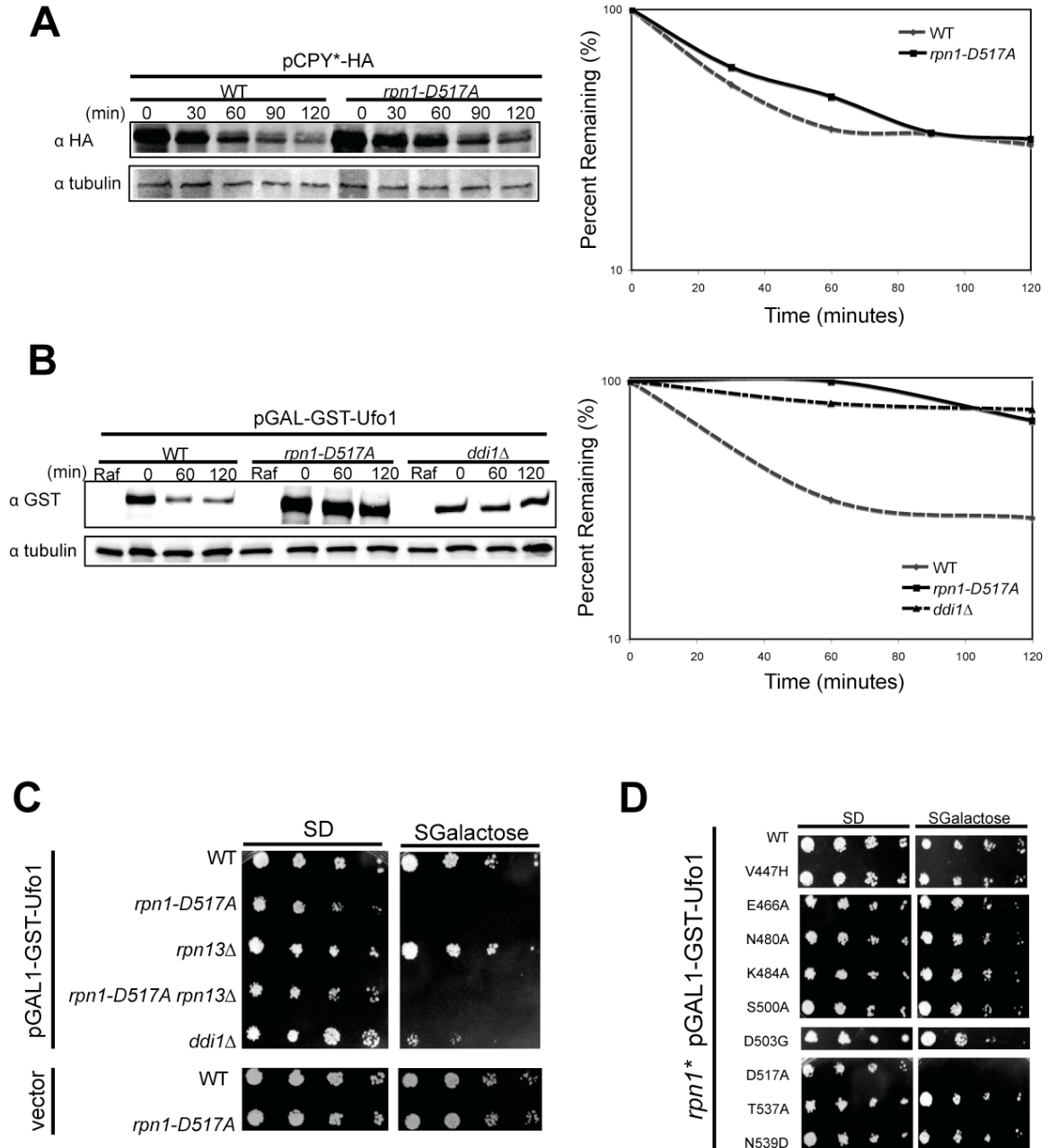
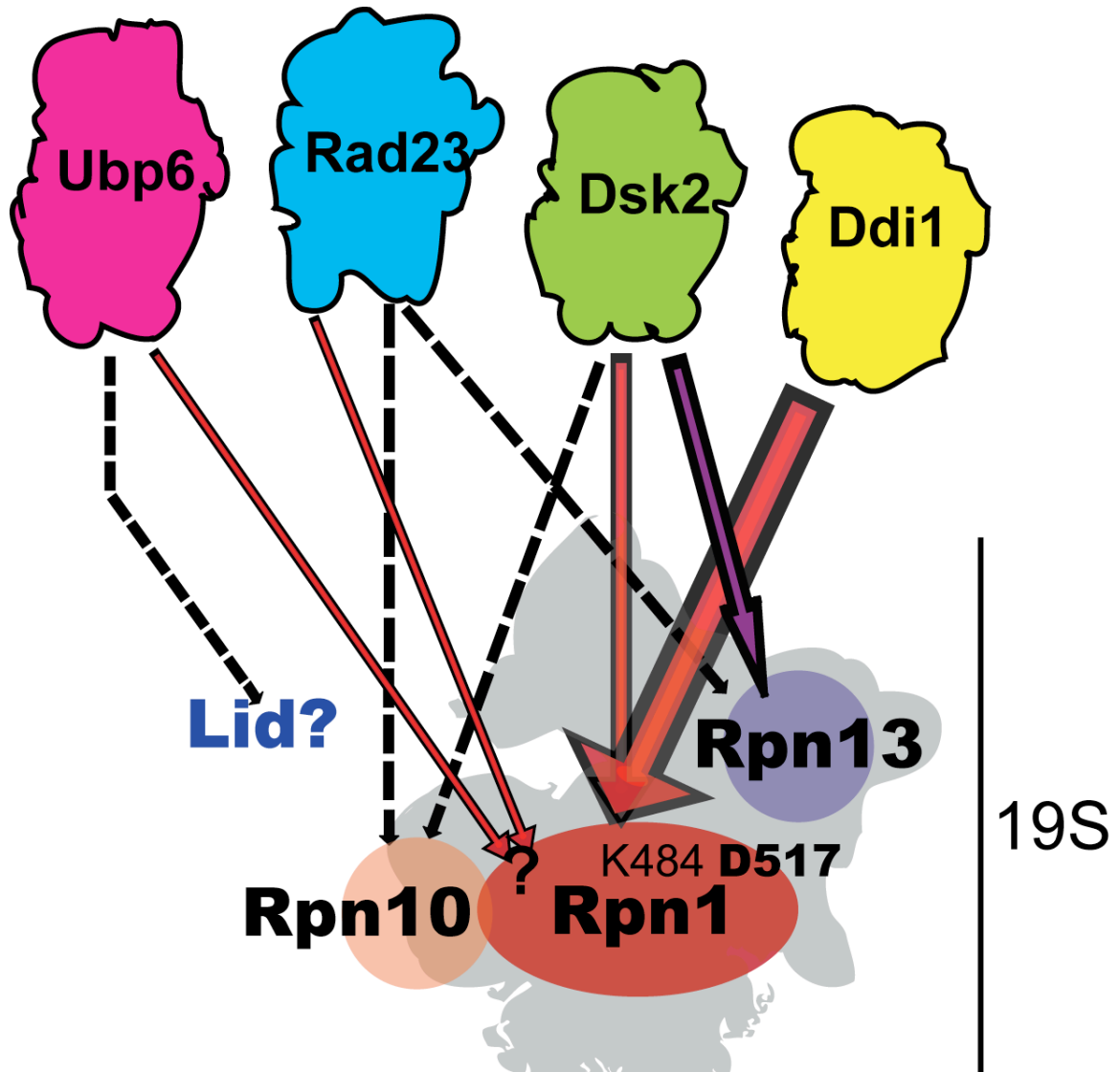


Figure 3.6. Model for UBL protein interfacing with the proteasome



## Supplementary data

**Supplemental Table 3.1. Additional rational Rpn1 mutants used in this study**

**Supplemental Table 3.2. *S. cerevisiae* strains used in this Study**

**Supplemental Table 3.3. Plasmids used in this study**

**Supplemental Table 3.4. Antibodies used in this study**

## Supplemental figure legends

**Figure S1. Mutant *rpn1* alleles derived from both the RY2H screen and rational mutations display genetic interactions with mutations in genes that encode ubiquitin receptors intrinsic to the proteasome.**

Five-fold serial dilutions of cells were plated onto the indicated media. The *rpn1* mutants (*rpn1*\*) were plasmid shuffled into an *rpn1Δ* strain containing either no additional mutations (A) or *rpn13Δ* (B). AZC refers to 5 mM of the proline analog l-azetidine-2-carboxylic acid (AZC). In panel B, mutations derived from the RY2H screen are indicated with a red box.

**Figure S2. *rpn1-D517A*, *rpn10-uim rpn1-D571A*, and *rpn10-uim rpn13-KKD rpn1-D571A* limit binding of UBA-UBL proteins Ddi1 and Dsk2.**

(A) Affinity-purified *rpn1-D517A* proteasomes contain reduced levels of Ddi1 and Ub conjugates. Levels of UBA-UBL proteins, the lid subunit Rpn12 and polyubiquitin are shown for affinity-purified proteasomes (IP) and in the whole cell extract input (WCE). (B) Affinity-purified *rpn10-uim rpn1-D571A* proteasomes similarly show diminished Ddi1 and Ub conjugates. (C) Affinity-purified *rpn10-uim rpn13-KKD rpn1-D571A* proteasomes contain reduced levels of Ddi1, Dsk2, and Ub conjugates in comparison to proteasomes from a *rpn10-uim rpn13-KKD* strain. Densitometric quantification of this

blot is shown on the right. The amounts of UBL proteins were normalized to Rpn11<sup>FLAG</sup> and wild-type levels were set at 100%.

**Figure S3. Mutations at Rpn1 residues A418, N549, F565, and G571 render unstable proteasomes.**

Pre1-myc13 tagged proteasomes from strains carrying plasmid-borne Rpn1 alleles in an *RPNI* null strain, were immunoprecipitated from whole cell extracts and analyzed by immunoblotting with the indicated antibodies. As shown, proteasomes with mutations at residues A418, N549, F565, and G571 exhibit dissociation of the 19S cap with the proteasomal base during immunoprecipitation experiments.

**Figure S4. *rpn1-D517A* mutants exhibit a selective defect in protein degradation.**

(A) Mutant *rpn1-D517A* cells degrade the Dsk2 substrate galactose inducible GST-Kre22 with normal kinetics. Strains carrying a plasmid that expressed GST-Kre22 from the GAL1 promoter were grown in raffinose medium and then induced with 2% galactose for 3 h. Dextrose was added at time zero to extinguish expression and samples were taken at the indicated time points. Below, cells were plated in a five-fold serial dilution onto either glucose or galactose containing media and monitored for growth after 2–3 days at 30°C. (B) Replicate of experiment seen in Figure 3.5A. Mutant *rpn1-D517A* cells degrade the Ufd1/Rad23/Dsk2 substrate CPY\* with normal kinetics in a cycloheximide chase. Equal loading of extracts was confirmed by blotting with an anti-tubulin antibody (lower panel). The quantification of these blots is shown. (C) Replicate of experiment seen in Figure 3.5B. Ufo1 is stabilized in *rpn1-D517A* and *ddi1Δ* mutants. Wild-type and mutant cells carrying a plasmid that expressed GST-Ufo1 from the GAL1 promoter were grown in raffinose medium and then induced with 2% galactose for 14 h. Dextrose was added at T<sub>0</sub> to extinguish expression and samples were taken at the indicated time points. Quantification is shown.

**Supplemental Table 3.1. Additional rational Rpn1 mutants used in this study**

<b>Rpn1 Residue Mutation(s)</b> <sup>1</sup>	<b>Binds Ubp6</b>	<b>Binds Rad23</b>	<b>Binds Dsk2</b>	<b>Binds Ddi1</b>
D482K	nd <sup>2</sup>	+	+	nd
T483R	nd	+	+	nd
D482K T483R K484A (KRA)	nd	+	+	nd
T516R	nd	+	+	nd
D517R	nd	+	+	nd
L518A	nd	+	+	nd
T516R D517R L518A (RRA)	nd	+	+	
I520E	nd	+	+	nd
E521K	nd	+	+	nd
T516R D517R L518A I520E E521K (RRAEK)	nd	+	+	nd
S500A T537A N539D (STN)	+ <sup>3</sup>	+	+	+
D503G T537A N539D (DTN)	+	+	+	+
V447H D517A (VD)	+	+	+	- <sup>4</sup>
V447H K484A D517A (VKD)	+	+	+	-

<sup>1</sup>All listed Rpn1 mutant strains were tested for UBL binding competence in an *rpn13Δ* background.

<sup>2</sup>“nd” indicates that no data was collected.

<sup>3</sup>“+” indicates that binding was observed.

<sup>4</sup>“-” indicates that no binding was observed.

**Supplemental Table 3.2. *S. cerevisiae* strains used in this study**

<b>RJD #</b>	<b>Genotype</b>	<b>Source</b>
4130	<i>MATa, leu2-3,112, trp1-901, his3D200, ade2-101, gal4D, gal80D, SPAL10::URA3, GAL1::lacZ, HIS3UAS GAL1::HIS3@LYS2, can1<sup>R</sup>, cyh2<sup>R</sup> (MaV203)</i>	Vidal Lab
4189	<i>Mata can1-100, leu2-3, his3-11,-15, trp1-1, ura3-1, ade2-1, rpn1::KanMX6 [pRS316-Rpn1-URA]</i>	this study
4626	<i>MATa leu2-3, his3-11,-15, trp1-1, ura3-1, ade2-1, rpn1::KanMX6 [pRS315-Rpn1-LEU]</i>	this study
4628	<i>MATa leu2-3, his3-11,-15, trp1-1, ura3-1, ade2-1, rpn1::KanMX6 [pRS315-Rpn1-V447H-LEU]</i>	this study
4748	<i>MATa leu2-3, his3-11,-15, trp1-1, ura3-1, ade2-1, rpn1::KanMX6 [pRS315-Rpn1-E466A-LEU]</i>	this study
4749	<i>MATa leu2-3, his3-11,-15, trp1-1, ura3-1, ade2-1, rpn1::KanMX6 [pRS315-Rpn1-N480A-LEU]</i>	this study
4750	<i>MATa leu2-3, his3-11,-15, trp1-1, ura3-1, ade2-1, rpn1::KanMX6 [pRS315-Rpn1-K484A-LEU]</i>	this study
4751	<i>MATa leu2-3, his3-11,-15, trp1-1, ura3-1, ade2-1, rpn1::KanMX6 [pRS315-Rpn1-S500A-LEU]</i>	this study
4629	<i>MATa leu2-3, his3-11,-15, trp1-1, ura3-1, ade2-1, rpn1::KanMX6 [pRS315-Rpn1-D503G-LEU]</i>	this study
4752	<i>MATa leu2-3, his3-11,-15, trp1-1, ura3-1, ade2-1, rpn1::KanMX6 [pRS315-Rpn1-D517A-LEU]</i>	this study
4633	<i>MATa leu2-3, his3-11,-15, trp1-1, ura3-1, ade2-1, rpn1::KanMX6 [pRS315-Rpn1-N539D-LEU]</i>	this study
4824	<i>MATa can1-100, leu2-3, his3-11,-15, trp1-1, ura3-1, ade2-1, rpn1::KanMX6 [pRS316-Rpn1-URA] rpn13::TRP1</i>	this study
5462	<i>MATa can1-100, leu2-3, his3-11,-15, trp1-1, ura3-1, ade2-1, rpn1::KanMX6 [pRS315-Rpn1-LEU] rpn13::TRP1</i>	this study
5463	<i>MATa can1-100, leu2-3, his3-11,-15, trp1-1, ura3-1, ade2-1, rpn1::KanMX6 [pRS315-Rpn1-K484A-LEU] rpn13::TRP1</i>	this study
5464	<i>MATa can1-100, leu2-3, his3-11,-15, trp1-1, ura3-1, ade2-1, rpn1::KanMX6 [pRS315-Rpn1-S500A-LEU] rpn13::TRP1</i>	this study
5465	<i>MATa can1-100, leu2-3, his3-11,-15, trp1-1, ura3-1, ade2-1, rpn1::KanMX6 [pRS315-Rpn1-D517A-LEU] rpn13::TRP1</i>	this study
5466	<i>MATa can1-100, leu2-3, his3-11,-15, trp1-1, ura3-1, ade2-1, rpn1::KanMX6 [pRS315-Rpn1-N539D-LEU] rpn13::TRP1</i>	this study
4920	<i>MATa leu2-3, his3-11,-15, trp1-1, ura3-1, ade2-1, rpn1::KanMX6 [pRS315-Rpn1-LEU] rpn13KKD::NatMX</i>	this study
4921	<i>MATa leu2-3, his3-11,-15, trp1-1, ura3-1, ade2-1, rpn1::KanMX6 [pRS315-Rpn1-N480A-LEU] rpn13KKD::NatMX</i>	this study
4922	<i>MATa leu2-3, his3-11,-15, trp1-1, ura3-1, ade2-1, rpn1::KanMX6 [pRS315-Rpn1-K484A-LEU] rpn13KKD::NatMX</i>	this study
4923	<i>MATa leu2-3, his3-11,-15, trp1-1, ura3-1, ade2-1, rpn1::KanMX6 [pRS315-Rpn1-S500A-LEU] rpn13KKD::NatMX</i>	this study
4924	<i>MATa leu2-3, his3-11,-15, trp1-1, ura3-1, ade2-1, rpn1::KanMX6 [pRS315-Rpn1-D517A-LEU] rpn13KKD::NatMX</i>	this study
4925	<i>MATa leu2-3, his3-11,-15, trp1-1, ura3-1, ade2-1, rpn1::KanMX6 [pRS315-Rpn1-N539D-LEU] rpn13KKD::NatMX</i>	this study
4926	<i>MATa leu2-3, his3-11,-15, trp1-1, ura3-1, ade2-1, rpn1::KanMX6 [pRS315-Rpn1-N480A-LEU] rpn10-UIM::KanMX</i>	this study
4927	<i>MATa leu2-3, his3-11,-15, trp1-1, ura3-1, ade2-1, rpn1::KanMX6 [pRS315-</i>	this study

	<i>Rpn1-K484A-LEU] rpn10-UIM::KanMX</i>	
4928	<i>MATa leu2-3, his3-11,-15, trp1-1, ura3-1, ade2-1, rpn1::KanMX6 [pRS315-Rpn1-S500A-LEU] rpn10-UIM::KanMX</i>	this study
4929	<i>MATa leu2-3, his3-11,-15, trp1-1, ura3-1, ade2-1, rpn1::KanMX6[pRS315-Rpn1-D517A-LEU] rpn10-UIM::KanMX</i>	this study
4930	<i>MATa leu2-3, his3-11,-15, trp1-1, ura3-1, ade2-1, rpn1::KanMX6 [pRS315-Rpn1-LEU] rpn13KKD::NatMX rpn10-UIM::KanMX</i>	this study
4931	<i>MATa leu2-3, his3-11,-15, trp1-1, ura3-1, ade2-1, rpn1::KanMX6 [pRS315-Rpn1-N480A-LEU] rpn13KKD::NatMX rpn10-UIM::KanMX</i>	this study
4932	<i>MATa leu2-3, his3-11,-15, trp1-1, ura3-1, ade2-1, rpn1::KanMX6 [pRS315-Rpn1-K484A-LEU] rpn13KKD::NatMX rpn10-UIM::KanMX</i>	this study
4933	<i>MATa leu2-3, his3-11,-15, trp1-1, ura3-1, ade2-1, rpn1::KanMX6[pRS315-Rpn1-S500A-LEU] rpn13KKD::NatMX rpn10-UIM::KanMX</i>	this study
4934	<i>MATa leu2-3, his3-11,-15, trp1-1, ura3-1, ade2-1, rpn1::KanMX6 [pRS315-Rpn1-D517A-LEU] rpn13KKD::NatMX rpn10-UIM::KanMX</i>	this study
4935	<i>MATa leu2-3, his3-11,-15, trp1-1, ura3-1, ade2-1, rpn1::KanMX6[pRS315-Rpn1-N539D-LEU] rpn13KKD::NatMX rpn10-UIM::KanMX</i>	this study
5106	<i>MATa leu2-3, his3-11,-15, trp1-1, ura3-1, ade2-1, rpn1::KanMX6 [pRS315-Rpn1-LEU] rpn4::TRP1</i>	this study
5107	<i>MATa leu2-3, his3-11,-15, trp1-1, ura3-1, ade2-1, rpn1::KanMX6[pRS315-Rpn1-N480A-LEU] rpn4::TRP1</i>	this study
5108	<i>MATa leu2-3, his3-11,-15, trp1-1, ura3-1, ade2-1, rpn1::KanMX6[pRS315-Rpn1-K484A-LEU] rpn4::TRP1</i>	this study
5109	<i>MATa leu2-3, his3-11,-15, trp1-1, ura3-1, ade2-1, rpn1::KanMX6[pRS315-Rpn1-S500A-LEU] rpnΔ::TRP1</i>	this study
5110	<i>MATa leu2-3, his3-11,-15, trp1-1, ura3-1, ade2-1, rpn1::KanMX6[pRS315-Rpn1-D517A-LEU] rpn4::TRP1</i>	this study
5111	<i>MATa leu2-3, his3-11,-15, trp1-1, ura3-1, ade2-1, rpn1::KanMX6 [pRS315-Rpn1-N539D-LEU] rpn4::TRP1</i>	this study
5459	<i>MATa leu2-3, his3-11,-15, trp1-1, ura3-1, ade2-1, rpn1::KanMX6 [pRS316-Rpn1-URA] rpn13::TRP1 arg4::KanMX lys2::HIS3 CAN1 rpn11::RPN11-FLAG-HphMX</i>	this study
5460	<i>MATa leu2-3, his3-11,-15, trp1-1, ura3-1, ade2-1, rpn1::KanMX6 [pRS315-Rpn1-K484A-LEU] rpn13::TRP1 arg4::KanMX lys2::HIS3 CAN1 rpn11::RPN11-FLAG-HphMX</i>	this study
5461	<i>MATa leu2-3, his3-11,-15, trp1-1, ura3-1, ade2-1, rpn1::KanMX6 [pRS315-Rpn1-D517A-LEU] rpn13::TRP1 arg4::KanMX lys2::HIS3 CAN1 rpn11::RPN11-FLAG-HphMX</i>	this study
5558	<i>MATa leu2-3, his3-11,-15, trp1-1, ura3-1, ade2-1, rpn1::KanMX6 [pRS315-Rpn1-A418V-LEU] rpn13::TRP1 arg4::KanMX lys2::HIS3 CAN1 rpn11::RPN11-FLAG-HphMX</i>	this study
5559	<i>MATa leu2-3, his3-11,-15, trp1-1, ura3-1, ade2-1, rpn1::KanMX6 [pRS315-Rpn1-V447H-LEU] rpn13::TRP1 arg4::KanMX lys2::HIS3 CAN1 rpn11::RPN11-FLAG-HphMX</i>	this study
5560	<i>MATa leu2-3, his3-11,-15, trp1-1, ura3-1, ade2-1, rpn1::KanMX6 [pRS315-Rpn1-E466A-LEU] rpn13::TRP1 arg4::KanMX lys2::HIS3 CAN1 rpn11::RPN11-FLAG-HphMX</i>	this study
5561	<i>MATa leu2-3, his3-11,-15, trp1-1, ura3-1, ade2-1, rpn1::KanMX6 [pRS315-Rpn1-N480A-LEU] rpn13::TRP1 arg4::KanMX lys2::HIS3 CAN1 rpn11::RPN11-FLAG-HphMX</i>	this study
5562	<i>MATa leu2-3, his3-11,-15, trp1-1, ura3-1, ade2-1, rpn1::KanMX6 [pRS315-Rpn1-S500A-LEU] rpn13::TRP1 arg4::KanMX lys2::HIS3 CAN1 rpn11::RPN11-FLAG-HphMX</i>	this study
5563	<i>MATa leu2-3, his3-11,-15, trp1-1, ura3-1, ade2-1, rpn1::KanMX6</i>	this study

	<i>[pRS315-Rpn1-V447H K484A D517A -LEU] rpn13::TRP1 arg4::KanMX lys2::HIS3 CAN1 rpn11::RPN11-FLAG-HphMX</i>	
4797	<i>MATa his3Δ1, leu2Δ0, met15Δ0, ura3Δ0, ddi1::KANMX</i>	Open Biosystems
5289	<i>MATA leu2-3, his3-11,-15, trp1-1, ura3-1, ade2-1, -LEU] rpn10- UIM::KanMX pre1::PRE1-FLAG-6XHIS-URA3</i>	this study
5290	<i>MATa leu2-3, his3-11,-15, trp1-1, ura3-1, ade2-1, rpn1::KanMX6 [pRS315-Rpn1 D517A-LEU rpn10-UIM::KanMX pre1::PRE1-FLAG- 6XHIS-URA3</i>	this study
5457	<i>MATa leu2-3, his3-11,-15, trp1-1, ura3-1, ade2-1, rpn1::KanMX6 [pRS315-Rpn1 -LEU] rpn13KKD::NatMX rpn10-UIM::KanMX pre1::PRE1- FLAG-6XHIS-URA3</i>	this study
5458	<i>MATa leu2-3, his3-11,-15, trp1-1, ura3-1, ade2-1, rpn1::KanMX6 [pRS315-Rpn1 D517A-LEU] rpn13KKD::NatMX rpn10-UIM::KanMX pre1::PRE1-FLAG-6XHIS-URA3</i>	this study

**Supplemental Table 3.3. Plasmids used in this study**

<b>Plasmid</b>	<b>Description</b>	<b>Source</b>
RDB834	pGEX 4T-3	RJD Lab
RDB1647	pGEX6P1-Rad23	H. Yokosawa
RDB1672	pGEX-KG-Dsk2	M. Funakoshi
RDB2448	pET42a-Ddi1	H. Fu
RDB2170	pEXP22(AD)-Rad23	this study
RDB2173	pEXP22(AD)-Dsk2	this study
RDB2488	pEXP22(AD)-Ddi1	this study
RDB2490	pEXP22(AD)-Ddi1Ddi1 $\Delta$ UBL (aa 78-428)	this study
RDB2179	pEXP22(AD)-Ubp6	this study
RDB2662	pEXP22(AD)-Rpn2	this study
RDB2115	pEXP32(DB)-Rpn1 <sup>391-642</sup>	this study
RDB2090	pRS316-Rpn1	this study
RDB2089	pRS315-Rpn1	this study
RDB2273	pRS315-Rpn1-V447H	this study
RDB2296	pRS315-Rpn1-E466A	this study
RDB2297	pRS315-Rpn1-N480A	this study
RDB2298	pRS315-Rpn1-K484A	this study
RDB2299	pRS315-Rpn1-S500A	this study
RDB2262	pRS315-Rpn1-D503G	this study
RDB2300	pRS315-Rpn1-D517A	this study
RDB2264	pRS315-Rpn1-N539D	this study
RDB2349	pRS315-Rpn1-S500A T537A N539D	this study
RDB2353	pRS315-Rpn1-D503G T537A N539D	this study
RDB2350	pRS315-Rpn1-V447H D517A	this study
RDB2354	pRS315-Rpn1-V447H K484A D517A	this study
RDB2407	pEGH-GAL-GST-Ufo1	OpenBiosystems
RDB2409	pEGH	Brenda Andrews
RDB1752	pCPY*HA/ <i>URA3</i>	R. Hampton
RDB2408	pEGH-GAL-GST-Kre22	OpenBiosystems

**Supplemental Table 3.4. Antibodies used in this study**

<b>Antibody</b>	<b>Source</b>	
	Kiran Madura, Robert Wood	
Rad23	Johnson Medical School	rabbit
Rad23	Santa Cruz (yG-20; sc-15556)	goat
	Michael Glickman, Technion, Haifa, Israel	
Dsk2		chicken
Dsk2	Abcam No.ab4119	rabbit
	Jeffrey Gerst, Weizmann Institute	
Ddi1		rabbit
Rpt5	Biomol No. PW8245	rabbit
	Keiji Tanaka, Tokyo Metropolitan Inst. of Med. Sci.	
Rpn3		rabbit
Rpn12	Daniel Finley, Harvard	rabbit
myc	Covance	mouse
flag	Sigma	mouse
UB	Chemicon	mouse
UB	Enzo	rabbit
Ubp6	Rohan Baker	rabbit

**Figure 3.S1. Mutant *rpn1* alleles derived from both the RY2H screen and rational mutations display genetic interactions with mutations in genes that encode ubiquitin receptors intrinsic to the proteasome.**

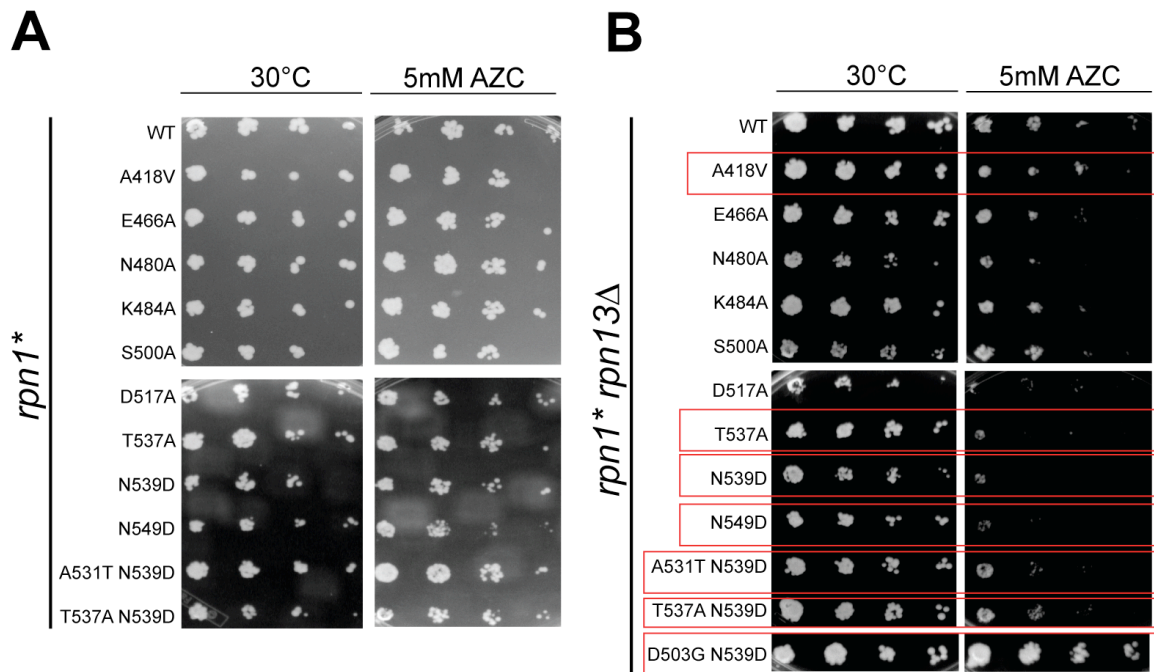


**Figure 3.S2.** *rpn1-D517A*, *rpn10-uim rpn1-D517A*, and *rpn10-uim rpn13-KKD rpn1-D517A* limit binding of UBA-UBL proteins Ddi1 and Dsk2.

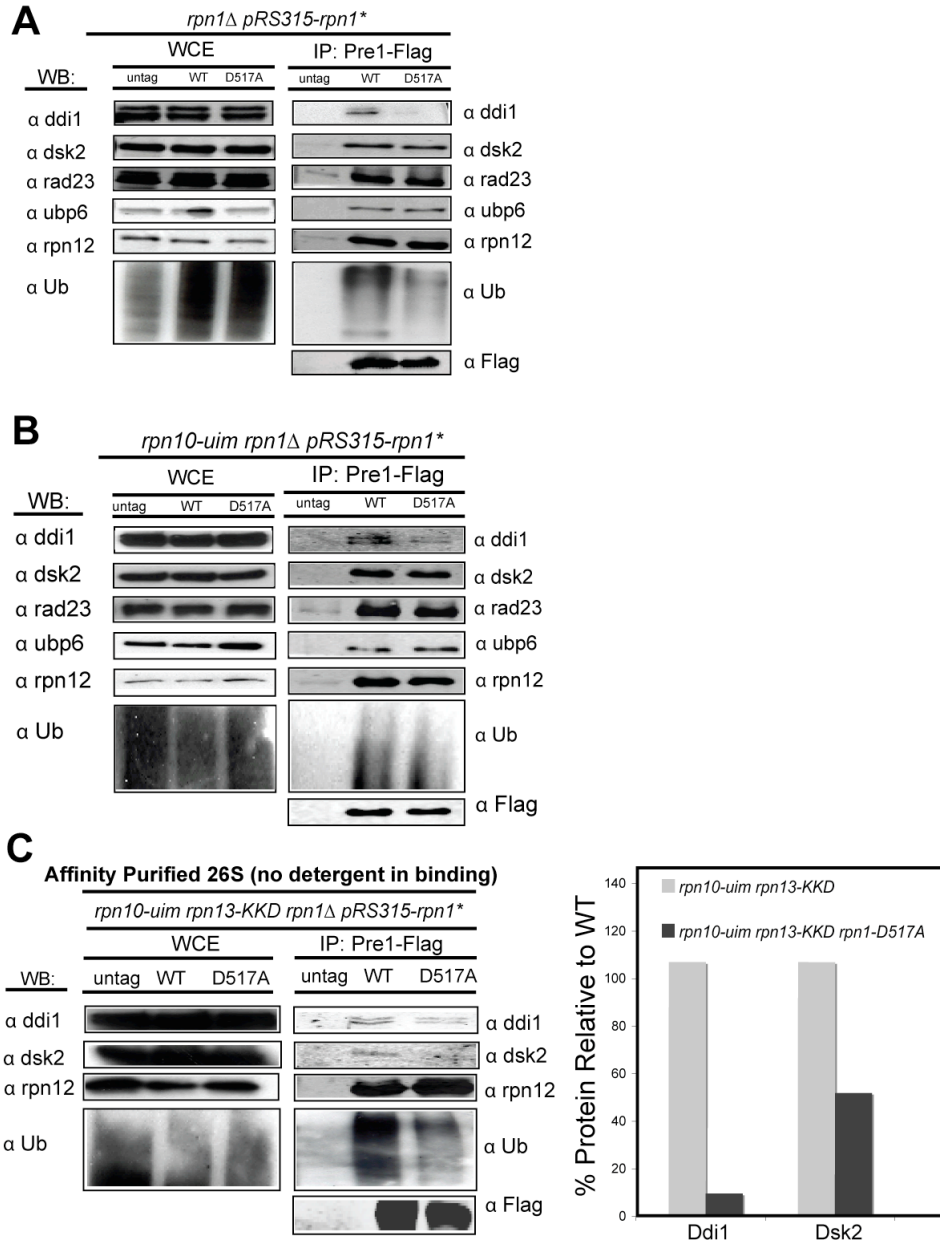


**Figure 3.S3. Mutations at Rpn1 residues A418, N549, F565, and G571 render unstable proteasomes.**

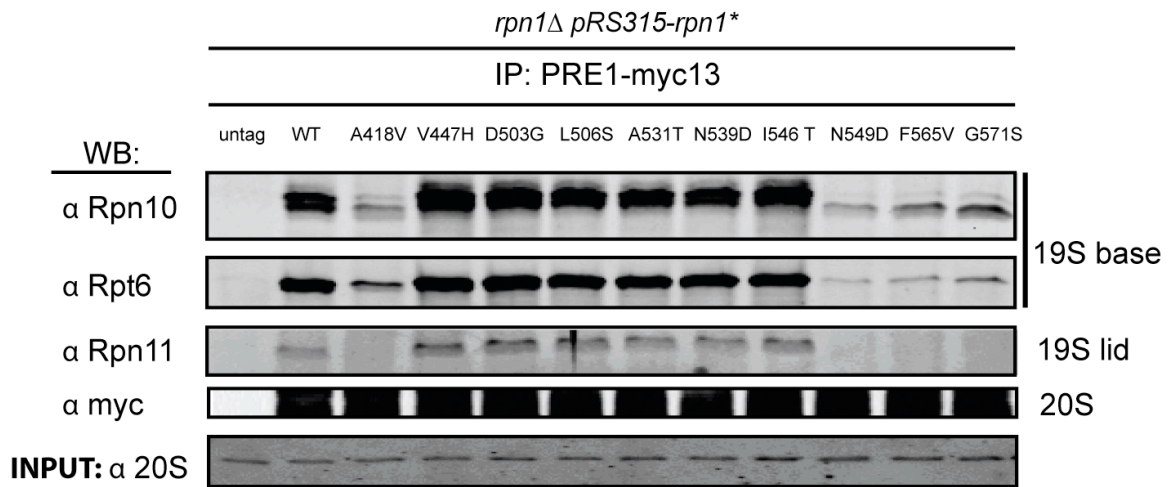
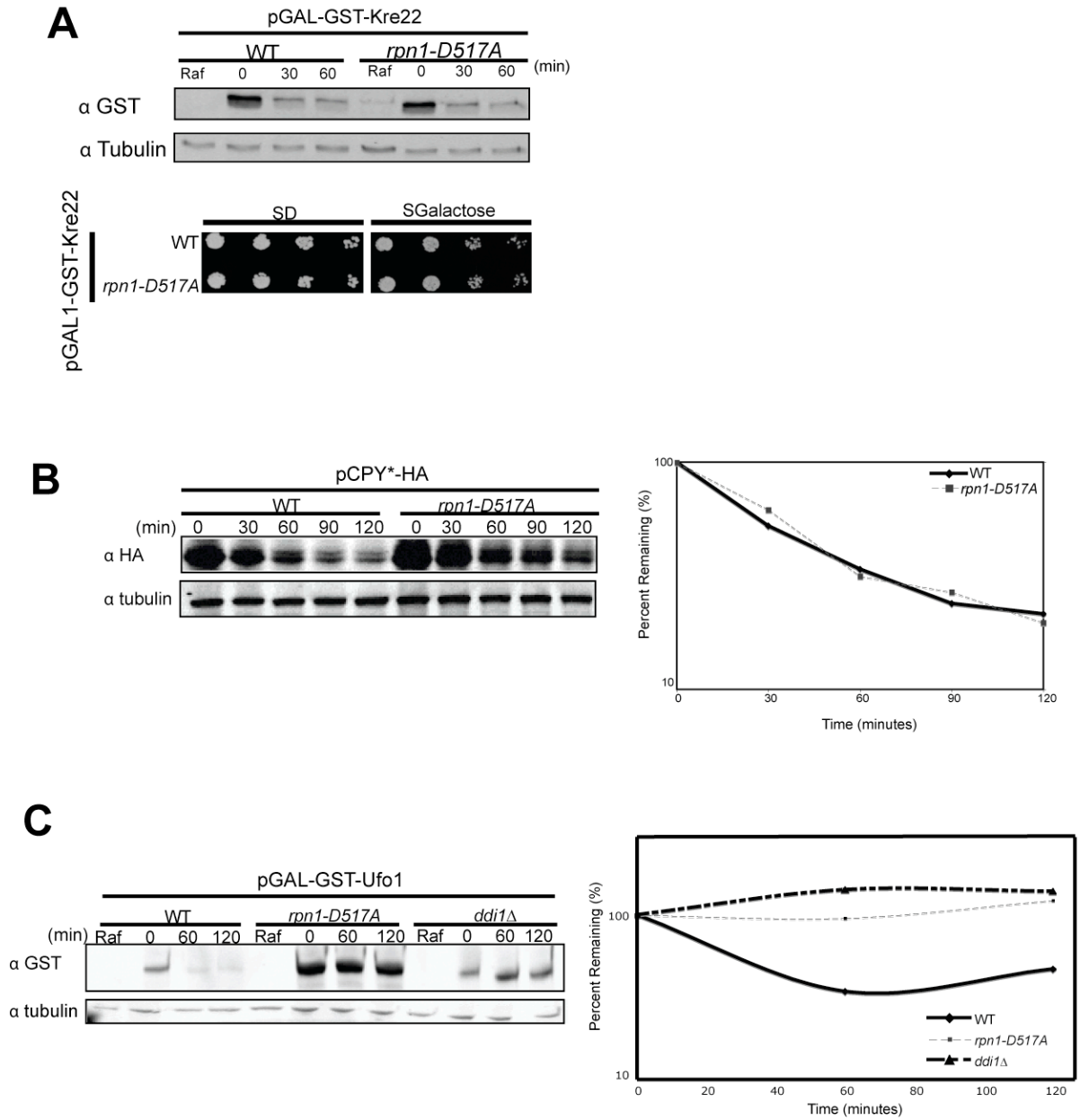


**Figure 3.S4. *rpn1-D517A* mutants exhibit a selective defect in protein degradation.**



## **Chapter 4:**

# **Comparative analysis of proteasome *cis* mutants to UBA-UBL null strains**

## Introduction

Rpn1 is the largest subunit of the proteasome and shares ~ 30% identity with Rpn2, the second largest subunit of the proteasome (Fôrster et al., 2010). Both proteins have two contiguous segments of nearly 250 repetitive residues that are classified as proteasome cyclosome (PC) repeats/leucine-rich repeats (LRR) (Lupas et al., 1997). LRR repeats are well conserved throughout the eukaryotes and participate in protein-protein interactions (Kobe and Kajava, 2001). These LRR repeats of Rpn1 and Rpn2 have been proposed to fold into repetitive  $\alpha$ -solenoid structures that curve into a nearly closed horseshoe shape (Kajava, 2002). Newer data suggest that Rpn1 and Rpn2 may actually form slightly opened horseshoes instead (Effantin et al., 2009).

It had been proposed that the horseshoe-shaped Rpn1 and Rpn2 proteins are stacked on top of each other, forming a pre-chamber preceding entry into the core of the proteasome (Effantin et al., 2009; Kajava, 2002; Rosenzweig et al., 2008). However, recent experimental evidence uncovering the mechanisms of proteasome biogenesis and electron microscopy work are not in agreement with this possibility (Fôrster et al., 2010; Nickell et al., 2009a; Tomko Jr et al., 2010)

Rpn1 has been proposed to play a scaffolding role in the proteasome. Its scaffolding functions include binding proteasome interacting proteins (PIPs) (Crosas et al., 2006; Elsasser et al., 2004), and serving as a structural support “beam” for supporting the formation of the proteasome base during biogenesis (Kaneko et al., 2009; Saeki et al., 2009).

In line with the proposed roles Rpn1 plays in the proteasome and the aforementioned structural evidence, it seems reasonable that one surface of the horeshoe may interact with the Rpt ring of the proteasome, while the other may be exposed for binding to PIPs. In this section I began querying this possibility by making a series of combinatorial mutations in two distinct surfaces of Rpn1 to test if they have differential effects on interaction with UBA-UBL proteins and on turnover of a Ddi1 substrate, Ufo1.

I was also interested in knowing if combinatorial mutations on one surface of Rpn1 could exacerbate the phenotypes observed in Chapter 3 of the *rpn1-D517A* mutant.

Here I show evidence that one surface of Rpn1 may be important for binding UBL-containing proteins. Although, in comparing the data presented here to that in Chapter 3, combinatorial mutants may only slightly exacerbate mutant phenotypes. For instance, an *rpn1-V447H K484A* mutant is sensitive to over expression of Ufo1, whereas as single mutants, they are not (Chapter 3).

With the overwhelming evidence that the *rpn1-D517A* mutation, and closely clustered mutations, contributed to binding of Ddi1 at the proteasome, the next question was: Is elimination of the *rpn1-D517A* site equivalent to the elimination of the UBA-UBL receptor, Ddi1, itself?

I report that the reduction of binding of Ddi1 to a *cis* proteasome mutant produces a cellular physiology distinct from a *ddi1Δ* null strain.

## Methods

### **Native immunoprecipitations of 26S proteasomes, growth assays, turnover of galactose inducible Ufo1, and yeast strains**

All methods were done as described in detail in Chapter 3. Strains used in this chapter are listed, Table 4.1.

### **HO steady-state concentration measurements**

The steady-state concentration of HO was measured as described (Kaplun et al., 2000).

Briefly, strains containing pCM190-HO-LacZ were grown to saturation in the presence of 2 mg/ml doxycycline to prevent *HO* expression. Next, strains were diluted to an OD<sub>600</sub> 0.3 and grown in the absence of doxycycline and allowed to reach steady state.

Approximately 1 mL of saturated culture was pelleted by centrifugation, washed in Z-buffer (10 mM KCl, 1 mM MgSO<sub>4</sub>, 60 mM Na<sub>2</sub>HPO<sub>4</sub>, 40 mM NaH<sub>2</sub>PO<sub>4</sub>, pH 7), pelleted again, and resuspended in 300 µl of Z-buffer before being flash frozen in liquid nitrogen for ~20 seconds. Frozen samples were thawed in a 30°C water bath for 1 minute, and then flash frozen and thawed for three subsequent cycles. Next, 160 µl of 4 mg/ml ONPG (Sigma) dissolved in Z-buffer was added to the cell mixture and incubated in a 30°C water bath. Color change was monitored every 5–10 minutes. After a yellow color developed, 0.4 ml of 1 M Na<sub>2</sub>CO<sub>3</sub> was added to quench the reaction. Approximately 2 µl of sample was used to measure the A<sub>420</sub> using a nanodrop.

## Results

### **One surface of Rpn1 may be necessary for binding UBA-UBL proteins.**

Since Rpn1 is the largest subunit of the proteasome, I wanted to investigate if only a distinct surface is dedicated to binding UBA-UBL proteins and Ub conjugates. Based on the structural model of Rpn1 and its role as a scaffold in the proteasome (Elsasser et al., 2004; Kajava, 2002; Nickell et al., 2009a), it seems plausible that one surface of Rpn1 may be necessary for interacting with shuttle receptors bearing Ub conjugates, while the other surface might interact with other proteasome subunits. For instance, we noticed that mutations in residues A418, N539, F565, and G571 caused the lid and base of the proteasome to nearly completely dissociate during immunoprecipitation experiments (Chapter 3). To test this idea, we assayed the binding of clustered mutations (Figure 4.1A) to ubiquitin conjugates and UBA-UBL proteins. Ddi1 binding and ubiquitin conjugate accumulation was vastly diminished for the *rpn13Δ rpn1-V447H K484A D517A* mutant ('VKD') but not for a *rpn13Δ rpn1-S500A T537A N539D* ('STN') triple-point mutant, although ubiquitin accumulation is equivalent in a whole cell extract (Figure 4.1A). This data is suggestive that the surface containing Rpn1 residues V447, K484, and D517 specifically binds UBL proteins, although caveats should also be considered. Given that Rpn1-D517A by itself has effects on Ddi1 and Ub-binding, it is possible that the phenotype of VKD mutant is due entirely to D517A and that the mutations at V447 and K484 are making no contribution. Further, it is hard to understand the role of the STN mutant without any other mutant phenotypes known.

**The *rpn1-VKD* mutant shows only slightly more dramatic synthetic lethality than *rpn1-STN* in combination with mutations of intrinsic ubiquitin receptors.**

To see if the roles of the ‘VKD’ surface could be distinguished genetically from the ‘STN’ surface of Rpn1, I tested if either an *rpn1-VKD* or an *rpn1-STN* mutant would be particularly sensitive to mutations in intrinsic ubiquitin receptors, Rpn10 and Rpn13. On their own, *rpn1-STN* and *rpn1-VKD* were unaffected by the addition of exogenous AZC, a proline analog that induces protein misfolding. In the presence of the *rpn13-KKD* mutation, a mutation that blocks the ability of Rpn13 to bind ubiquitin (Husnjak et al., 2008), both strains appear slightly sensitive, although *rpn1-VKD* shows a more dramatic sensitivity. I next tested whether these *rpn1* mutants exhibited genetic interaction with *RPN10*. The ubiquitin-interaction motif (UIM) of Rpn10 is mutated in the *rpn10-UIM* strain. In the *rpn10-UIM* background, both *rpn1* mutants showed a subtle increase in sensitivity to AZC. In an *rpn10-UIM rpn13-KKD* background, both *rpn1* mutants were hypersensitive to AZC, however, the *rpn1-VKD* mutant exhibited the most striking sensitivity (Figure 4.1B). As a test for specificity, the *rpn1-VKD* and *rpn1-STN* mutations were also tested in an *rpn4Δ* background and appeared wild type (Figure 4.1B).

While it is hard to differentiate the cellular roles of the ‘VKD’ surface from the ‘STN’ surface based on this sensitivity, two facts of notable importance are worth mentioning. First, known proteasome assembly mutants show sensitivity to AZC (Saeki et al., 2009), hence it is not inconceivable that ‘STN’ mutants may show defects in combination with these mutations for reasons other than directly affecting UBA-UBL

recruitment. Secondly, the *rpn1-VKD* mutant did, in fact, show the most severe phenotypes in combinations with intrinsic receptors.

### **Only Rpn1 ‘VKD’ surface mutations stabilize the Ddi1 substrate Ufo1.**

As seen, the *rpn1-D517A* mutation stabilizes Ufo1 (Chapter 3). I hypothesized that a mutant containing multiple mutations on the ‘VKD’ surface should similarly do so. First, I tested if over expression of Ufo1 causes lethality in any combination of ‘VKD’ or ‘STN’ surface mutants. Only *rpn1* mutants with combined mutations on the ‘VKD’ surface exhibited lethality when Ufo1 was over expressed. Notably, a mutant that did not contain the D517A mutation, the *rpn1-V447H K484A*, exhibited sensitivity to Ufo1 over-expression. This effect was exquisitely specific—no ‘STN’ surface mutant conferred sensitivity to over-expression of Ufo1 (Figure 4.1C). Since only mutations on the ‘VKD’ surface reduced Ddi1 binding (Figure 4.1A) and were sensitive to over expression of Ufo1, I postulated that only ‘VKD’ surface mutants would stabilize Ufo1 in a turnover experiment. I observed nearly complete stabilization of Ufo1 in an *rpn1-VD* mutant in comparison to a wild-type strain and an *rpn1-SN* mutant (Figure 4.1D).

### **Rpn1-D517A and Ddi1 interact genetically.**

My biochemical data suggest that the *rpn1-D517A* point mutation has a direct impact on Ddi1 binding, and this is supported by the Ufo1 degradation assay (Figure 4.1D and Chapter 3). Hence, we hypothesized that if we looked at AZC sensitivity of an *rpn1-D517A ddi1Δ* double mutant, we would see no exacerbated effects in comparison to either single mutant. Contrary to our prediction, we noted that *rpn1-D517A ddi1Δ* double mutants displayed reduced viability compared to either single mutant (Figure 4.2A). I

also tested the sensitivity of an *rpn1-D517A ddi1Δ rpn13Δ* strain, but no exacerbated sensitivity was conferred by the loss of *RPN13* (Figure 4.2A). These puzzling data may suggest at least one of two things. Firstly, the D517 residue of Rpn1 may do more than inhibit binding of Ddi1, for instance, it may reduce the binding of other UBA-UBL proteins. Although the reduction of Dsk2 binding was only detected in immunoprecipitation experiments, if there was a loss of ubiquitin binding by the intrinsic receptors (Chapter 3) it is still plausible that even a subtle inhibition of binding could have a physiological impact. Secondly, the *rpn1-D517A* may not completely block binding of Ddi1, otherwise, a *ddi1Δ* mutation would not aggravate the phenotype of *rpn1-D517A*. From densitometric quantification of Ddi1 on *rpn1-D517A* proteasomes, approximately 80% of Ddi1 binding appears to be lost (Chapter 3). However, maybe the 20% of residual Ddi1 binding is just enough to yield a seemingly parallel genetic interaction between *rpn1-D517A* and *ddi1Δ*.

**The *rpn1-D517A* does not mimic a *ddi1Δ* mutant in steady-state accumulation of *HO* endonuclease.**

Since I had previously determined that *rpn1-D517A* and *rpn1-VD* mutants stabilized Ddi1 substrate Ufo1 (Chapter 3 and Figure 4.1D), I sought to determine if all known Ddi1 substrates would be stabilized by these mutations. Further, considering the genetic relationship between *rpn1-D517A* and *ddi1Δ*, I postulated that understanding how universal Ddi1 substrate stabilization is by the *rpn1-D517A* mutant should give insights into if Ddi1 binding to mutant *rpn1* is not completely blocked, or if *rpn1-D517A* does more than just inhibit Ddi1 binding.

*HO* endonuclease is a protein that is important in yeast mating type switching. It has been shown to be reliant upon Ddi1 for turnover. In *ddi1Δ* mutants, HO is stabilized and steady-state levels are high (Kaplun et al., 2005). The doxycycline inducible pCM190-*HO-LacZ* constructs were transformed into wild-type and *rpn1-D517A* cells. Transformants were grown in the absence of doxycycline and allowed to reach saturation, at which point, β-galactosidase activity was determined. A very high level of β-galactosidase activity was detected in *ddi1Δ* cells whereas *rpn1-D517A* had a considerably lower level of β-galactosidase activity that was comparable to wild-type levels (Figure 4.2B). The lack of increased steady-state *HO* concentrations in the *rpn1-D517A* mutant may be indicative that not all known Ddi1 substrates will be reliant on the D517A residue of Rpn1 for turnover. Alternatively, steady-state levels of *HO* may not be fairly representative of turnover defects.

**The *ddi1Δ dsk2Δ* mutant does not have diminished Ub conjugate binding to the proteasome.**

A *ddi1Δdsk2Δ* strain accumulates cellular Ub conjugates in comparison to a wild-type yeast strain (Figure 4.2C, left panel). Rpn1 ‘VKD’ surface mutants do not accumulate Ub conjugates in a whole cell extract (Figure 4.1A), so I wondered how Ub accumulation would appear at *ddi1Δdsk2Δ* mutant proteasomes. Proteasomes from a fully wild-type strain and a double *ddi1Δdsk2Δ* mutant whose Pre1 subunit contained a Flag epitope, were affinity purified and analyzed for ubiquitin conjugate accumulation. I observed that similar levels of Ub conjugates are found at a *ddi1Δdsk2Δ* proteasome as at a wild-type proteasome (Figure 4.2C). Similar results were seen when I did the same experiment with

a single *ddi1*Δ strain (data not shown). This result was unexpected considering that *rpn1-VKD* mutants actually have fewer ubiquitin conjugates that immunoprecipitate with their proteasomes.

## Discussion

Since only *rpn1-VD* and *rpn1-VKD* surface mutants show diminished binding of Ddi1, only mutants on this surface show toxicity in the presence of over expressed Ufo1 and stabilization of Ufo1. Hence, I have shown that multiple mutations on the ‘VKD’ surface of Rpn1 reduce binding to Ub conjugates, Ddi1, and lead to stabilization of Ufo1.

It is hard to say definitively that the ‘STN’ surface plays a role in scaffolding to other subunits to maintain proteasome structure, since I do not have an assay to explicitly test this hypothesis. However, one could imagine testing for interaction of the ‘STN’ surface with the Rpt1 and Rpt2 subunits that were found to form subcomplexes with Rpn1 during proteasome biogenesis (Roelofs et al., 2009; Saeki et al., 2009). Further testing will be needed to prove my hypothesis: the ‘VKD’ surface of Rpn1 is exposed for binding of proteasome interacting proteins.

The biochemical mimicry of mutations on the ‘VKD’ surface begged me to test if genetically a *ddi1* and *rpn1-D517A* mutant would prove to be working in the same functional pathway. However, the genetic analysis produced two intriguing questions:

- 1) Does the D517 residue of Rpn1 do more than inhibit binding of Ddi1?
- 2) Does the *rpn1-D517A* not completely block binding of Ddi1, such that genetically they will appear to work in parallel pathways?

The loss of ubiquitin conjugates at *rpn1-D517A* proteasomes seems to imply that this mutation does do ‘more’ than just bind Ddi1, since loss of *DDI* and, even jointly, *DDI1* and *DSK2* does not reduce Ub conjugate binding by the proteasome (Figure 4.2C and data not shown). Interestingly, *rad23Δdsk2Δ* mutants do exhibit loss of ubiquitin conjugate binding at their proteasomes (Elsasser et al., 2004). With the aforementioned result in mind, in terms of a functional role for the Rpn1-D517A mutation, what could the ‘more’ be? One hypothesis is that the ‘VKD’ surface of Rpn1 binds unidentified receptors and/or has even subtle effects on delivery of Rad23 substrates to the proteasome.

Explaining the genetic interaction between *rpn1-D517A* and Ddi1 is also challenging because based on a strict genetic view, it appears that they are contributing in parallel to protein turnover. One hypothesis is that the lack of Ddi1 binding at the proteasome in a *rpn1-D517A* causes a more distinct phenotype than does the deletion of Ddi1. Perhaps the upstream roles Ddi1 plays before binding to the proteasome leads to this apparent difference in physiology. For instance, Ddi1 is known to have an aspartyl protease domain, although no functional role has been identified for this domain other than it is necessary for homodimerization (Gabriely et al., 2008). It is possible that the intrinsic protease activity of Ddi1 may preclude having an *rpn1-D517A* mutant fully mimic its phenotype. Additionally, the greatest loss of Ddi1 binding to *rpn1-D517A* proteasomes I have seen is an 80% decrease in comparison to wild-type levels. Perhaps the remaining 20% of Ddi1 binding is what creates the unique physiology.

Finally, the redundancy of UBA-UBL binding at the proteasome that I have discovered (Chapter 3) might further confound the analysis of *RPNI* mutant alleles and

may contribute to the disparity between these proteasome *cis* mutants and UBA-UBL null strains. Future studies will be needed to investigate this complexity. For instance, it would be interesting to determine if UBA-UBL proteins deliver a different set of substrates to each of their different docking sites at the proteasome and how this is altered in a *cis* proteasome mutant.

## Figure legends

### Figure 4.1. The ‘VKD’ surface of Rpn1 may be responsible for binding UBA-UBL proteins.

(A) Ddi1 and Ub conjugate accumulation is diminished for the *rpn1-V447H K484A D517A* triple mutant ('VKD') and *rpn1-V447H D517A* double mutant ('VD') proteasomes but not for *rpn1-S500A T537A N539D* ('STN') and *rpn1-D503G T537A N539D* ('DTN') which harbor mutations on the opposing surface of Rpn1. Rpn1-Flag tagged proteasomes were immunoprecipitated and immunoblotted with the indicated antibodies. Inputs, whole cell extracts (WCE) are also shown. (B) Five-fold serially diluted cells were plated onto either YPD or YPD containing 4 mM AZC, a proline analog. The Rpn1 allele mutants (*rpn1\**) were plasmid shuffled into an *rpn1* null strain containing (from top to bottom) either no additional mutations or in an *rpn13-KKD*, *rpn10-UIM*, *rpn13-KKD rpn10-UIM* double, or *rpn4Δ* background. (C) Sensitivity to GST-Ufo1 over expression by *rpn1* mutants of clustered residues on the same surface (*rpn1-VK* and *rpn1-VD*) is specific (i.e., not shown by other *rpn1* mutants from the ‘STN’ surface). (D) Ufo1 is stabilized in the *rpn1-V447H D517A* mutant. Wild-type and mutant cells containing a *GAL1* promoter regulated GST tagged Ufo1 were grown in raffinose media preceding induction of expression with 2% galactose. Samples were taken after promoter shut off with the addition of dextrose at the indicated time points.

**Figure 4.2. *rpn1-D517A* and *ddi1* $\Delta$  mutants may have some parallel functions in protein turnover.**

(A) The indicated strains were serially diluted to equal concentrations of cells and grown on either YPD (control) or YPD media containing 5 mM AZC, a proline analog. (B) The steady-state levels of HO-LacZ were determined by an ONPG assay. Strains (wild type, *rpn1-D517A*, and *ddi1* $\Delta$ ) were transformed with pCM190-*HO-LacZ* constructs and  $\beta$ -galactosidase activity was determined after transformants were allowed to reach saturation after 18 hours of growth in the absence of doxycycline. (C) Pre1 flag tagged affinity-purified proteasomes from wild type and *ddi1* $\Delta$ *dsk2* $\Delta$  mutants were resolved on SDS PAGE and immunoblotted with the indicated antibodies (IP, right panel). Input whole cell extracts are also shown (WCE, left).

**Table 4.1 Strains used in this chapter****Yeast strains**

<b>RJD #</b>	<b>Genotype</b>	<b>Source</b>
Tgy38	<i>MATa leu2-3, his3-11,-15, trp1-1, ura3-1, ade2-1, rpn1::KanMX6 [pRS315-Rpn1 S500A T537A N539D-LEU] rpn13::TRP1 arg4::KanMX lys2::HIS3 CAN1 rpn11::RPN11-FLAG-HphMX</i>	this study
Tgy39	<i>MATa leu2-3, his3-11,-15, trp1-1, ura3-1, ade2-1, rpn1::KanMX6 [pRS315-Rpn1 D503G T537A N539D-LEU] rpn13::TRP1 arg4::KanMX lys2::HIS3 CAN1 rpn11::RPN11-FLAG-HphMX</i>	this study
Tgy40	<i>MATa leu2-3, his3-11,-15, trp1-1, ura3-1, ade2-1, rpn1::KanMX6 [pRS315-Rpn1 V447H D517A-LEU] rpn13::TRP1 arg4::KanMX lys2::HIS3 CAN1 rpn11::RPN11-FLAG-HphMX</i>	this study
Tgy41	<i>MATa leu2-3, his3-11,-15, trp1-1, ura3-1, ade2-1, rpn1::KanMX6 [pRS315-Rpn1 V447H K484A D517A-LEU] rpn13::TRP1 arg4::KanMX lys2::HIS3 CAN1 rpn11::RPN11-FLAG-HphMX</i>	this study
5377	<i>MATa leu2-3, his3-11,-15, trp1-1, ura3-1, ade2-1, rpn1::KanMX6 [pRS315-Rpn1 S500A T537A N539D-LEU]</i>	this study
5378	<i>MATa leu2-3, his3-11,-15, trp1-1, ura3-1, ade2-1, rpn1::KanMX6 [pRS315-Rpn1 V447H K484A D517A-LEU]</i>	this study
5402	<i>MATa leu2-3, his3-11,-15, trp1-1, ura3-1, ade2-1, rpn1::KanMX6 [pRS315-Rpn1 S500A T537A N539D-LEU] rpn13::TRP1</i>	this study
5403	<i>MATa leu2-3, his3-11,-15, trp1-1, ura3-1, ade2-1, rpn1::KanMX6 [pRS315-Rpn1 V447H K484A D517A-LEU] rpn13::TRP1</i>	this study
5381	<i>MATa leu2-3, his3-11,-15, trp1-1, ura3-1, ade2-1, rpn1::KanMX6 [pRS315-Rpn1 S500A T537A N539D-LEU] rpn13KKD::NatMX</i>	this study
5382	<i>MATa leu2-3, his3-11,-15, trp1-1, ura3-1, ade2-1, rpn1::KanMX6 [pRS315-Rpn1 V447H K484A D517A-LEU] rpn13KKD::NatMX</i>	this study
5383	<i>MATa leu2-3, his3-11,-15, trp1-1, ura3-1, ade2-1, rpn1::KanMX6 [pRS315-Rpn1 S500A T537A N539D-LEU] rpn10-UIM::KanMX</i>	this study
5384	<i>MATa leu2-3, his3-11,-15, trp1-1, ura3-1, ade2-1, rpn1::KanMX6 [pRS315-Rpn1 V447H K484A D517A-LEU] rpn10-UIM::KanMX</i>	this study
5385	<i>MATa leu2-3, his3-11,-15, trp1-1, ura3-1, ade2-1, rpn1::KanMX6 [pRS315-Rpn1 S500A T537A N539D-LEU] rpn13KKD::NatMX rpn10-UIM::KanMX</i>	this study
5386	<i>MATa leu2-3, his3-11,-15, trp1-1, ura3-1, ade2-1, rpn1::KanMX6 [pRS315-Rpn1 V447H K484A D517A-LEU] rpn13KKD::NatMX rpn10-UIM::KanMX</i>	this study
5379	<i>MATa leu2-3, his3-11,-15, trp1-1, ura3-1, ade2-1, rpn1::KanMX6 [pRS315-Rpn1 S500A T537A N539D-LEU] rpn4::TRP1</i>	this study
5380	<i>MATa leu2-3, his3-11,-15, trp1-1, ura3-1, ade2-1, rpn1::KanMX6 [pRS315-Rpn1 V447H K484A D517A-LEU] rpn4::TRP1</i>	this study
5154	<i>MATa leu2-3, his3-11,-15, trp1-1, ura3-1, ade2-1, rpn1::KanMX6 [pRS316-Rpn-URA] ddi1::HIS3</i>	this study
5347	<i>MATa leu2-3, his3-11,-15, trp1-1, ura3-1, ade2-1, rpn1::KanMX6 [pRS315-Rpn1 D517A-LEU] ddi1::HIS3</i>	this study
5456	<i>MATa leu2-3, his3-11,-15, trp1-1, ura3-1, ade2-1, rpn1::KanMX6 [pRS316-Rpn-URA] ddi1::HIS3 rpn13::TRP1</i>	this study
5348	<i>MATa leu2-3, his3-11,-15, trp1-1, ura3-1, ade2-1, rpn1::KanMX6 [pRS315-Rpn1 D517A-LEU] ddi1::HIS3 rpn13::TRP1</i>	this study
5456	<i>MatA ddi1::KanMX dsk2::KANMX bar1Δ pre1::PRE1-Flag-6XHIS (URA3)</i>	this study

**Figure 4.1. The 'VKD' surface of Rpn1 may be responsible for binding UBA-Ubl proteins.**

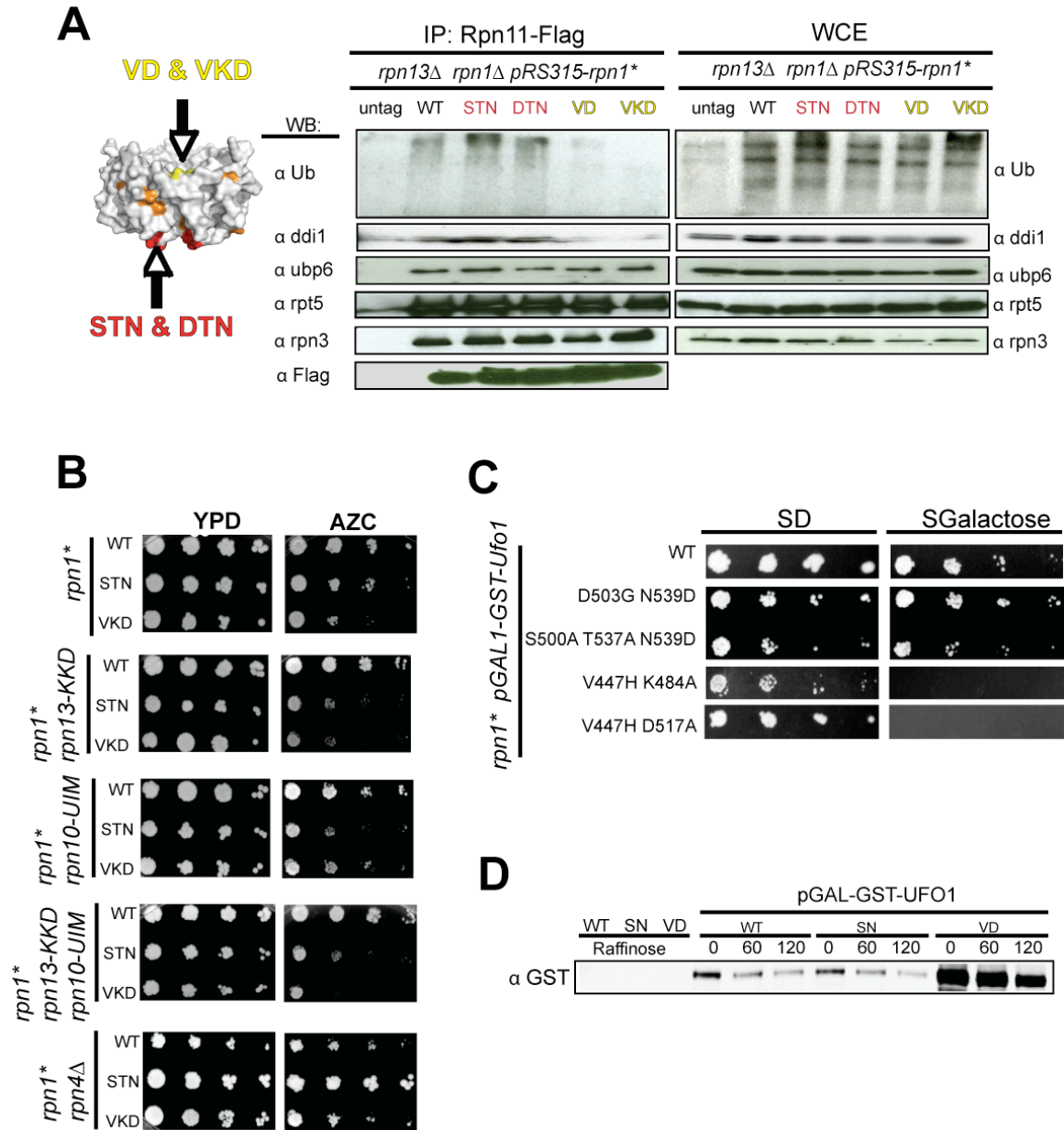
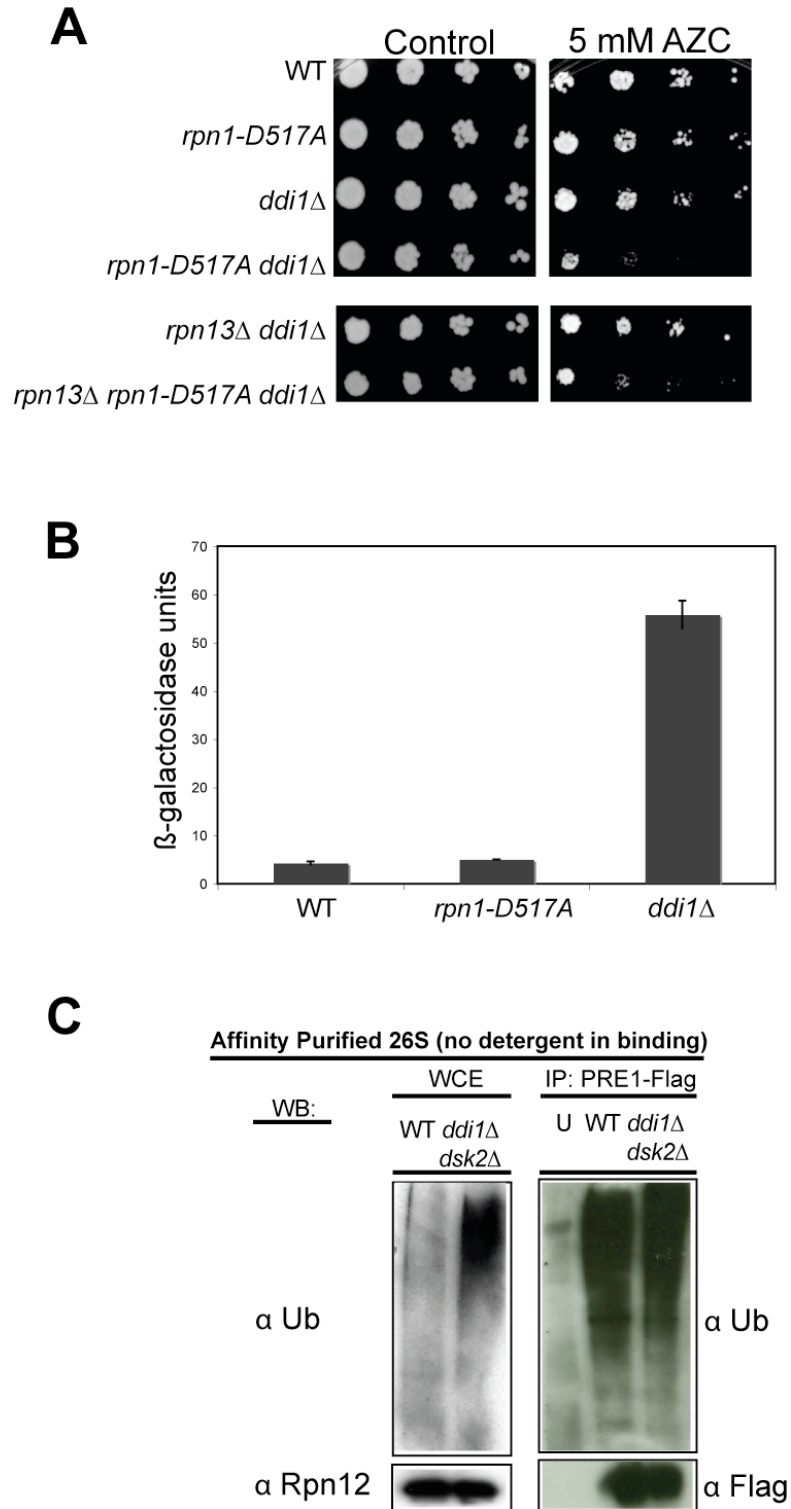


**Figure 4.2.** *rpn1-D517A* and *ddi1Δ* mutants may have some parallel functions in protein turnover.



**Chapter 5:**

**Insights into the binding of  
Rad23 and Ubp6  
to the 26S proteasome**

## Introduction

After an exhaustive genetic screen for mutations in the proteasome base subunit, Rpn1 (Chapter 3), that would inhibit binding of all UBL domain proteins, Ubp6, Rad23, Dsk2, and Ddi1, only two residues were verified to partially disrupt binding of Ddi1 and Dsk2. Interestingly, the effects on Dsk2 were only seen in the absence of one or more mutations in intrinsic receptors Rpn10 and Rpn13. However, no combination of manipulations to Rpn1, discussed in Chapter 3, seems to disrupt binding of Rad23 and Ubp6. In addition to Rpn1, Ubp6 is known to bind subunits within the lid of the proteasome, Rad23 may bind Rpn10, and human hHR23 binds hRpn13 (Husnjak et al., 2008; Leggett et al., 2002; Matiuhin et al., 2008b). Hence, in this chapter, I queried a small number of additional proteasomal perturbations to see if there was any reasonable genetic approach to impinge upon binding of Rad23 and Ubp6 to the proteasome.

Here, I report that Rad23 binding to the proteasome is diminished in a *rpn10-uim rpn13-kkd* double mutant and in an *ufd2Δ* mutant in comparison to a fully wild-type strain. Furthermore, a reduction in the levels of Rad23 at the proteasome appears to coincide with an increase in Ubp6. This is an unexpected result since it has been reported that Rad23 and Ubp6 do not compete for binding at the proteasome (Elsasser et al., 2004). To the best of my knowledge, no reports indicate that Ubp6 binds Rpn13 and Rpn10. It therefore seems reasonable that the increase in abundance of Ubp6 at Rad23-diminished proteasomes may be a physiological response to the loss of receptor docking. This data raises the question: Contrary to published reports, is Rpn1 truly the major docking site for Rad23 and Ubp6 (Fatimababy et al., 2010)?

## Methods

All methods are the same as those described in Chapter 3. Please see Table 5.1 for a list of strains used in this chapter.

## Results

### **Rpn10 and Rpn13 contribute to docking of UBA-UBL receptor proteins.**

I was interested in understanding the contribution of the roles of Rpn10 and Rpn13 to binding UBA-UBL proteins in a *rpn10-uim rpn13-KKD rpn1-D517A* mutant. To address this, I compared proteasomes from a fully wild-type strain containing no genetic perturbations in receptor genes to proteasomes from the *rpn10-uim rpn13-KKD rpn1-D517A* strain. As expected, Ub conjugates, Ddi1, and Dsk2 were again reduced (Figure 5.1C). However, unexpectedly, we noticed that the levels of Rad23 were reduced while those of Ubp6 were increased. The decrease in Rad23 levels in mutant proteasomes is not dependent upon the Rpn1-D517A mutation as when *rpn10-uim rpn13-KKD rpn1-D517A* proteasomes are compared to *rpn10-uim rpn13-KKD* proteasomes, no difference is seen in the levels of Rad23 binding (Figure 5.1B). Hence, this is likely to be an effect due to either Rpn10 or Rpn13 or to the combinatorial deletion of both of their ubiquitin binding domains.

**A sole deletion of Rpn13 is not sufficient to interrupt binding of any ubiquitin receptor protein to the proteasome.**

The possible or dual necessity for Rpn10 and Rpn13 in binding UBA-UBL proteins was intriguing. To investigate this further, I used a quantitative mass spectrometry technique, stable isotope labeling with amino acids, SILAC, to analyze if the levels of ubiquitin receptors and/or UBL proteins were dependent on the presence of Rpn13. To assay this, *rpn13Δ* Rpn11<sup>FLAG</sup> cells were labeled with light lysine and arginine while wild-type Rpn11<sup>FLAG</sup> cells were labeled with heavy lysine and arginine. The cells were mixed prior to lysing, and a proteasome affinity purification was carried out. The immunoprecipitate was analyzed on a mass spectrometer. I confirmed that all of the 26S subunits had approximately a 1:1 ratio (data not shown). There were also a plethora of proteins that were less (Table 5.2) and more (Table 5.3) abundant at *rpn13Δ* proteasomes. However, amongst the proteins that were unchanged between wild-type and *rpn13Δ* proteasomes, were Rad23, Ddi1, Ubp6, and intrinsic ubiquitin receptor Rpn10 (Table 5.4).

Unfortunately, Dsk2 was not measured in this experiment. Other PIPs such as the deubiquitinases Ubp3 and Ubp1 were also unaltered. Interestingly, I also saw Cdc48 in the proteasome preparation and there were no changes in the levels of this protein. The Cdc48/p97 pathway is also involved in the targeted delivery of specific substrates to the proteasome (Barbin et al., 2010; Verma et al., 2011), although it is unknown how Cdc48 binds to the proteasome.

**Proteasomes from *ufd2*Δ are less abundant for Rad23.**

There could be any number of factors that could potentially be restricting the Rpn1-Rad23 interaction *in vivo*. Ufd2 is one such factor, and Pth2 is another. It has been shown that Pth2, a mitochondrially-localized peptidyl-tRNA hydrolase, interacts with Rad23 and Dsk2 (Ishii et al., 2006). However, there is no evidence that speaks to the significance of such an interaction. I questioned if Rad23 or Dsk2 are bound to proteasomes in a *PTH2* null strain. Ufd2, an E4/chain elongation enzyme, has been postulated to hand off Rad23 to the proteasome (Kim et al., 2004). So, I questioned how the levels of Rad23 might be affected in a deletion mutant. Proteasomes purified from a *pth2*Δ null mutant have wild-type levels of Rad23 and Dsk2 proteins, however, *ufd2*Δ proteasomes have less Rad23 associated with them than a wild-type proteasome does (Figure 5.2) although they have equivalent amounts of another UBA-UBL protein, Dsk2.

**Discussion**

Here I observed that the simultaneous absence of the ubiquitin interaction domains of Rpn10 and Rpn13 was sufficient for reducing Rad23 interaction with proteasomes. However, since the sole loss of Rpn13 does not impinge on loss of Rad23 (Table 5.4), it may be true that either only Rpn10 contributes to binding of Rad23, or that both intrinsic receptors must be mutated to create this change. While no perturbation in Rpn1 in combination with either Rpn10 or Rpn13 diminished binding, it seems questionable as to which subunit of the proteasome is the main docking site for Rad23.

I also show that deletion of Ufd2, an E4 enzyme, decreases the presence of Rad23 at the proteasome. The structure of Ufd2 binding to the UBL domains of Rad23 and Dsk2 has been solved (Hänzelmann et al., 2010). The interaction of Rad23/Dsk2 with Ufd2 has been shown to be important for the turnover of some substrates (Richly et al., 2005). Hence, this interaction is physiologically relevant towards protein turnover. Since Ufd2 promotes substrate degradation and delivery, it is not likely that it competes for binding to Rad23 and Dsk2 with the proteasome. It seems more reasonable that there is some cooperativity between Ufd2 and the proteasomes. It is unclear, how the UBL domains of Rad23/Dsk2 could potentially interact simultaneously with Ufd2 and docking sites on the proteasome.

No mutational perturbations decreased Ubp6 binding to the proteasome, and binding to either Rpn1 and/or lid subunits is enhanced by dual mutations in Rpn10 and Rpn13. Dissecting the increased presence of Ubp6 at Rad23-derived proteasomes may prove to be challenging. Perhaps studying the activity of substrates and PIPs known to rely on Ubp6 might shed some light in this arena.

Taken together, the interaction of UBA-UBL proteins creates a very complicated binding landscape. The interactions for Dsk2 and Rad23 appear to be, at a minimum, bidentate.

## Figure legends

### Figure 5.1. **Rpn10 and Rpn13 contribute to docking of UBA-UBL receptor proteins.**

(A) Affinity-purified *rpn10-UIM rpn13-KKD rpn1-D517A* proteasomes contain reduced levels of Ub conjugates in comparison to proteasomes from an *rpn10-UIM rpn13-KKD* strain. (B) *rpn10-UIM rpn13-KKD rpn1-D517A* proteasomes contain less Ddi1 and Dsk2 in comparison to proteasomes from a *rpn10-UIM rpn13-KKD*, as shown in the densitometric quantification of UBA-UBL proteins found in affinity-purified proteasomes represented in (A). (C) Affinity-purified *rpn10-UIM rpn13-KKD rpn1-D517A* proteasomes contain reduced levels of Rad23, Dsk2, Ddi1, and Ub conjugates in comparison to a fully WT strain containing no genetic manipulations in receptor genes. Levels of UBA-UBL proteins, the lid subunit Rpn12, and polyubiquitin are shown for affinity-purified proteasomes (IP) and in the whole cell extract input (WCE). (D) Affinity purified fully wild-type proteasomes are compared to *rpn10-UIM rpn13-KKD* proteasomes.

### Figure 5.2. **Ufd2 contributes to recruitment of Rad23 to the 26S proteasomes.**

(A) PRE1<sup>FLAG</sup> *ufd2Δ* and *pth2Δ* proteasomes were immunoprecipitated from cells under native conditions. Immunoprecipitates were resolved by SDS-PAGE, transferred to nitrocellulose and immunoblotted with the indicated antibodies.

**Table 5.1 Strains used in this chapter****Yeast strains**

<b>RJD #</b>	<b>Genotype</b>	<b>Source</b>
RJD4299	<i>Mata leu2 his3 ad2 pth2::KanMX pre1::PRE1-FlagHIS6</i>	this study
RJD4300	<i>Mata leu2 his3 ad2 ufd22::KanMX pre1::PRE1-FlagHIS6</i>	this study
RJD5034	<i>MATA leu2-3, his3-11,-15, trp1-1, ura3-1, ade2-1, rpn1::KanMX6 [pRS316-Rpn1-URA] arg4::KanMX lys2::HIS3 CAN1 rpn11::RPN11-FLAG-HphMX</i>	this study
RJD4830	<i>MATA leu2-3, his3-11,-15, trp1-1, ura3-1, ade2-1, rpn1::KanMX6 [pRS316-Rpn1-URA] rpn13::TRP1 arg4::KanMX lys2::HIS3 CAN1 rpn11::RPN11-FLAG-HphMX</i>	this study

**Table 5.2. PIPS that are less abundant in *rpn13Δ* proteasomes**

<b>Gene</b>	<b>Peptides</b>	<b>Sequence Coverage [%]</b>	<b>Ratio H/L</b>	<b>Significance</b>	<b>Variability [%]</b>
DLD3	4	9.5	1.7	6.5E-04	14.5
PMA2	5	7.1	1.6	9.7E-04	13.5
G3P2	17	52.1	1.5	5.4E-03	13.7
MXR1	5	28.3	1.5	6.9E-03	14.2
OYE2	3	10.2	1.5	7.1E-03	30.3
REI1	8	27.2	1.5	7.3E-03	9.3
FAF1	2	2.9	1.5	8.0E-03	2.5
YJ11B	10	7.9	1.4	8.6E-03	3.9
DHYS	2	5.2	1.4	1.2E-02	0.3
YG3Y	3	9.8	1.4	1.4E-02	16.4
SPE3	2	9.6	1.4	1.5E-02	15.6
ENO2	18	48.1	1.4	1.5E-02	18.8
TRM8	3	11.5	1.4	1.6E-02	19.7
RRB1	4	11	1.4	1.7E-02	26.5
RIO1	4	9.9	1.4	1.7E-02	16.9
APA1	1	4	1.4	1.9E-02	4.7
NOP4	14	26.1	1.4	2.0E-02	20.9
DBP2	19	41	1.4	2.1E-02	20.6
IF4A	2	8.1	1.4	2.4E-02	7.0
REX4	1	5.5	1.4	2.6E-02	6.3
SSF1	7	21	1.3	2.9E-02	5.7
LEU1	44	53.8	1.3	3.1E-02	17.2
REP2	1	5.1	1.3	3.2E-02	12.5
YNL010W	1	4.1	1.3	3.5E-02	10.7
RNT1	4	10.4	1.3	3.7E-02	4.6
SDA1	2	3.8	1.3	3.9E-02	0.4
NSR1	17	40.1	1.3	3.9E-02	14.5
MAE1	4	9	1.3	3.9E-02	15.0
ALFT	8	36.2	1.3	4.0E-02	10.2
NMD3	9	19.7	1.3	4.0E-02	10.2
PGK	11	33.9	1.3	4.1E-02	10.8
YC16	2	13.1	1.3	4.3E-02	9.6
MRD1	11	15.8	1.3	4.5E-02	15.0
MAS5	15	37.2	1.3	4.6E-02	8.9
NOP13	14	36.7	1.3	4.9E-02	33.9
NOC3	2	3.2	1.3	4.9E-02	17.7
ESF1	24	43.5	1.3	5.0E-02	8.6
CCT1	5	12	1.3	5.1E-02	14.6
YD173	2	6.1	1.3	5.2E-02	8.4
CF130	2	1.1	1.3	5.3E-02	20.7
ARP5	4	6	1.3	5.4E-02	13.8
OTU2	5	18.6	1.3	5.5E-02	27.2

PYC2	3	3.3	1.3	5.6E-02	16.5
GLN1	6	15.9	1.3	5.6E-02	15.2
URA3	5	19.9	1.3	5.7E-02	21.0
YIJ1	4	6.2	1.3	5.8E-02	7.6
YDR341C	4	7.6	1.3	5.8E-02	11.2
SQT1	1	4.2	1.3	5.8E-02	13.9
CPR1	2	21	1.3	5.9E-02	6.2
IPI3	7	16	1.3	6.2E-02	13.3
AROC	6	18.6	1.3	6.3E-02	10.7
ADH1	14	45.1	1.3	6.7E-02	6.4
TEF4	16	37.1	1.3	6.7E-02	9.9
RL22B	4	45.1	1.3	6.8E-02	4.7

**Table 5.3. PIPS that are more abundant in *rpn13Δ* proteasomes**

<b>Gene</b>	<b>Peptides</b>	<b>Sequence Coverage [%]</b>	<b>Ratio H/L</b>	<b>Significance</b>	<b>Variability [%]</b>
YPL168W	1	1.6	0.02	2.4E-04	31.794
PDC1	29	69.1	0.04	6.0E-03	145.27
OSH6	3	10.7	0.05	1.0E-02	126.98
SIL1	1	5.5	0.05	1.1E-02	27.955
PYK1	47	81.8	0.05	1.2E-02	118.92
SAM2	27	62	0.05	1.4E-02	81.893
GPM1	22	83	0.05	1.5E-02	106.42
MET6	54	68.3	0.05	1.5E-02	100.29
PGK1	42	80	0.06	1.8E-02	95.571
ADH1	25	68.7	0.06	2.0E-02	135.93
FUR1	7	51.9	0.06	2.0E-02	89.866
YNL010W	10	62.2	0.06	2.1E-02	80.56
PMI40	5	26.1	0.06	2.1E-02	102.34
HEM2	2	11.7	0.06	2.2E-02	69.463
TDH2	27	63.9	0.06	2.2E-02	65.311
ELP4	2	9.2	0.06	2.4E-02	17.587
TDH3	36	91.3	0.06	2.5E-02	116.57
TMA19	6	31.1	0.06	2.7E-02	80.741
TIF11	3	22.9	0.06	2.8E-02	71.455
INO1	12	33.8	0.07	2.8E-02	126.63
GND1	17	42.9	0.07	2.8E-02	89.841
HAM1	4	42.6	0.07	2.9E-02	44.718
SAH1	27	57.2	0.07	2.9E-02	129.49
RPE1	4	24.8	0.07	3.1E-02	133.26
FBA1	21	69.6	0.07	3.3E-02	105.88
FUM1	2	6.6	0.07	3.5E-02	19.147
TIM44	2	7.7	0.07	3.5E-02	66.81
ADE8	2	15	0.07	3.5E-02	45.027
SPE3	9	38.6	0.07	3.5E-02	77.763
FPR1	6	57.9	0.07	3.5E-02	87.846
TPI1	13	50	0.07	3.6E-02	75.258
EFT1	46	64.4	0.07	4.0E-02	91.02
YPL184C	2	5.4	0.07	4.1E-02	102.96
ACO1	18	36	0.07	4.1E-02	92.781
IPP1	11	61.7	0.08	4.2E-02	99.526
ENO2	41	74.4	0.08	4.2E-02	114.84
HPT1	8	40.7	0.08	4.3E-02	110.13
TAL1	20	56.1	0.08	4.4E-02	93.278
PGM1	2	3.9	0.08	4.4E-02	2.9083
ACS2	13	27.8	0.08	4.5E-02	64.316
YKR043C	2	11.4	0.08	4.5E-02	75.563
HOM6	13	57.4	0.08	4.5E-02	91.978

YNL134C	9	38	0.08	4.6E-02	57.544
TRM10	1	2.7	0.08	4.7E-02	33.759
FPP1	7	29.3	0.08	4.7E-02	96.144
ARG3	10	44.7	0.08	4.8E-02	71.591
OLA1	21	63.7	0.08	4.8E-02	95.232
ARF1	6	34.3	0.11	4.9E-02	60.556

**Table 5.4. Ubiquitin receptor levels are unchanged in *rpn13Δ* proteasomes.**

<b>Gene</b>	<b>Peptides</b>	<b>Sequence Coverage [%]</b>	<b>Ratio H/L Normalized</b>	<b>Significance</b>	<b>Variability [%]</b>
DDI1	1	6.8	1.01	0.44	17.9
RAD23	7	24.6	0.90	0.31	13.1
UBP6	8	18	0.93	0.36	27.9
RPN10	11	47.8	0.94	0.39	26.1
UBP3	5	5.6	0.97	0.45	36.5
UBP1	7	13.8	0.97	0.44	14.6
CDC48	36	47.2	0.99	0.49	12.1

**Figure 5.1. Rpn10 and Rpn13 contribute to docking of UBA-UBL receptor proteins.**

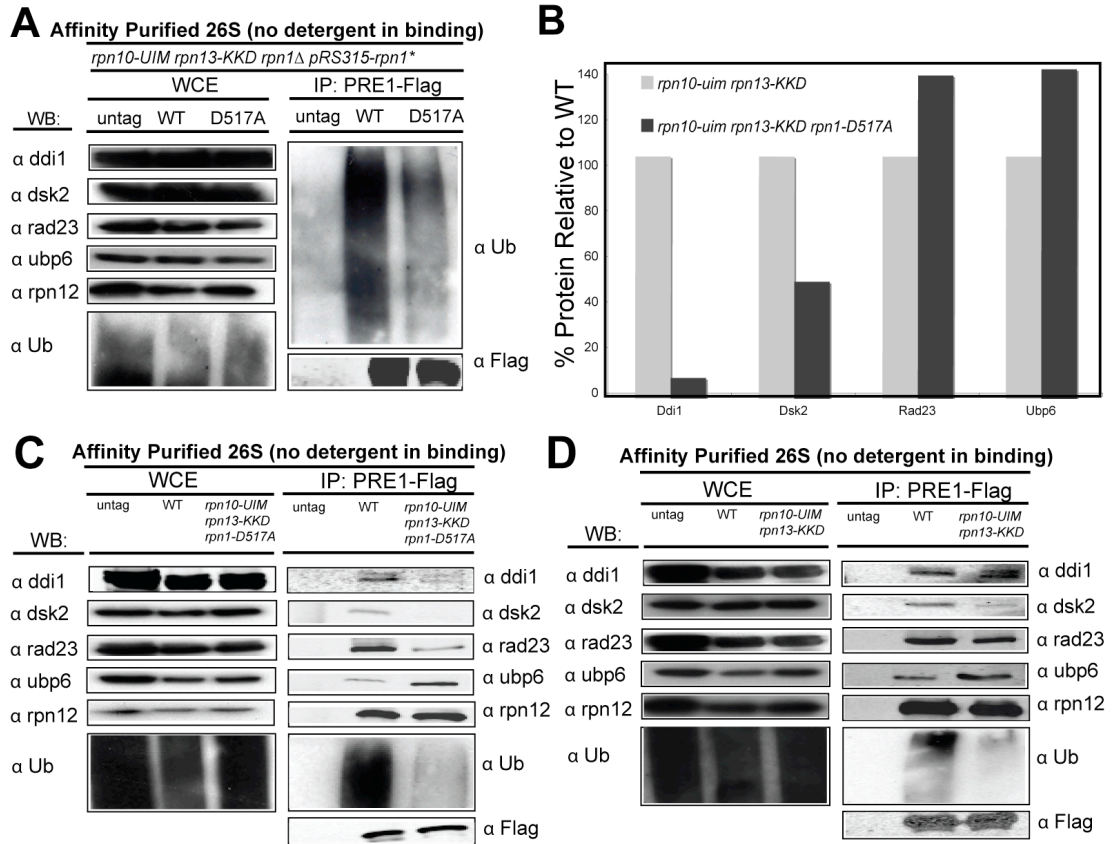
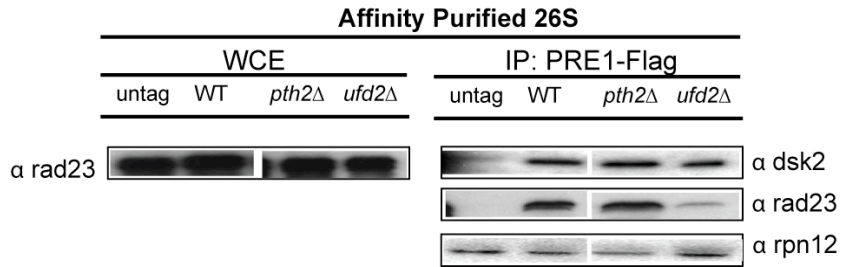


**Figure 5.2. Ufd2 contributes to recruitment of Rad23 to the 26S proteasomes.**



## **Chapter 6:**

**Mitochondrial import and methionine synthesis pathways are perturbed by interference of UBA-UBL binding to the proteasome**

## Introduction

I recently described the *rpn1-D517A* mutant that impairs binding of the UBA-UBL protein Ddi1 (Chapter 3). Little is known about the contribution Ddi1 makes to substrate delivery to the proteasome. This question has been hard to tackle considering the breadth of roles Ddi1 plays in other biochemical pathways that may or may not be related to its role in the UPS (Díaz-Martínez et al., 2006; Gabriely et al., 2008; Lustgarten and Gerst, 1999).

Here, I use the *rpn1-D517A* proteasome *cis* mutant as an indicator of how a specific impingement upon Ddi1 binding to the proteasome may perturb cell physiology in a UPS-dependent manner. Although the *rpn1-D517A* mutant does not strictly mimic loss of *DDI1* (Chapter 4), probing further into the physiology of this mutant may provide revelations even towards that point.

Each UBA-UBL receptor has a specific substrate repertoire it delivers to the proteasome (Verma et al., 2004). One natural question was: can novel Ddi1-specific UPS substrates be discovered with the *rpn1-D517A* mutant? To identify novel substrates and understand the physiological consequences of the deletion of the natural Ddi1 binding site, *rpn1-D517A* mutant proteasomes were analyzed using a quantitative mass spectrometry technique. Proteins that were found both more and less abundant at mutant proteasomes were probed further and revealed novel roles for the proteasome in cysteine and methionine biosynthetic pathways and in mitochondrial protein import. Further, I identify a potential new substrate of the proteasome, Aac2, a mitochondrial ADP/ATP carrier.

## Methods

### Yeast strains and culture methods

Strains were grown and crossed according to standard procedures. Table 6.1 lists all strains used in this chapter.

### SILAC analysis of 26S proteasomes

Done as described in detail in Chapter 3.

### Rpn1-D517A strain construction

For the preparation of the *rpn1-D517A strain*, a 3.2 kb fragment was PCR amplified using primers TG269 and TG270 from RDB2300 bearing 85 bp in the 5' UTR, the entire Rpn1 ORF containing internal *AvrII* and *EagI* silent mutations and a D517A mutation, and 85 bp past the stop codon. A second PCR product of 1.6 kb was amplified using primers TG271 and TG272 from pFA6a-KanMX6 (Longtine et al., 1998) containing flanking overlapping sequences with primer TG270, the entire KanMX6 cassette, and sequences overlapping with nucleotides beginning 86 bp downstream of the Rpn1 stop codon. A fusion PCR was performed to fuse these amplification products together. This 4.8 kb fusion PCR product was then transformed into RJD4006 using a standard LiAc protocol creating RJD5151. Integrants were verified by PCR, and the presence of the mutation was determined by restriction mapping with *AvrII* and *EagI* and sequencing.

### High-throughput yeast strain crossing

High-throughput crossing via the SGA method was used to cross GFP-tagged ORF strains to RJD4006 or RJD5151 (Tong et al., 2001). For SGA analysis, the *MAT $\alpha$*  starting strains, *lyp1 $\Delta$  his3 $\Delta$ 1 leu2 $\Delta$ 0 ura3 $\Delta$ 0 met15 $\Delta$ 0 can1 $\Delta$ ::STE2pr-LEU2 pdr5 $\Delta$ ::ADHpr-NLS-mRFP1-URA3* (RJD 4006) or *lyp1 $\Delta$  his3 $\Delta$ 1 leu2 $\Delta$ 0 ura3 $\Delta$ 0 met15 $\Delta$ 0 can1 $\Delta$ ::STE2pr-LEU2 pdr5 $\Delta$ ::ADHpr-NLS-mRFP1-URA3 rpn1::rpn1-D517A-KanMX6* (RJD 5151), were mated to 87 individual *MAT $\alpha$*  strains from the Invitrogen yeast GFP collection, *his3 $\Delta$  leu2 $\Delta$ , met15 $\Delta$  ura3 $\Delta$  XXX-GFP-HIS3*. These strains were mated on SC–His–Ura. Diploids were selected on SC–His–Ura plates for 1 day at 30°C and then pre-sporulated for 1.5 days at 25°C on GNA plates. Cells were sporulated on SPO plates at 25°C for 10–14 days. To select for *MAT $\alpha$*  *lyp1 $\Delta$  his3 $\Delta$ 1 leu2 $\Delta$ 0 ura3 $\Delta$ 0 met15 $\Delta$ 0 can1 $\Delta$ ::STE2pr-LEU2 pdr5 $\Delta$ ::ADHpr-NLS-mRFP1-URA3 XXX-GFP-HIS3 (+/- rpn1::rpn1-D517A-KanMX)* haploids, spores were haploid selected on either SD-Ura–Arg-Lys supplemented with canavanine and S-AEC +/- MSG and G418 for 2 days at 30°C. Haploids were again reselected in the appropriate haploid selection media prior to preparation of glycerol stocks of the resultant strains.

### High-throughput microscopy

Cells were grown in 96-well plates until saturated in haploid selection liquid culture. Three hundred microliters of C/AA/Dex liquid media (1.6 g Yeast Nitrogen Base without ammonium sulfate and amino acids, 5 g Ammonium Sulfate, 11 g Succinic Acid, 6.9 g Sodium Hydroxide, +amino acids, +2% dextrose, up to 1 L with water) was inoculated with 5  $\mu$ L of saturated culture and allowed to grow overnight. The next day, 100  $\mu$ L of

C/AA/Dex media was inoculated with 5  $\mu$ l of overnight culture and grown at 30°C for 2 hours. Cells were pelleted, washed in TE, and then resuspended in 100  $\mu$ l of TE, in which they are transferred to glass-bottom 96-well plates coated with Concanavalin A. Cells were allowed to settle for 20 minutes before imaging on the 96-well plate microscope. A fluorescence microscopy system (Image Express Micro; Molecular Devices) was used to acquire images. The data collected was analyzed in MatLab.

### **Protein turnover experiments**

For galactose promoter shutoffs, yeast transformed with *GALI* promoter-driven expression plasmids were grown in synthetic medium with raffinose as the sole carbohydrate source. When the cultures reached an OD<sub>600</sub> 0.5, galactose was added to 2% for 2–3 hours. Expression was shut off by the addition of 2% dextrose, at which point samples were collected for up to 120 minutes after promoter shut off. For cycloheximide chases, yeast strains were grown to an OD<sub>600</sub> ~ 0.5, and then treated with 100  $\mu$ g/ml cycloheximide, at which point a chase was initiated. Lysates were prepared by making boiling extracts. Immunoblotting was done using the indicated antibodies. The Aac2 antibody was a kind gift from Carla Koehler (UCLA).

### ***In vivo* Hsp60 precursor accumulation assay**

Assessment of Hsp60 precursor accumulation was done as described (Schiller et al., 2008). Briefly, strains were grown in YPD at 30°C until they reached an OD<sub>600</sub> ~ 0.5, at which point half of the culture was shifted to 37°C for 4–5 hours. Samples were taken and prepared by making boiling extracts. Lysates were resolved by 6% SDS-PAGE,

transferred onto nitrocellulose membranes, and immunoblotted with anti-Hsp60 (Novus Biologicals).

### **Yeast boiling extract preparation**

Cells were pelleted and washed in stop buffer (50 mM Tris-HCl pH 7.5, 0.02% NaN<sub>3</sub>, 50 mM NaF). Next, 0.3 mL of glass beads per 8 OD units were directly added to the cell pellets and the samples were boiled for 3 minutes. An equal volume of 1X SDS buffer was added prior to fastprepping for 60 seconds at maximum speed. The samples are then boiled again for another 5 minutes and spun at top speed for 2 minutes prior to being loaded onto SDS-PAGE gels.

## **Results**

### **Rpn1-D517A proteasomes show diminished amounts of specific PIPs.**

In our efforts to understand the physiological consequence of having a *cis* mutation in the proteasome, we performed quantitative mass spectrometry using the st<sub>a</sub>b<sub>l</sub>e is<sub>o</sub>t<sub>o</sub>p<sub>e</sub> la<sub>b</sub>e<sub>l</sub>i<sub>n</sub>g wi<sub>t</sub>h am<sub>i</sub>n<sub>o</sub> ac<sub>i</sub>d<sub>s</sub> me<sub>t</sub>h<sub>o</sub>d (SILAC). Rpn1<sup>FLAG</sup> *rpn13Δ* cells were labeled with heavy lysine and arginine while Rpn1<sup>FLAG</sup> *rpn13Δ rpn1-D517A* cells were labeled with light lysine and arginine. The cells were mixed prior to lysing, and a proteasome affinity purification was carried out. The SILAC analysis revealed a list of proteins that were found less abundantly in light-labeled *rpn13Δ rpn1-D517A* proteasomes when compared to heavy-labeled *rpn13Δ* proteasomes (Table 6.2). Some of the less-abundant PIPs were also identified in a prior report as specific proteasome-interacting proteins (Guerrero et

al., 2008). Others had been identified as unstable proteins (Belle et al., 2006), or even UPS substrates (SCUD; <http://scud.kaist.ac.kr/index.html>). I hypothesized that novel substrates may be represented in this class of SILAC hits in which the protein was found less abundantly in Rpn1-D517A-containing proteasomes and that were known unstable proteins. Based on further suggested criteria for selecting putative UPS substrates (Verma et al., 2011), I chose a handful of SILAC hits to test for their dependence on *rpn1-D517A*. In turnover experiments (done either by galactose promoter shutoff or cycloheximide chases), I observed that most of the proteins I tested were fairly stable proteins (Figure 6.1). There were a few proteins that were unstable (Rot1, Aro8, Sam1, Rrp6, and Aac2). Notably, Aac2 appeared to be the only protein whose turnover may have been slightly stabilized in the *rpn1-D517A* mutant. For the other tested proteins, it is unclear what their role is at the proteasome and if the decrease in their abundance is directly or indirectly related to mutation of Rpn1.

### **Galactose-inducible Aac2 appears to be stabilized in *rpn1-D517A*.**

I was intrigued by the subtle, but consistent stabilization of galactose-inducible HA-tagged Aac2 (Figure 6.1I). A replicate of this experiment is shown (Figure 6.2A). Interestingly, at least two lower-molecular-weight species also appear more stable in the *rpn1-D517A* mutant cells than in a wild-type strain. Aac2 is an inner mitochondrial membrane ADP/ATP carrier (Lawson and Douglas, 1988). I questioned if I would see turnover defects of endogenous pools of Aac2. Using an Aac2 antibody, I analyzed endogenous Aac2 turnover by initiating a cycloheximide chase at 30°C for 90 minutes. Under these experimental conditions, endogenous Aac2 appears to be only slightly

unstable and the *rpn1-D517A* mutant does not seem to have a drastic effect on turnover (Figure 6.2B).

### **Cellular concentrations of Sam2, Cys3, and Fsr1 are shifted in *rpn1-D517A* mutants.**

In the search for more novel substrates and insights into the potential physiological consequences of the *rpn1-D517A* mutation, I chose to look at steady-state levels of proteins that were both less abundant (Table 6.3) and more abundant (Table 6.4) at *rpn1-D517A* containing proteasomes via a high-throughput method. Using SGA technology, I mated an *rpn1-D517A* containing strain against 87 GFP-tagged ORFs that were selected from the SILAC datasets. The resultant strains were then analyzed on a high-throughput microscope that quantified the fluorescence intensity of each cell line. I hypothesized that proteins that were less abundant in mutant proteasome preparations and which met the proposed substrate criterion would have higher steady-state concentrations (Verma et al., 2011). To my surprise, from the proteins found in Table 6.3 that were used in the high-throughput analysis, two proteins appeared to have a higher steady-state concentration (Sam2 and Cox4) and two proteins had lower steady state concentrations in an *rpn1-D517A* background (Cys3, Ado1). No proteins queried from those selected from Table 6.4 were found to have steady-state levels outside of the GFP fluorescence standard deviation (Figure 6.3).

Based on these results, Sam2, Cox4, Cys3, and Ado1 were analyzed further by immunoblotting lysates of log phase cells that were treated with a translation inhibitor, cycloheximide, for 1 hour, and cells that were not treated. Several other potentially

unstable proteins (Belle et al., 2006) were also tested in parallel for dependence on *rpn1-D517A* for turnover. Surprisingly, no tested proteins appeared unstable after cycloheximide treatment. In agreement with the GFP fluorescence experiment, more lower-molecular-weight species of Sam2 were present in *rpn1-D517A* cells while a higher-molecular-weight species of Cys3 was less abundant. However, no effect on Ado1 and Cox4 was detected. Interestingly, I also observed less of a lower-molecular-weight species of Frs1 in the *rpn1-D517A* mutant (Figure 6.4).

No changes were noted in steady-state levels of some of the mitochondrial proteins that were found to be more abundant in mutant proteasomes (Table 6.4) when they were similarly probed by immunoblotting log phase cell lysates with or without cycloheximide (Figure 6.5).

### **Methionine and cysteine biosynthesis pathways appear perturbed in *rpn1-D517A* cells.**

The change in steady-state levels of potential modified and unmodified forms of these metabolic enzymes I discovered to be perturbed in *rpn1-D517A* cells is intriguing because these enzymes are known to regulate interconnected metabolic pathways, cysteine/methionine biosynthesis, and the methyl cycle (Lafaye et al., 2005).

Furthermore, I found that many of the other enzymes in this pathway, including: Met6 and Sah1 were also found in decreased levels at mutant proteasomes (Table 6.3).

Additionally, over expression of Met6 caused slow growth in an *rpn1-D517A* mutant.

Taken together, there appears to be some perturbation in this pathway that could be probed further (Figure 6.6).

***rpn1-D517A* mutants have an abundance of mitochondrial proteins at their proteasomes and respiration defects.**

From the SILAC dataset of proteins that were found more abundantly at *rpn1-D517A* mutant proteasomes, there appeared to be enrichment for mitochondrial proteins (Table 6.4). In fact, more than 60% of these SILAC hits were mitochondrial proteins (Figure 6.7A). Similarly, in my prior *rpn13Δ* SILAC analysis, I found that mitochondrial proteins are also enriched at mutant proteasomes in comparison to wild type, albeit to a lower extent (Chapter 5, Table 5.3). This result caused me to postulate that the *rpn1-D517A* mutant may have mitochondrial defects. Many yeast strains with mitochondrial defects are characterized by an inability to respire/grow on a non-fermentable carbon source, such as glycerol (Sherman and Slonimski, 1964). I observed that *rpn1-D517A* cells did not have respiratory defects. However, since the SILAC analysis was performed on *rpn13Δ rpn1-D517A* cells, I also tested this cell line and found it to show lethality on glycerol media. Similarly a  $\rho^{\circ}$  strain lacking mitochondrial DNA also shows lethality on glycerol (Figure 6.7B).

***rpn13Δ rpn1-D517A* mutants accumulate precursor forms of Hsp60.**

Interestingly, 100% of the mitochondrial proteins that accumulate at *rpn13Δ rpn1-D517A* proteasomes are encoded by nuclear DNA (Table 6.4). Since these proteins must be imported into the mitochondria, I asked if there is an accompanying defect in the import of mitochondrial preproteins *in vivo*. Hsp60 is a nuclear-DNA-encoded heat shock protein that is imported into mitochondria (Cheng et al., 1989). To test for the accumulation of precursors *in vivo*, mutant strains were grown to mid-logarithmic phase

and then shifted to 37°C for 4-6 hours. Cell extracts were analyzed for precursor and mature forms of Hsp60. As a control, a *tim44-R180K* strain, a strain harboring a mutant in a mitochondrial inner membrane transport protein, was also used in this assay (Schiller et al., 2008). The *rpn13Δ rpn1-D517A* mutant accumulated Hsp60 precursors similarly to the *tim44-180K* mutant after growing at 37°C (Figure 6.8A). To test if general proteasome perturbation influences accumulation of Hsp60 precursors, a panel of proteasome subunit mutants was also tested. A proteasome mutant containing a mutation in an ATPase subunit, *rpt6-1*, also showed pHsp60 accumulation, even when grown at just 30°C (Figure 6.8B). Additionally, an *rpn4Δ rpn1-D517A* accumulated precursors as well as a *rpn10-uim rpn1-D517A* mutant, although to a lesser extent (Figure 6.8C). Since binding of both Ddi1 and Dsk2 is reduced in an *rpn13Δ rpn1-D517A* strain, a *ddi1Δ dsk2Δ* strain was also tested, and appears to accumulate precursor Hsp60 as well (Figure 6.8C). A *pdr5Δ* strain treated with proteasome inhibitor, MG132, also appeared to accumulate a barely detectable level of pHsp60. Taken together, this data is indicative that inhibition of proteasome degradation, by mutation, drug treatment, or elimination of Ub receptor docking, leads to accumulation of precursor Hsp60 *in vivo*.

## Discussion

Here I report that the mitochondrial ADP/ATP carrier, Aac2 is slightly stabilized in an *rpn1-D517A* mutant when over expressed. To validate Aac2 further as a substrate, an observation of ubiquitlyated Aac2, identifying Ddi1 as a receptor of Aac2 and finding the ideal conditions for turnover of endogenous Aac2 would be essential. Already, two

proteomic studies have independently assigned Aac2 as a UPS substrate (Mayor et al., 2007; Tagwerker et al., 2006).

The notion of Aac2 acting as a UPS substrate is intriguing since very few mitochondrial proteins have ever been validated as proteasome substrates. Fzo1, a mitochondrial transmembrane GTPase important for mitochondrial fusion, has been validated as an UPS substrate through basic biochemical methods and in a proteomic screen (Cohen et al., 2008; Tagwerker et al., 2006), although there also appears to be a non-proteolytic pathway that may also degrade it (Escobar-Henriques et al., 2006). The mitochondria does itself not have a UPS system, although there appear to be some bacterial-like proteases (Weber et al., 1996), and an N-end rule type protease system that controls mitochondrial protein stability (Vögtle et al., 2009). Since proteasomes are localized to the cytoplasm and nucleus, how do mitochondrial proteins become proteasome substrates? It has been postulated that Cdc48, in conjunction with Vsm1 as an adaptor, acts as segregase at the mitochondria, extracting mitochondrial proteins so that they are accessible to the proteasome for degradation. Such a role has already been shown to be essential for degradation of Fzo1 (Heo et al., 2010).

In further probing possible physiological consequences of having a *cis* proteasome mutant, I stumbled across changes in the equilibrium of potentially modified and unmodified forms of proteins, Fsr1, Cys3, and Sam2. *FRS1* is an essential gene that codes for a subunit of cytoplasmic phenylalanyl-tRNA synthetase (Sanni et al., 1991). My SILAC could not be used to determine how Fsr1 is possibly post translationally modified in cells. It will be interesting to see if the disequilibrium of the forms of Fsr1 has any effects on protein translation.

Levels of potentially modified forms of the enzymes Sam2 and Cys3 also exhibited perturbations in an *rpn1-D517A* mutant. More interestingly, a seemingly large number of closely related enzymes are also perturbed. Since this class of enzymes regulates the synthesis of methionine, cysteine, sulfur metabolism, and the methyl cycle (the flux between *S*-Adenosylhomocysteine and homocysteine (Lafaye et al., 2005) it may be interesting to use biochemical testing for observing possible defects in the levels of key biosynthetic intermediates. Additionally, are these putative posttranslational modifications I observe in my immunoblots active/unactive forms of these enzymes? Currently, to my knowledge, there is no published data indicating if these enzymes are regulated by post-translational modifications.

I have also demonstrated that chemical or mutational perturbations to proteasome degradation led to import defects of Hsp60. The UPS has already been implicated in playing a role in mitochondria metabolism, however, I report the first role for the UPS in the import of mitochondrial proteins. The reported roles for the UPS in mitochondria function are broad and have no mechanistic basis. Pth2, a protein that binds Rad23 and Dsk2, is a negative regulator of mitochondrial function (Ishii et al., 2006). Rpn11, a deubiquitinase enzyme that is a lid subunit of the proteasome, causes mitochondria fission defects (Rinaldi et al., 2002). Human Rpn13 has also been observed to effect the localization of mitochondria within the cell and tRNA import into the mitochondria (Brandina et al., 2007; Qiu et al., 2006). To my knowledge, there is no literature which links the UPS to mitochondrial protein import.

I propose that the *rpn13Δ rpn1-D517A* mutant may effect import of Hsp60 in one of two ways. First, accumulation of some unknown substrate may have inhibitory effects

on mitochondrial import. Alternatively, *rpn13Δ rpn1-D517A* may have defects in degrading precursor Hsp60 that is not imported, due to damage, misfolding or other cellular events that would limit translocation of mitochondrial proteins (Figure 6.9).

In summary, the *rpn1-D517A* mutation limits binding of Ddi1 (Chapter 3) and disrupts the equilibrium of steady-state levels of Frs1, Cys3, and Sam2. The *rpn13Δ rpn1-D517A* mutant diminishes binding of Dsk2 and Ddi1 (Chapter 3), and leads to mitochondrial respiration and Hsp60 import defects. Hence, as a whole, the *rpn1-D517A* mutant leads to a broad pleiotrophic defects in multiple biochemical pathways. The *rpn1-D517A* mutant can be used as a tool, not only for studying docking of UBA-UBL proteins to the proteasome, but also for uncovering unknown facets of these diverse biochemical pathways.

## Figure legends

### Figure 6.1. **Screening for putative *rpn1-D517A* substrates from the SILAC data set**

Wild-type and *rpn1-D517A* cells carrying a plasmid that expressed GST-X or HA-X from the *GAL1* promoter were grown in raffinose medium and then induced with 2% galactose for 1–3 hours. Dextrose was added at  $T_0$  to extinguish expression and samples were taken at the indicated time points. Some turnover experiments were done as cycloheximide chases where either GFP or HA tagged ORFs which were integrated at the endogenous gene locus. For cycloheximide chases, cells were grown to an  $OD_{600}$  0.5–1 before initiation of a chase period with cycloheximide. Multiple proteins were screened by one of these methods: Rot1 (A), Dop1 (B), Gde1 (C), Aro8 (D), Sam1 (E), Met6 (F), Aro9 (E), Rrp6 (G), Dop1 (H), and Aac2 (I).

### Figure 6.2. **Galactose-inducible Aac2 is slightly stabilized in *rpn1-D517A*.**

(A) Wild-type and *rpn1-D517A* cells carrying a pGAL1-HA-Aac2 were grown in raffinose medium prior to induction with 2% galactose for 2 hours. Dextrose was added at  $T_0$  to extinguish expression and samples were taken at the indicated time points. To the right, quantification is shown. (B) Endogenous Aac2 turnover was assayed in a cycloheximide chase initiated once the indicated strains had reached an  $OD_{600} \sim 1$ . Boiling extracts were made at the indicated time points, resolved by SDS-PAGE, transferred to nitrocellulose and immunoblotted with an Aac2 antibody. (C) Schematic of Aac2 in the mitochondrial innermembrane.

**Figure 6.3. Steady-state concentrations of multiple GFP tagged ORFs change in an *rpn1-D517A* mutant.**

ORFS identified in the SILAC analysis as either more or less abundant in *rpn1-D517A rpn13Δ* cells in comparison to *rpn13Δ* were crossed into either a wild-type or a *rpn1-D517A* strain using SGA high-throughput crossing methodology. The resultant strains were grown to log phase, and GFP intensity was measured on a high-throughput fluorescence microscope. The change in fluorescence intensity between wild type and *rpn1* mutant strains was quantified in MatLab. The dashed line indicates the standard deviation. Any change falling within the standard deviation is considered non-significant. Several ORFS appeared to have either higher (Sam2 and Cox4) or lower (Cys3 and Ado1) steady-state concentrations in the *rpn1-D517A* mutant background.

**Figure 6.4. Steady-state concentrations of ORFs found less abundantly in *rpn13Δ rpn1-D517A* proteasomes**

GFP-tagged ORFS of proteins identified in the SILAC analysis as less abundant in *rpn13Δ rpn1-D517A* proteasomes were crossed into either a wild-type or *rpn1-D517A* mutant strain background using SGA methodology. Some of the strains were individually analyzed for being unstable (by treatment with cycloheximide for one hour) and for any changes in steady state (no cycloheximide treatment). Frs1, Sam2, and Cys3 were found to have differences in steady states of particular molecular weight species. An anti-GFP was used for immunoblotting and ponceaus S is shown to demonstrate even loading of all samples.

**Figure 6.5. Steady-state concentrations of ORFs found more abundant in *rpn13Δ rpn1-D517A* proteasomes**

GFP-tagged ORFs of proteins identified in the SILAC analysis as more abundant in *rpn13Δ rpn1-D517A* proteasomes were crossed into either a wild-type or *rpn1-D517A* mutant strain background using SGA methodology. Some of the strains were individually analyzed for being unstable (by treatment with cycloheximide for one hour) and for any changes in steady state (no cycloheximide treatment). An anti-GFP was used for immunoblotting and ponceaus S is shown to demonstrate even loading of all samples

**Figure 6.6. Methionine and cysteine biosynthetic pathways contain multiple enzymes that are perturbed in *rpn1-D517A*.**

A summary figure of the methionine and cysteine biosynthetic pathways. Bolded enzymes were found in the SILAC data set to be less abundant in *rpn13Δ rpn1-D517A* proteasomes. Interestingly, when GFP-ORF cell lines were assayed with and without cycloheximide, Cys3 and Sam2 showed different compositions of high and low molecular weight species in an *rpn1-D517A* strain. Additionally, over expression of galactose-inducible Met6 is slightly toxic in an *rpn1-D517A* strain.

**Figure 6.7. *rpn13Δ rpn1-D517A* mutants have mitochondrial defects**

(A) The data in this graph is a cellular functional grouping of the proteins represented in Table 6.4. More than 60% of proteins that are found more abundantly at proteasomes from *rpn13Δ rpn1-D517A* mutants are mitochondrial proteins. Nearly 55% of the mitochondrial proteins found are ribosomal (inset). (B) Equivalent concentrations of the

indicated strains, including a  $\rho^{\circ}$  mutant (a strain lacking mitochondrial DNA) were spotted at five-fold dilutions on plates containing either dextrose (YPD) or glycerol (YPG) at 30°C or 37°C for 2–3 days.

**Figure 6.8. *rpn13*Δ *rpn1-D517A* mutants accumulate Hsp60 precursor proteins.**

Accumulation of Hsp60 preprotein *in vivo* was assayed in the indicated yeast strains, including a *tim44-R810K* mutant that was used as a positive control (A). Cells were grown at 30°C until they reached an OD<sub>600</sub> 0.5, and subsequently shifted to 37°C for 4–6 hours. Extracts were analyzed by SDS-PAGE and immunoblotted with an Hsp60 antibody. Premature Hsp60 (p) and mature Hsp60 (m) are indicated on the figure. Panels A, B, and C are three separate experiments.

**Figure 6.9 Two hypotheses describe pHsp60 accumulation in proteasome mutants.**

The genetic or chemical inhibition of the proteasome may affect import of Hsp60 in one of two ways. First, accumulation of some unknown substrate may have inhibitory effects on mitochondrial import (A). Alternatively, *rpn13*Δ *rpn1-D517A* may have defects in degrading precursor Hsp60 that is not imported due to damage, misfolding, or other cellular events that would limit translocation across the mitochondrial membrane (B).

**Table 6.1. Strains used in this chapter**

<b>Yeast strains</b>		
<b>RJD #</b>	<b>Genotype</b>	<b>Source</b>
RJD5133	<i>Mata can1-100, leu2-3, his3-11,-15, trp1-1, ura3-1, ade2-1, rpn1::KanMX6 [pRS315-Rpn1-LEU] aro8::ARO8-3HA</i>	this study
RJD5134	<i>Mata can1-100, leu2-3, his3-11,-15, trp1-1, ura3-1, ade2-1, rpn1::KanMX6 [pRS315-Rpn1-D517A-LEU] aro8::ARO8-3HA</i>	this study
RJD5136	<i>Mata can1-100, leu2-3, his3-11,-15, trp1-1, ura3-1, ade2-1, rpn1::KanMX6 [pRS315-Rpn1-LEU] sam1::SAM1-3HA</i>	this study
RJD5136	<i>Mata can1-100, leu2-3, his3-11,-15, trp1-1, ura3-1, ade2-1, rpn1::KanMX6 [pRS315-Rpn1-D517A-LEU] sam1::SAM1-3HA</i>	this study
RJD4006	<i>lyp1Δ his3Δ1 leu2Δ0 ura3Δ0 met15Δ0 can1Δ::STE2pr-LEU2 pdr5Δ::ADHpr-NLS-mRFP1-URA3</i>	David Toczyski
RJD5151	<i>lyp1Δ his3Δ1 leu2Δ0 ura3Δ0 met15Δ0 can1Δ::STE2pr-LEU2 pdr5Δ::ADHpr-NLS-mRFP1-URA3 rpn1::rpn1-D517A-KanMX6</i>	this study
RJD5352	<i>MATa lyp1Δ his3Δ1 leu2Δ0 ura3Δ0 met15Δ0 can1Δ::STE2pr-LEU2 pdr5Δ::ADHpr-NLS-mRFP1-URA3 Gde1-GFP-HIS3</i>	this study
RJD5355	<i>MATa lyp1Δ his3Δ1 leu2Δ0 ura3Δ0 met15Δ0 can1Δ::STE2pr-LEU2 pdr5Δ::ADHpr-NLS-mRFP1-URA3 Gde1-GFP-HIS3 rpn1::rpn1-D517A-KanMX</i>	this study
TGY96well plate	<i>MATa lyp1Δ his3Δ1 leu2Δ0 ura3Δ0 met15Δ0 can1Δ::STE2pr-LEU2 pdr5Δ::ADHpr-NLS-mRFP1-URA3 Vas1-GFP-HIS3</i>	this study
TGY96well plate	<i>MATa lyp1Δ his3Δ1 leu2Δ0 ura3Δ0 met15Δ0 can1Δ::STE2pr-LEU2 pdr5Δ::ADHpr-NLS-mRFP1-URA3 Vas1-GFP-HIS3 rpn1::rpn1-D517A-KanMX</i>	this study
TGY96well plate	<i>MATa lyp1Δ his3Δ1 leu2Δ0 ura3Δ0 met15Δ0 can1Δ::STE2pr-LEU2 pdr5Δ::ADHpr-NLS-mRFP1-URA3 Cdc60-GFP-HIS3</i>	this study
TGY96well plate	<i>MATa lyp1Δ his3Δ1 leu2Δ0 ura3Δ0 met15Δ0 can1Δ::STE2pr-LEU2 pdr5Δ::ADHpr-NLS-mRFP1-URA3 Cdc60-GFP-HIS3 rpn1::rpn1-D517A-KanMX</i>	this study
TGY96well plate	<i>MATa lyp1Δ his3Δ1 leu2Δ0 ura3Δ0 met15Δ0 can1Δ::STE2pr-LEU2 pdr5Δ::ADHpr-NLS-mRFP1-URA3 Sac6-GFP-HIS3</i>	this study
TGY96well plate	<i>MATa lyp1Δ his3Δ1 leu2Δ0 ura3Δ0 met15Δ0 can1Δ::STE2pr-LEU2 pdr5Δ::ADHpr-NLS-mRFP1-URA3 Sac6-GFP-HIS3 rpn1::rpn1-D517A-KanMX</i>	this study
TGY96well plate	<i>MATa lyp1Δ his3Δ1 leu2Δ0 ura3Δ0 met15Δ0 can1Δ::STE2pr-LEU2 pdr5Δ::ADHpr-NLS-mRFP1-URA3 Dpm1-GFP-HIS3</i>	this study
TGY96well plate	<i>MATa lyp1Δ his3Δ1 leu2Δ0 ura3Δ0 met15Δ0 can1Δ::STE2pr-LEU2 pdr5Δ::ADHpr-NLS-mRFP1-URA3 Dpm1-GFP-HIS3 rpn1::rpn1-D517A-KanMX</i>	this study
RJD5568	<i>MATa lyp1Δ his3Δ1 leu2Δ0 ura3Δ0 met15Δ0 can1Δ::STE2pr-LEU2 pdr5Δ::ADHpr-NLS-mRFP1-URA3 Frs1-GFP-HIS3</i>	this study
RJD5569	<i>MATa lyp1Δ his3Δ1 leu2Δ0 ura3Δ0 met15Δ0 can1Δ::STE2pr-LEU2 pdr5Δ::ADHpr-NLS-mRFP1-URA3 Frs1-GFP-HIS3 rpn1::rpn1-D517A-KanMX</i>	this study
TGY96well plate	<i>MATa lyp1Δ his3Δ1 leu2Δ0 ura3Δ0 met15Δ0 can1Δ::STE2pr-LEU2 pdr5Δ::ADHpr-NLS-mRFP1-URA3 Tif3-GFP-HIS3</i>	this study
TGY96well	<i>MATa lyp1Δ his3Δ1 leu2Δ0 ura3Δ0 met15Δ0 can1Δ::STE2pr-LEU2</i>	this study

plate	<i>pdr5Δ::ADHpr-NLS-mRFP1-URA3 Tif3-GFP-HIS3 rpn1::rpn1-D517A-KanMX</i>	
RJD5353	<i>MATa lyp1Δ his3Δ1 leu2Δ0 ura3Δ0 met15Δ0 can1Δ::STE2pr-LEU2 pdr5Δ::ADHpr-NLS-mRFP1-URA3 Sam2-GFP-HIS3</i>	this study
RJD5356	<i>MATa lyp1Δ his3Δ1 leu2Δ0 ura3Δ0 met15Δ0 can1Δ::STE2pr-LEU2 pdr5Δ::ADHpr-NLS-mRFP1-URA3 Sam2-GFP-HIS3 rpn1::rpn1-D517A-KanMX</i>	this study
TGY96well plate	<i>MATa lyp1Δ his3Δ1 leu2Δ0 ura3Δ0 met15Δ0 can1Δ::STE2pr-LEU2 pdr5Δ::ADHpr-NLS-mRFP1-URA3 Aro2-GFP-HIS3</i>	this study
TGY96well plate	<i>MATa lyp1Δ his3Δ1 leu2Δ0 ura3Δ0 met15Δ0 can1Δ::STE2pr-LEU2 pdr5Δ::ADHpr-NLS-mRFP1-URA3 Aro2-GFP-HIS3 rpn1::rpn1-D517A-KanMX</i>	this study
RJD5570	<i>MATa lyp1Δ his3Δ1 leu2Δ0 ura3Δ0 met15Δ0 can1Δ::STE2pr-LEU2 pdr5Δ::ADHpr-NLS-mRFP1-URA3 Cox4-GFP-HIS3</i>	this study
RJD5571	<i>MATa lyp1Δ his3Δ1 leu2Δ0 ura3Δ0 met15Δ0 can1Δ::STE2pr-LEU2 pdr5Δ::ADHpr-NLS-mRFP1-URA3 Cox4-GFP-HIS3 rpn1::rpn1-D517A-KanMX</i>	this study
TGY96well plate	<i>MATa lyp1Δ his3Δ1 leu2Δ0 ura3Δ0 met15Δ0 can1Δ::STE2pr-LEU2 pdr5Δ::ADHpr-NLS-mRFP1-URA3 Ado1-GFP-HIS3</i>	this study
TGY96well plate	<i>MATa lyp1Δ his3Δ1 leu2Δ0 ura3Δ0 met15Δ0 can1Δ::STE2pr-LEU2 pdr5Δ::ADHpr-NLS-mRFP1-URA3 Ado1-GFP-HIS3 rpn1::rpn1-D517A-KanMX</i>	this study
TGY96well plate	<i>MATa lyp1Δ his3Δ1 leu2Δ0 ura3Δ0 met15Δ0 can1Δ::STE2pr-LEU2 pdr5Δ::ADHpr-NLS-mRFP1-URA3 Gpp1-GFP-HIS3</i>	this study
TGY96well plate	<i>MATa lyp1Δ his3Δ1 leu2Δ0 ura3Δ0 met15Δ0 can1Δ::STE2pr-LEU2 pdr5Δ::ADHpr-NLS-mRFP1-URA3 Gpp1-GFP-HIS3 rpn1::rpn1-D517A-KanMX</i>	this study
RJD5351	<i>MATa lyp1Δ his3Δ1 leu2Δ0 ura3Δ0 met15Δ0 can1Δ::STE2pr-LEU2 pdr5Δ::ADHpr-NLS-mRFP1-URA3 Dop1-GFP-HIS3</i>	this study
RJD5354	<i>MATa lyp1Δ his3Δ1 leu2Δ0 ura3Δ0 met15Δ0 can1Δ::STE2pr-LEU2 pdr5Δ::ADHpr-NLS-mRFP1-URA3 Dop1-GFP-HIS3 rpn1::rpn1-D517A-KanMX</i>	this study
RJD5566	<i>MATa lyp1Δ his3Δ1 leu2Δ0 ura3Δ0 met15Δ0 can1Δ::STE2pr-LEU2 pdr5Δ::ADHpr-NLS-mRFP1-URA3 Met6-GFP-HIS3</i>	this study
RJD5567	<i>MATa lyp1Δ his3Δ1 leu2Δ0 ura3Δ0 met15Δ0 can1Δ::STE2pr-LEU2 pdr5Δ::ADHpr-NLS-mRFP1-URA3 Met6-GFP-HIS3 rpn1::rpn1-D517A-KanMX</i>	this study
TGY96well plate	<i>MATa lyp1Δ his3Δ1 leu2Δ0 ura3Δ0 met15Δ0 can1Δ::STE2pr-LEU2 pdr5Δ::ADHpr-NLS-mRFP1-URA3 Aro9-GFP-HIS3</i>	this study
TGY96well plate	<i>MATa lyp1Δ his3Δ1 leu2Δ0 ura3Δ0 met15Δ0 can1Δ::STE2pr-LEU2 pdr5Δ::ADHpr-NLS-mRFP1-URA3 Aro9-GFP-HIS3 rpn1::rpn1-D517A-KanMX</i>	this study
RJD5564	<i>MATa lyp1Δ his3Δ1 leu2Δ0 ura3Δ0 met15Δ0 can1Δ::STE2pr-LEU2 pdr5Δ::ADHpr-NLS-mRFP1-URA3 Cys3-GFP-HIS3</i>	this study
RJD5565	<i>MATa lyp1Δ his3Δ1 leu2Δ0 ura3Δ0 met15Δ0 can1Δ::STE2pr-LEU2 pdr5Δ::ADHpr-NLS-mRFP1-URA3 Cys3-GFP-HIS3 rpn1::rpn1-D517A-KanMX</i>	this study
TGY96well plate	<i>MATa lyp1Δ his3Δ1 leu2Δ0 ura3Δ0 met15Δ0 can1Δ::STE2pr-LEU2</i>	this study

	<i>pdr5Δ::ADHpr-NLS-mRFP1-URA3 MSS116-GFP-HIS3</i>	
TGY96well plate	<i>MATa lyp1Δ his3Δ1 leu2Δ0 ura3Δ0 met15Δ0 can1Δ::STE2pr-LEU2 pdr5Δ::ADHpr-NLS-mRFP1-URA3 MSS116-GFP-HIS3 rpn1::rpn1-D517A-KanMX</i>	this study
TGY96well plate	<i>MATa lyp1Δ his3Δ1 leu2Δ0 ura3Δ0 met15Δ0 can1Δ::STE2pr-LEU2 pdr5Δ::ADHpr-NLS-mRFP1-URA3 MRPL4-GFP-HIS3</i>	this study
TGY96well plate	<i>MATa lyp1Δ his3Δ1 leu2Δ0 ura3Δ0 met15Δ0 can1Δ::STE2pr-LEU2 pdr5Δ::ADHpr-NLS-mRFP1-URA3 MRPL4-GFP-HIS3 rpn1::rpn1-D517A-KanMX</i>	this study
TGY96well plate	<i>MATa lyp1Δ his3Δ1 leu2Δ0 ura3Δ0 met15Δ0 can1Δ::STE2pr-LEU2 pdr5Δ::ADHpr-NLS-mRFP1-URA3 MRPL10-GFP-HIS3</i>	this study
TGY96well plate	<i>MATa lyp1Δ his3Δ1 leu2Δ0 ura3Δ0 met15Δ0 can1Δ::STE2pr-LEU2 pdr5Δ::ADHpr-NLS-mRFP1-URA3 MRPL10-GFP-HIS3 rpn1::rpn1-D517A-KanMX</i>	this study
TGY96well plate	<i>MATa lyp1Δ his3Δ1 leu2Δ0 ura3Δ0 met15Δ0 can1Δ::STE2pr-LEU2 pdr5Δ::ADHpr-NLS-mRFP1-URA3 PDB1-GFP-HIS3</i>	this study
TGY96well plate	<i>MATa lyp1Δ his3Δ1 leu2Δ0 ura3Δ0 met15Δ0 can1Δ::STE2pr-LEU2 pdr5Δ::ADHpr-NLS-mRFP1-URA3 PDB1-GFP-HIS3 rpn1::rpn1-D517A-KanMX</i>	this study
RJD5152	<i>W303 ρ°</i>	David Chan Lab
RJD5255	<i>his3 leu2 lys2-801 trp1 ura3-1 ade2-1 met2 tim44::LYS2 ycplac33-TIM44-R180K</i>	Elizabeth Craig Lab
RJD1786	<i>MATa can1 leu2 his3 trp1 ura3 ade2 rho+ mrp1-1</i>	RJD Lab
RJD3330	<i>MATa Ura3 leu2Δ his3Δ TRP+ pep4::KanMX rpt6-1</i>	J. Dohmen Lab
RJD4340	<i>MATa leu2Δ his3Δ ade2-101 trp1 ura3Δ::TRP1 rpn2-1</i>	Mark Hochstrasser Lab
RJD5427	<i>MatA ddi1::KanMX dsk2::KANMX bar1Δ</i>	DJ Clarke Lab

**Table 6.2. Plasmids used in this chapter**

<b>Plasmid</b>	<b>Description</b>	<b>Source</b>
RDB2492	pEGH-GAL-GST-Rot1	OpenBiosystems
RDB2506	pBG1805-Met6	OpenBiosystems
RDB2507	pBG1805-Aro9	OpenBiosystems
RDB2500	pBG1805-Rrp6	OpenBiosystems
RDB2499	pBG1805-Dop1	OpenBiosystems
RDB2501	pBG1805-Aac2	OpenBiosystems

**Table 6.3. PIPs that are reduced in *rpn13Δ rpn1-D517A* 26S proteasome preparations**

ORF	H/L Ratio	Peptides	Seq. Coverage (%)	No. of Experiments
GCV3	38.5**	2	11.8	1/3
AAC2	32.4**	1	6.3	1/3
HXK2 <sup>†</sup>	29.0**	2	6	1/3
DPM1 <sup>†</sup>	11.8**	2	16.9	1/3
COX4	24.9**	2	25.2	1/3
GPP1	25.7**	2	11.2	1/3
URA3	19.7**	4	19.1	1/3
DPM1	11.8**	2	16.9	1/3
PPX1	11.4**	2	7.8	1/3
VPH1 <sup>†</sup>	9.9**	2	4.2	1/3
DLD3 <sup>†</sup>	8.3**	2	5.8	1/3
CBR1	7.3**	2	13.4	1/3
SEC53 <sup>†</sup>	6.7**	6	23.2	1/3
BAT1 <sup>†</sup>	6.6**	3	11.2	1/3
SAC6 <sup>†</sup>	6.4**	3	7.9	1/3
ARP4	5.9**	3	4.7	3/3
CYS3	5.7**	2	18	1/3
ARO9	4.9**	2	3.9	1/3
PTC2	4.7**	2	6.5	1/3
VAS1 <sup>†</sup>	4.5**	3	3.5	1/3
LEU1 <sup>†</sup>	4.5**	65	73.9	3/3
URA7 <sup>†</sup>	4.4**	6	14	1/3
SPA2	4.2**	3	2.8	2/3
RNR2 <sup>†</sup>	3.7**	7	10.8	1/3
TIF3 <sup>†</sup>	3.6**	5	20.9	2/3
TRP5 <sup>†</sup>	3.3**	4	7.5	1/3
GFA1 <sup>†</sup>	3.3**	7	13.8	2/3
SAM1 <sup>†</sup>	3.0**	19	51.8	2/3
MET6 <sup>†</sup>	2.9**	16	31.8	3/3
APA1 <sup>†</sup>	2.9**	2	7.8	1/3
RSM25	2.7**	2	7.6	1/3
CDC60 <sup>†</sup>	2.7**	3	3.4	1/3
ADO1 <sup>†</sup>	2.5**	10	46.2	3/3
SYN8	2.5**	5	18	3/3
SAM2 <sup>†</sup>	2.5**	20	58.3	3/3
ERG6 <sup>†</sup>	2.5**	7	18	1/3
TUB2 <sup>†</sup>	2.4**	7	24.3	2/3
FRS1 <sup>†</sup>	2.4**	7	17.3	2/3
BGL2	2.4**	2	5.8	1/3
VMA2 <sup>†</sup>	2.2**	19	48.7	3/3
SAH1 <sup>†</sup>	2.1**	13	30.1	3/3

ILV5 <sup>†</sup>	1.8 <sup>**</sup>	13	41	3/3
ARO8 <sup>†</sup>	1.8 <sup>**</sup>	13	32	3/3
RRP6	1.8 <sup>**</sup>	4	32	3/3
KRE6	1.6 <sup>*</sup>	11	7.4	3/3
DED1 <sup>†</sup>	1.6 <sup>*</sup>	19	44.9	3/3
ARO2 <sup>†</sup>	1.6 <sup>*</sup>	2	6.1	2/3
ROT1	1.6 <sup>*</sup>	2	17.2	3/3
PBI2	1.6 <sup>*</sup>	2	22.7	3/3
GUA1 <sup>†</sup>	1.5 <sup>*</sup>	5	13.5	1/3
IPP1 <sup>†</sup>	1.3 <sup>*</sup>	5	17.1	3/3
URA6	1.2 <sup>*</sup>	4	24.5	1/3
PPN1	1.2 <sup>*</sup>	2	3	1/3

<sup>†</sup> Indicated PIPs are proteasome interacting proteins that were seen in the SILAC assay reported here and in Guerrero et al., 2008.

\* Denotes  $0.005 < P < 0.05$ .

\*\* Denotes  $P \ll 0.005$ .

**Table 6.4. PIPs that are increased in *rpn13Δ rpn1-D517A* 26S proteasome preparations<sup>†</sup>**

ORF	H/L Ratio	Peptides	Seq. Coverage (%)	No. of Experiments
TDH1	0.3 <sup>**</sup>	12	36.7	3/3
PIM1	0.3 <sup>**</sup>	31	32.6	3/3
ATP3	0.3 <sup>**</sup>	2	11.6	3/3
PMA1	0.4 <sup>**</sup>	15	24.4	3/3
MNP1	0.4 <sup>**</sup>	5	28.4	3/3
YML6	0.4 <sup>**</sup>	3	20.3	3/3
EXG1	0.4 <sup>**</sup>	5	13.4	3/3
MRPL24	0.4 <sup>**</sup>	3	12.8	3/3
MRP7	0.4 <sup>**</sup>	8	20.8	3/3
IDH1	0.4 <sup>**</sup>	4	13.6	3/3
YGP1	0.4 <sup>**</sup>	6	23.7	3/3
MRPL22	0.4	5	26.5	2/3
MRPL17	0.4 <sup>**</sup>	4	10.7	3/3
MRPL10	0.4 <sup>**</sup>	2	5.6	2/3
MRPL25	0.4 <sup>**</sup>	4	25.5	2/3
MRPL40	0.4 <sup>**</sup>	6	24.2	3/3
MRPL32	0.4 <sup>**</sup>	1	6	2/3
MRPL35	0.4 <sup>**</sup>	10	27	3/3
MRPL1	0.5 <sup>**</sup>	3	11.9	2/3
YGL004C	0.5 <sup>**</sup>	15	39.6	3/3
ATP2	0.5 <sup>**</sup>	5	17.6	3/3
MRPL31	0.5 <sup>**</sup>	3	26.7	3/3
MRPL13	0.5 <sup>**</sup>	5	35.2	3/3
RML2	0.5 <sup>**</sup>	4	14.8	2/3
ENO1	0.5 <sup>**</sup>	15	41.2	3/3
QCR2	0.5 <sup>**</sup>	5	17.9	2/3
PFK26	0.5 <sup>**</sup>	38	55.4	3/3
IDH2	0.5 <sup>**</sup>	5	22.8	3/3
MRPL4	0.5 <sup>**</sup>	3	14.1	2/3
MRPL16	0.5 <sup>**</sup>	4	20.3	2/3
PDB1	0.6 <sup>**</sup>	10	37.7	3/3
MSS116	0.6 <sup>**</sup>	9	19.4	3/3
HSP60	0.6 <sup>**</sup>	27	57	3/3
ESC1	0.6 <sup>**</sup>	58	41.7	3/3
THI20	0.6 <sup>**</sup>	39	72.6	3/3
RIM15	0.6 <sup>**</sup>	3	2.5	3/3
MRPL9	0.6 <sup>**</sup>	2	7.1	2/3
GDE1	0.6 <sup>**</sup>	19	20.9	3/3
NAS2	0.6 <sup>**</sup>	6	25	3/3
RNH202	0.6 <sup>*</sup>	4	14.6	3/3

PGK1	0.7*	20	63	3/3
ADH1	0.7	18	67.2	3/3
PDA1	0.7*	24	57.9	3/3
ASK10	0.7*	6	6.4	3/3
PDX1	0.7*	12	40.7	3/3
MPM1	0.8*	3	16.7	3/3
SLK19	0.8*	7	10.6	3/3

\* Denotes  $0.005 < P < 0.05$ .

\*\* Denotes  $P \ll 0.005$ .

**Figure 6.1. Screening for putative *rpn1-D517A* substrates from the SILAC data set**

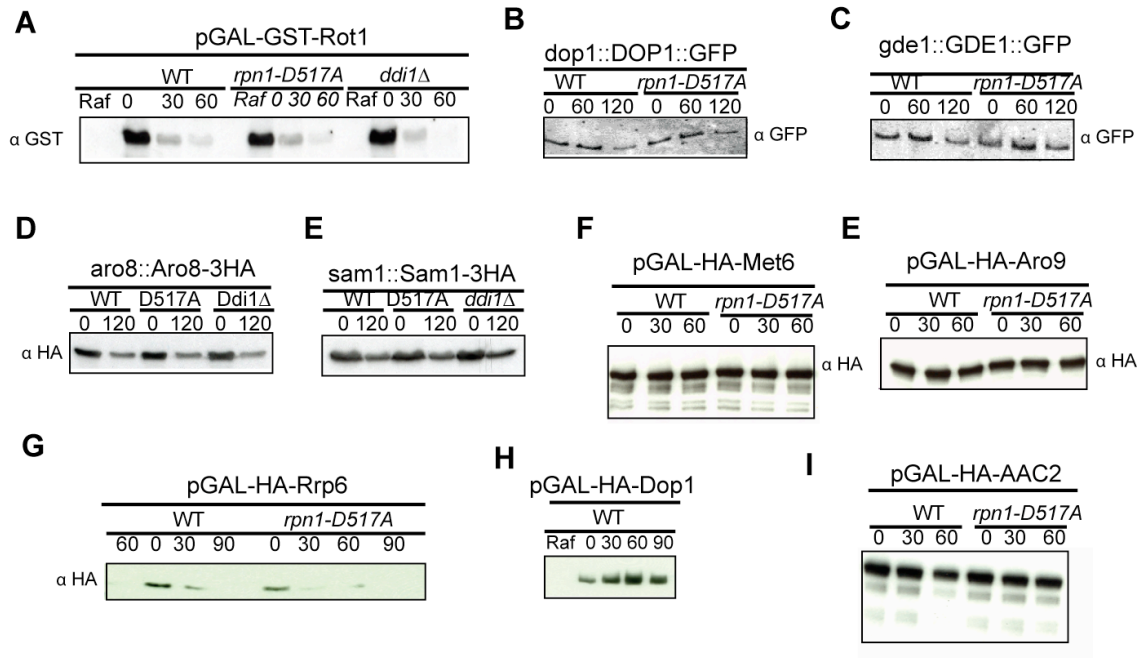


**Figure 6.2. Galactose-inducible Aac2 is slightly stabilized in an *rpn1-D517A* strain.**

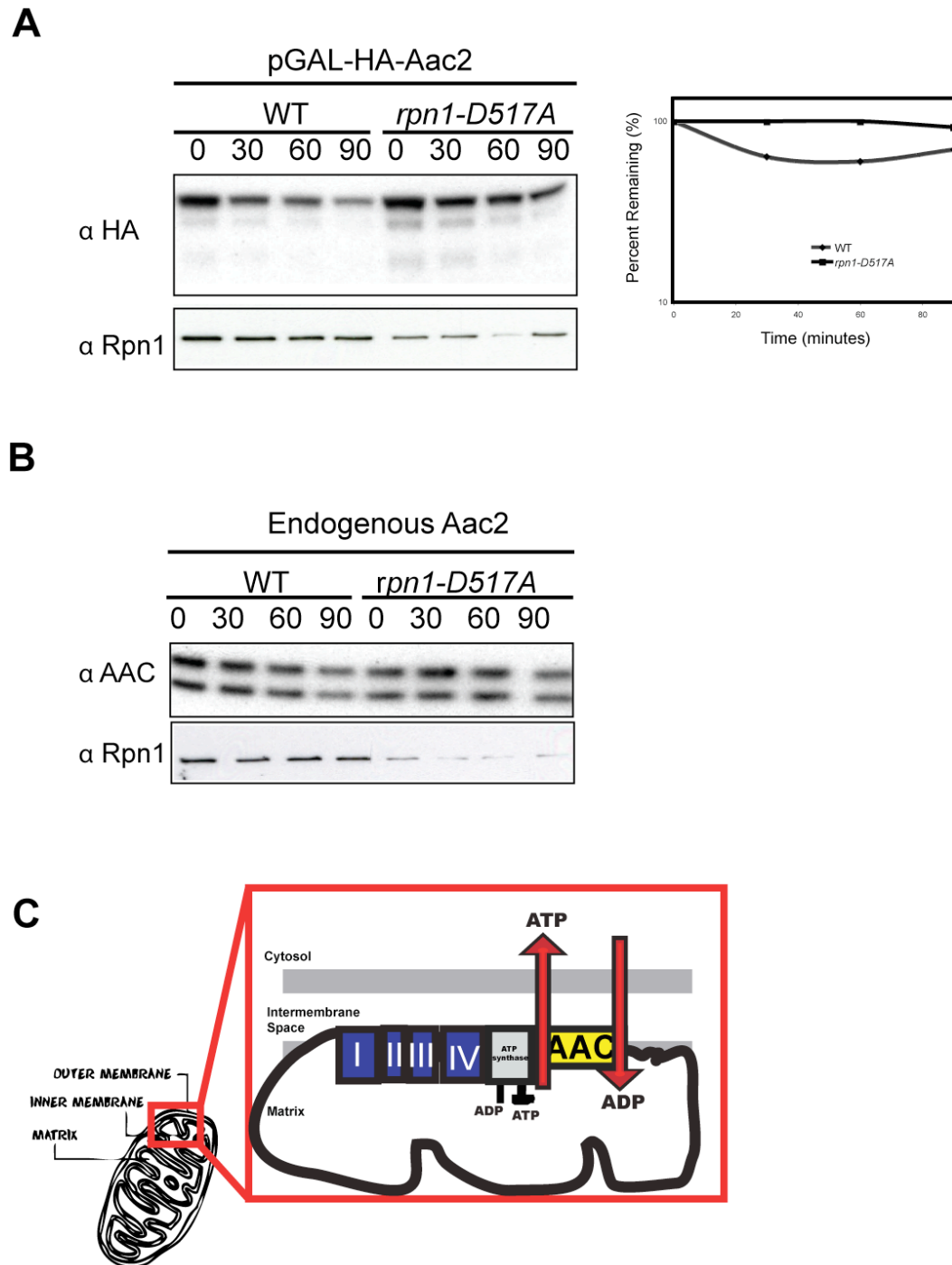


**Figure 6.3. Steady-state concentrations of multiple GFP tagged ORFs change in an *rpn1-D517A* mutant.**

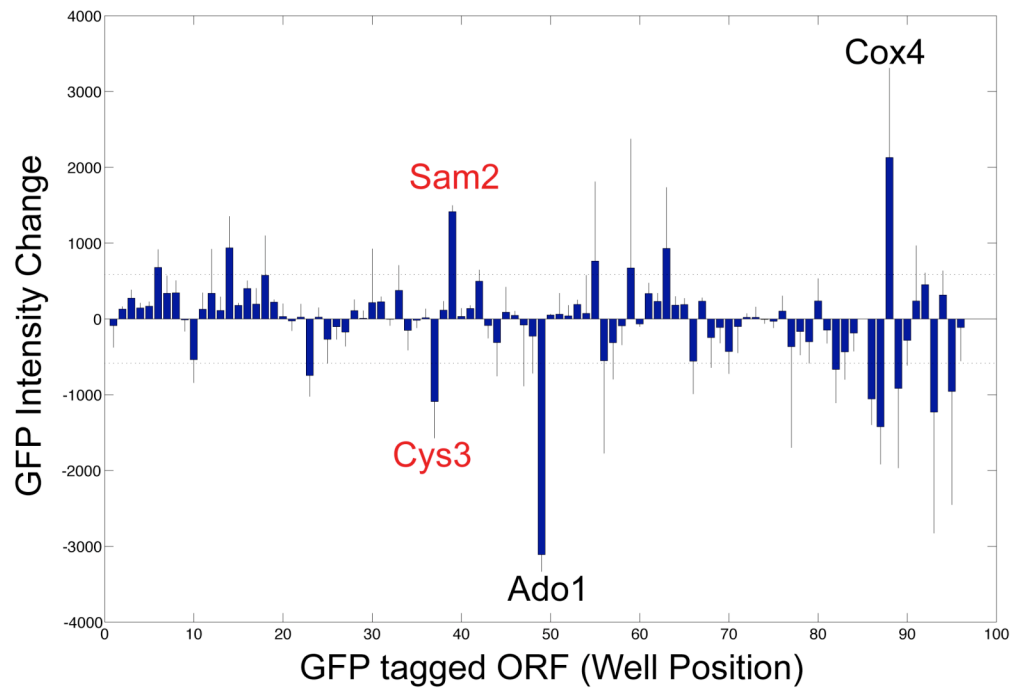


**Figure 6.4. Steady-state concentrations of ORFs found less abundantly in *rpn13Δ rpn1-D517A* proteasomes.**

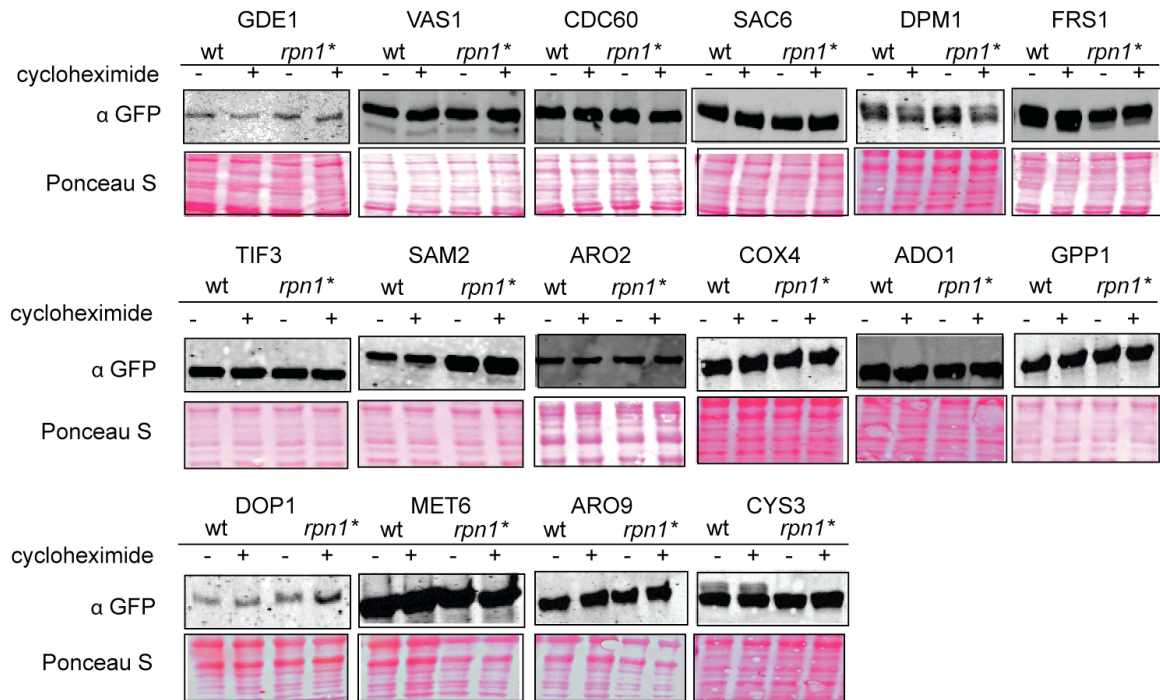


**Figure 6.5. Steady-state concentrations of ORFs found more abundant in *rpn13Δ rpn1-D517A* proteasomes.**

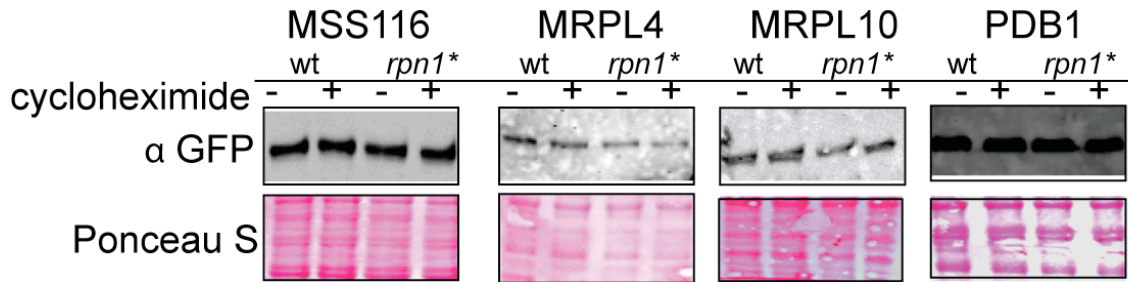


**Figure 6.6. Methionine and cysteine biosynthetic pathways contain multiple enzymes that are perturbed in *rpn1-D517A*.**

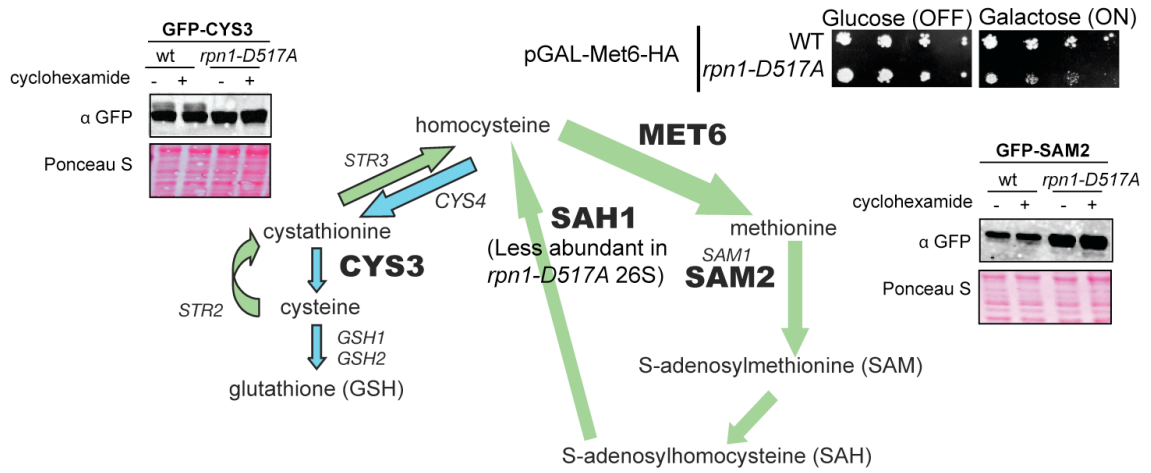
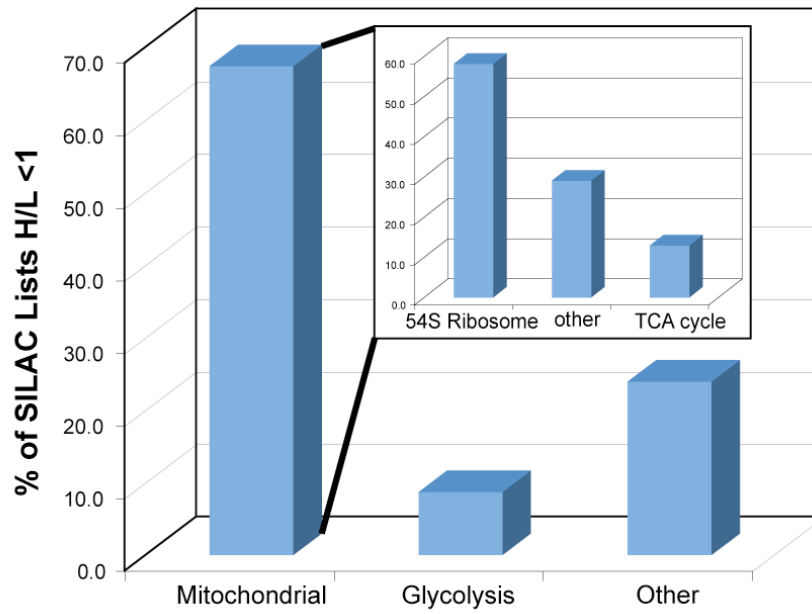
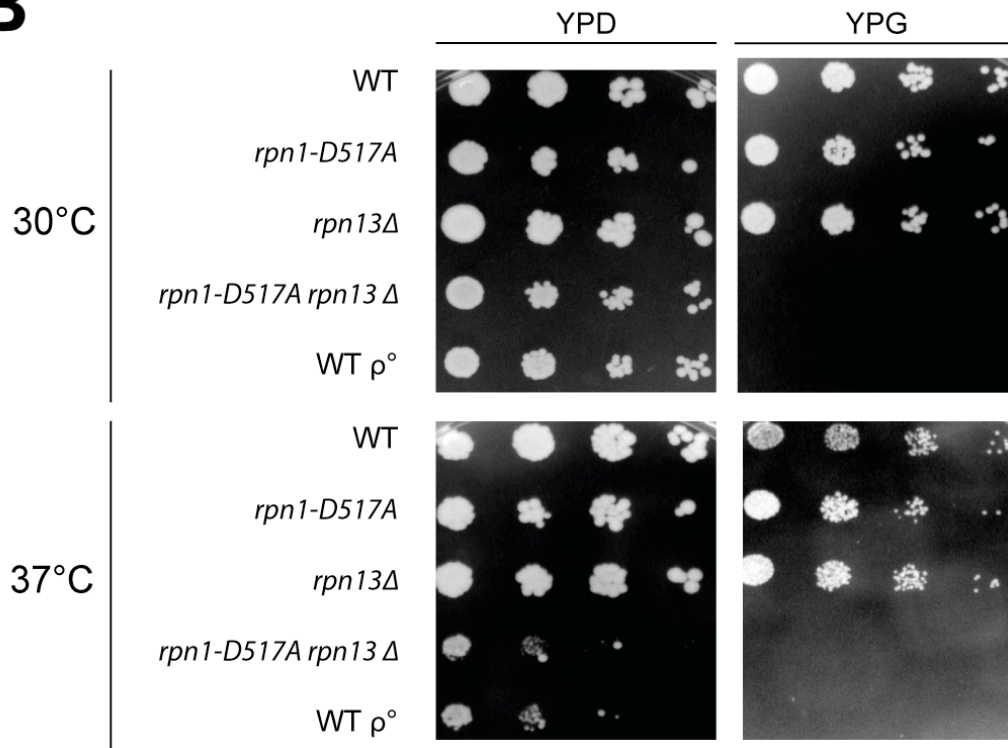
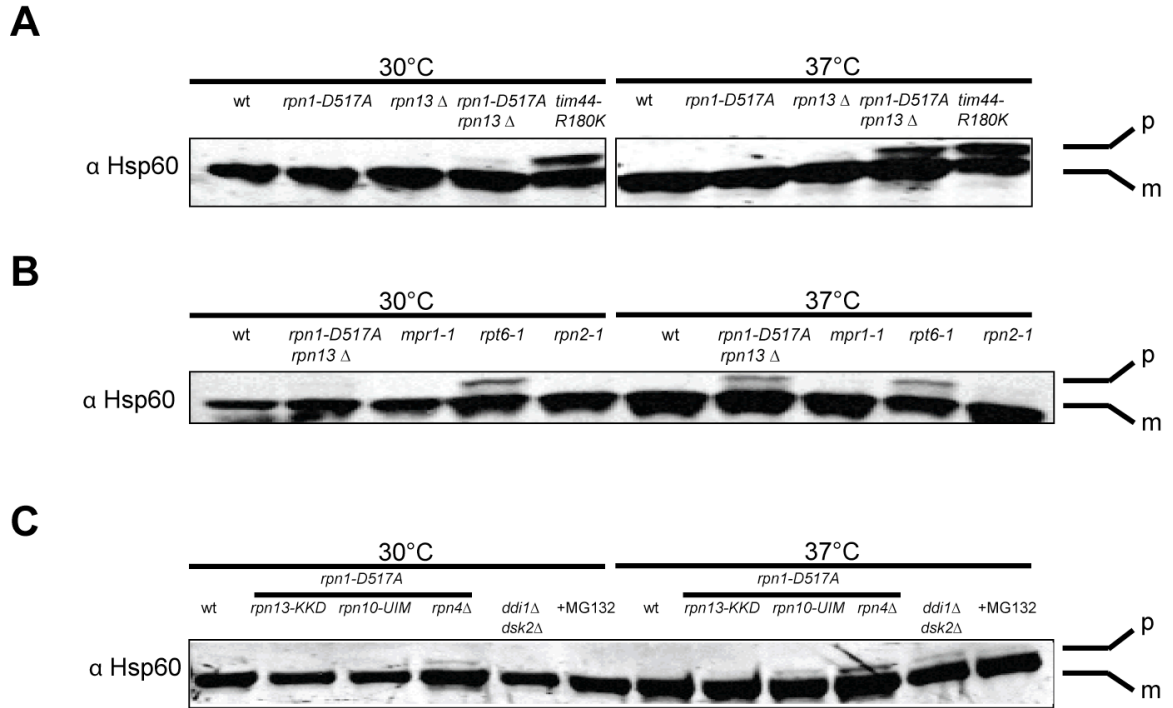
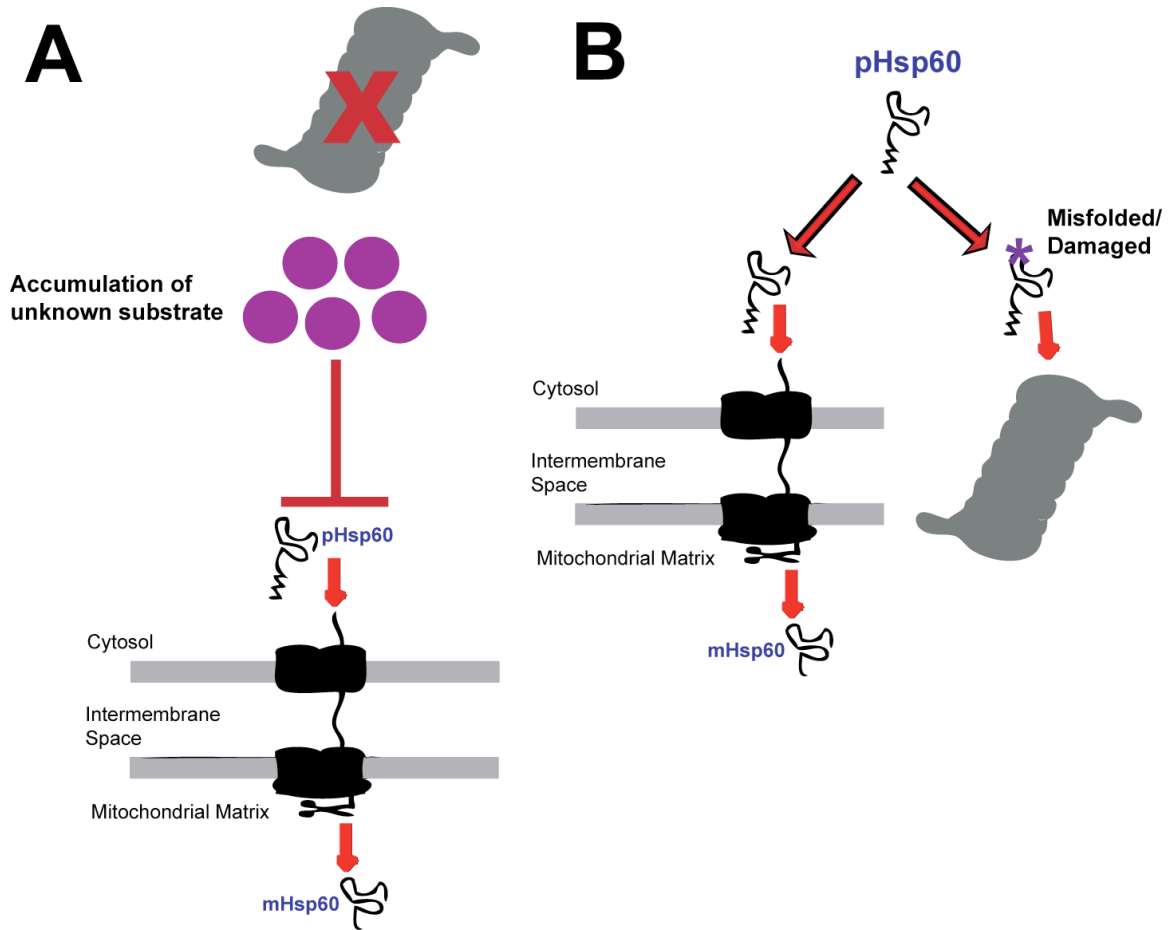


Figure 6.7. *rpn13Δ rpn1-D517A* mutants have mitochondrial defects.**A****B**

**Figure 6.8. *rpn13Δ rpn1-D517A* mutants accumulate Hsp60 precursor proteins.**



**Figure 6.9** Two hypotheses describe pHsp60 accumulation in proteasome mutants.



**Chapter 7:**  
**Findings, implications,**  
**and**  
**future directions**

## Summary

The goal of this dissertation work was to map key residues on the largest subunit of the proteasome, Rpn1, that are essential for docking the UBA-UBL ubiquitin shuttle receptors, Rad23, Dsk2, and Ddi1, to the 26S proteasome. Secondly, such a *cis* proteasome mutant was to be used as a tool for discovering the consequences yielded by selective inhibition of substrate delivery.

The largest contribution of my dissertation work is the proof I have provided that Ddi1 does in fact interact with the proteasome as a shuttle receptor. Such a point has been controversial and my genetic evidence closes the book on such controversy, however, there are undoubtedly enigmas and differences in the way Ddi1 may contribute to substrate turnover in comparison to the other UBA-UBL receptors (Chapter 4).

Secondly, on the tails of *in vitro* studies that show that other proteasomal subunits, such as the intrinsic ubiquitin receptors (Rpn10 and Rpn13) are important for binding UBA-UBL proteins, I provide the first genetic evidence that such interactions are physiologically relevant (Fatimababy et al., 2010; Husnjak et al., 2008; Matiuhin et al., 2008b). I show that the binding landscape at the 26S proteasome is very complicated and there are layers of built in redundancy that potentially help to ensure proper degradation of ubiquitylated substrates.

Mutation of Rpn1 alone was not sufficient for disrupting interactions with all UBL domain-containing proteins. Below I summarize my major findings for the three shuttle receptors I followed, as well as Ubp6, a UBL domain containing deubiquitinase that is also presumed to bind Rpn1 (Leggett et al., 2002).

**Rad23**

In the present study, no mutations made in Rpn1 diminished binding of Rad23 to the proteasome. However, simultaneous deletion of the ubiquitin binding domains of Rpn10 and Rpn13 limit binding of Rad23 (Chapter 5). Since multiple independent studies, including my own, have verified *in vitro* binding of Rpn1 to Rad23, I believe the interaction is real (Elsasser et al., 2002; Fatimababy et al., 2010; Rosenzweig et al., 2008). Therefore, Rad23 may interact with up to three subunits at the proteasome *in vivo*, Rpn1, Rpn10, and Rpn13. There are two modes of additional binding to the 26S proteasome that Rad23 might utilize that I did not test in combination with my genetic perturbations: docking at Rpt6 (Fatimababy et al., 2010) and stabilization to the proteasome through the ubiquitin chains it carries (Ghaboosi and Deshaies, 2007).

**Dsk2**

Dsk2 interacts with Rpn1 using residues D517, and to a lesser extent, K484. Mutation of Rpn1 alone is not sufficient to disrupt binding of Dsk2. Dsk2 also appears to interact with Rpn13 and possibly Rpn10 in intact proteasomes. Deletion of Rpn13 or simultaneous deletion of the Ub interaction motifs of Rpn10 and Rpn13 in an *rpn1-D517A* or *rpn1-K484A* background reduce binding of Dsk2 to the proteasome. However, deletion of the UIM of Rpn10 alone is not sufficient for reducing Dsk2 interaction with the proteasome.

**Ddi1**

Rpn1 residues D517 and K484 are also important for binding Ddi1. Ddi1 may interact solely with Rpn1, as great diminishment of Ddi1 is seen with just singular mutations in this base subunit.

**Ubp6**

Intriguingly, no genetic conditions tested decreased association of Ubp6 with the proteasome. However, under conditions in which all three UBA-UBL protein levels were diminished (in a *rpn10-uim rpn13-kkd* background), Ubp6 levels actually increase at the proteasome. A correlative increase in Ubp6 is puzzling since Ubp6 has been shown to not compete for binding with Rad23 at the proteasome (Elsasser et al., 2004). It should be noted that Ubp6 may also bind lid subunits of the proteasome (Leggett et al., 2002).

It will be interesting for future research to follow up on how the substrate repertoire of these UBA-UBL proteins depends, if at all, on which subunit of the proteasome they dock to. Furthermore, my Rpn1 *cis* proteasome mutant can be used as a tool for the discovery of novel UPS substrates, and for dissecting the substrate specificity of each dockings site.

## Future directions

My work on the consequences of the deletion of the Ddi1 docking site to the proteasome also led to several other key findings, some of which have great potential for future research projects:

1) The mitochondrial ADP/ATP carrier, Aac2, may be a substrate dependent on docking at Rpn1-D517. I suggest follow up studies on this result.

2) To my knowledge, no other study has shown that proteasome function is essential for mitochondrial import of nuclear encoded proteins. Unraveling the mechanism behind this observation will likely yield novel insights into the UPS and mitochondrial metabolism.

3) I suggest follow-up studies on the role of the UPS in the yeast methyl cycle. I see great changes in the steady-state and proteasome association levels of enzymes that regulate this cycle.

4) My SILAC data indicates that the deubiquitinase, Otu2, is less abundant in *rpn13Δ* proteasomes. Human Rpn13 has been shown to associate with a DUB.

Overall, this thesis characterizes a *cis* proteasome mutant that could be used to study the implications of inhibiting the ubiquitin-proteasome pathway in a very selective manner. I hope that this tool, and the future directions I have laid out, will help contribute to understanding the plethora of cellular roles in which the UPS plays a vital role.

## Bibliography

- Barbin, L., Eisele, F., Santt, O., and Wolf, D. (2010). The Cdc48-Ufd1-Npl4 complex is central in ubiquitin-proteasome triggered catabolite degradation of fructose-1, 6-bisphosphatase. *Biochemical and biophysical research communications* 394, 335-341.
- Belle, A., Tanay, A., Bitincka, L., Shamir, R., and O'Shea, E.K. (2006). Quantification of protein half-lives in the budding yeast proteome. *Proceedings of the National Academy of Sciences* 103, 13004.
- Bertolaet, B., Clarke, D., Wolff, M., Watson, M., Henze, M., Divita, G., and Reed, S. (2001a). UBA domains of DNA damage-inducible proteins interact with ubiquitin. *Nature structural & molecular biology* 8, 417-422.
- Bertolaet, B.L., Clarke, D.J., Wolff, M., Watson, M.H., Henze, M., Divita, G., and Reed, S.I. (2001b). UBA domains of DNA damage-inducible proteins interact with ubiquitin. *Nature structural & molecular biology* 8, 417-422.
- Biggins, S., Ivanovska, I., and Rose, M.D. (1996). Yeast ubiquitin-like genes are involved in duplication of the microtubule organizing center. *The Journal of cell biology* 133, 1331.
- Bohn, S., Beck, F., Sakata, E., Walzthoeni, T., Beck, M., Aebersold, R., Förster, F., Baumeister, W., and Nickell, S. (2010). Structure of the 26S proteasome from *Schizosaccharomyces pombe* at subnanometer resolution. *Proceedings of the National Academy of Sciences* 107, 20992.
- Brandina, I., Smirnov, A., Kolesnikova, O., Entelis, N., Krasheninnikov, I.A., Martin, R.P., and Tarassov, I. (2007). tRNA import into yeast mitochondria is regulated by the ubiquitin-proteasome system. *FEBS letters* 581, 4248-4254.
- Burns, K.E., Liu, W.T., Boshoff, H.I.M., Dorrestein, P.C., and Barry, C.E. (2009). Proteasomal protein degradation in *Mycobacteria* is dependent upon a prokaryotic ubiquitin-like protein. *Journal of Biological Chemistry* 284, 3069.
- Chandra, A., Chen, L., Liang, H., and Madura, K. (2010). Proteasome Assembly Influences Interaction with Ubiquitinated Proteins and Shuttle Factors. *Journal of Biological Chemistry* 285, 8330.
- Chang, L., van Dyk Dewald, L.Y., and Hai, R. A genome-wide synthetic dosage lethality screen reveals multiple pathways that require the functioning of ubiquitin-binding proteins Rad23 and Dsk2. *BMC biology* 7.

- Chen, L., Shinde, U., Ortolan, T., and Madura, K. (2001). Ubiquitin-associated (UBA) domains in Rad23 bind ubiquitin and promote inhibition of multi-ubiquitin chain assembly. *EMBO reports* 2, 933-938.
- Cheng, M.Y., Hartl, F.U., Martin, J., Pollock, R.A., Kalousek, F., Neupert, W., Hallberg, E.M., Hallberg, R.L., and Horwich, A. (1989). Mitochondrial heat-shock protein hsp60 is essential for assembly of proteins imported into yeast mitochondria.
- Ciosk, R., Zachariae, W., Michaelis, C., Shevchenko, A., Mann, M., and Nasmyth, K. (1998). An ESP1/PDS1 complex regulates loss of sister chromatid cohesion at the metaphase to anaphase transition in yeast. *Cell* 93, 1067-1076.
- Clarke, D.J., Mondesert, G., Segal, M., Bertolaet, B.L., Jensen, S., Wolff, M., Henze, M., and Reed, S.I. (2001). Dosage suppressors of pds1 implicate ubiquitin-associated domains in checkpoint control. *Molecular and cellular biology* 21, 1997.
- Cohen, M.M.J., Leboucher, G.P., Livnat-Levanon, N., Glickman, M.H., and Weissman, A.M. (2008). Ubiquitin-proteasome-dependent degradation of a mitofusin, a critical regulator of mitochondrial fusion. *Molecular biology of the cell* 19, 2457.
- Cox, J., and Mann, M. (2008). MaxQuant enables high peptide identification rates, individualized ppb-range mass accuracies and proteome-wide protein quantification. *Nature biotechnology* 26, 1367-1372.
- Crosas, B., Hanna, J., Kirkpatrick, D.S., Zhang, D.P., Tone, Y., Hathaway, N.A., Buecker, C., Leggett, D.S., Schmidt, M., and King, R.W. (2006). Ubiquitin chains are remodeled at the proteasome by opposing ubiquitin ligase and deubiquitinating activities. *Cell* 127, 1401-1413.
- Deveraux, Q., Jensen, C., and Rechsteiner, M. (1995a). Molecular cloning and expression of a 26 S protease subunit enriched in dileucine repeats. *Journal of Biological Chemistry* 270, 23726.
- Deveraux, Q., van Nocker, S., Mahaffey, D., Vierstra, R., and Rechsteiner, M. (1995b). Inhibition of ubiquitin-mediated proteolysis by the Arabidopsis 26 S protease subunit S5a. *Journal of Biological Chemistry* 270, 29660.
- Díaz-Martínez, L., Kang, Y., Walters, K., and Clarke, D. (2006). Yeast UBL-UBA proteins have partially redundant functions in cell cycle control. *Cell Division* 1, 28.
- Effantin, G., Rosenzweig, R., Glickman, M., and Steven, A. (2009). Electron Microscopic Evidence in Support of [alpha]-Solenoid Models of Proteasomal Subunits Rpn1 and Rpn2. *Journal of molecular biology* 386, 1204-1211.
- Elsasser, S., Chandler-Militello, D., Mller, B., Hanna, J., and Finley, D. (2004). Rad23 and Rpn10 serve as alternative ubiquitin receptors for the proteasome. *Journal of Biological Chemistry* 279, 26817.

- Elsasser, S., Gali, R., Schwickart, M., Larsen, C., Leggett, D., Müller, B., Feng, M., T'bing, F., Dittmar, G., and Finley, D. (2002). Proteasome subunit Rpn1 binds ubiquitin-like protein domains. *Nature cell biology* 4, 725-730.
- Elsasser, S., Schmidt, M., and Finley, D. (2005). Characterization of the proteasome using native gel electrophoresis. *Methods in enzymology* 398, 353-363.
- Escobar-Henriques, M., Westermann, B., and Langer, T. (2006). Regulation of mitochondrial fusion by the F-box protein Mdm30 involves proteasome-independent turnover of Fzo1. *The Journal of cell biology* 173, 645.
- Fatimababy, A., Lin, Y., Usharani, R., Radjacommaré, R., Wang, H., Tsai, H., Lee, Y., and Fu, H. (2010). Cross species divergence of the major recognition pathways of ubiquitylated substrates for ubiquitin/26S proteasome mediated proteolysis. *FEBS Journal* 277, 796-816.
- Finley, D. (2009). Recognition and processing of ubiquitin-protein conjugates by the proteasome. *Annual review of biochemistry* 78, 477-513.
- Fisher, R.I., Bernstein, S.H., Kahl, B.S., Djulbegovic, B., Robertson, M.J., de Vos, S., Epner, E., Krishnan, A., Leonard, J.P., and Lonial, S. (2006). Multicenter phase II study of bortezomib in patients with relapsed or refractory mantle cell lymphoma. *Journal of Clinical Oncology* 24, 4867-4874.
- Förster, F., Lasker, K., Nickell, S., Sali, A., and Baumeister, W. (2010). Toward an Integrated Structural Model of the 26S Proteasome. *Molecular & Cellular Proteomics* 9, 1666.
- Fowden, L., and Richmond, M. (1963). Replacement of proline by azetidine-2-carboxylic acid during biosynthesis of protein. *Biochimica et Biophysica Acta* 71, 459-461.
- Fu, H., Lin, Y., and Fatimababy, A. (2010). Proteasomal recognition of ubiquitylated substrates. *Trends in plant science*.
- Fu, H., Sadis, S., Rubin, D.M., Glickman, M., van Nocker, S., Finley, D., and Vierstra, R.D. (1998). Multiubiquitin chain binding and protein degradation are mediated by distinct domains within the 26 S proteasome subunit Mcb1. *Journal of Biological Chemistry* 273, 1970.
- Funakoshi, M., Sasaki, T., Nishimoto, T., and Kobayashi, H. (2002). Budding yeast Dsk2p is a polyubiquitin-binding protein that can interact with the proteasome. *Proceedings of the National Academy of Sciences of the United States of America* 99, 745.
- Funakoshi, M., Tomko Jr, R.J., Kobayashi, H., and Hochstrasser, M. (2009). Multiple assembly chaperones govern biogenesis of the proteasome regulatory particle base. *Cell* 137, 887-899.

- Gabriely, G., Kama, R., Gelin-Licht, R., and Gerst, J.E. (2008). Different domains of the UBL-UBA ubiquitin receptor, Ddi1/Vsm1, are involved in its multiple cellular roles. *Molecular biology of the cell* *19*, 3625.
- Ghaboosi, N., and Deshaies, R. (2007). A conditional yeast E1 mutant blocks the ubiquitin-proteasome pathway and reveals a role for ubiquitin conjugates in targeting Rad23 to the proteasome. *Molecular biology of the cell* *18*, 1953.
- Glickman, M.H., Rubin, D.M., Coux, O., Wefes, I., Pfeifer, G., Cjeka, Z., Baumeister, W., Fried, V.A., and Finley, D. (1998). A subcomplex of the proteasome regulatory particle required for ubiquitin-conjugate degradation and related to the COP9-signalosome and eIF3. *Cell* *94*, 615-623.
- Glockzin, S., Ogi, F.X., Hengstermann, A., Scheffner, M., and Blattner, C. (2003). Involvement of the DNA repair protein hHR23 in p53 degradation. *Molecular and cellular biology* *23*, 8960.
- Gonzalez, F., Delahodde, A., Kodadek, T., and Johnston, S.A. (2002). Recruitment of a 19S proteasome subcomplex to an activated promoter. *Science* *296*, 548.
- Grabbe, C., Husnjak, K., and Dikic, I. (2011). The spatial and temporal organization of ubiquitin networks. *Nature Reviews Molecular Cell Biology*.
- Gray, P.N., Busser, K.J., and Chappell, T.G. (2007). A novel approach for generating full-length, high coverage allele libraries for the analysis of protein interactions. *Molecular & Cellular Proteomics* *6*, 514.
- Guerrero, C., Milenkovi, T., Prùlj, N., Kaiser, P., and Huang, L. (2008). Characterization of the proteasome interaction network using a QTAX-based tag-team strategy and protein interaction network analysis. *Proceedings of the National Academy of Sciences* *105*, 13333.
- Hampton, R., Gardner, R., and Rine, J. (1996). Role of 26S proteasome and HRD genes in the degradation of 3-hydroxy-3-methylglutaryl-CoA reductase, an integral endoplasmic reticulum membrane protein. *Molecular biology of the cell* *7*, 2029.
- Hänzelmann, P., Stingele, J., Hofmann, K., Schindelin, H., and Raasi, S. (2010). The Yeast E4 ubiquitin ligase Ufd2 interacts with the ubiquitin-like domains of Rad23 and Dsk2 via a novel and distinct ubiquitin-like binding domain. *Journal of Biological Chemistry* *285*, 20390.
- Heessen, S., Masucci, M.G., and Dantuma, N.P. (2005). The UBA2 domain functions as an intrinsic stabilization signal that protects Rad23 from proteasomal degradation. *Molecular cell* *18*, 225-235.
- Heo, J.M., Livnat-Levanon, N., Taylor, E.B., Jones, K.T., Dephoure, N., Ring, J., Xie, J., Brodsky, J.L., Madeo, F., and Gygi, S.P. (2010). A stress-responsive system for mitochondrial protein degradation. *Molecular cell* *40*, 465-480.

- Hershko, A. (1997). Roles of ubiquitin-mediated proteolysis in cell cycle control. *Current opinion in cell biology* 9, 788-799.
- Hershko, A., and Ciechanover, A. (1998). The ubiquitin system. *Annual review of biochemistry* 67, 425-479.
- Hiyama, H., Yokoi, M., Masutani, C., Sugasawa, K., Maekawa, T., Tanaka, K., Hoeijmakers, J.H.J., and Hanaoka, F. (1999). Interaction of hHR23 with S5a. *Journal of Biological Chemistry* 274, 28019.
- Hobeika, M., Brockmann, C., Iglesias, N., Gwizdek, C., Neuhaus, D., Stutz, F., Stewart, M., Divita, G., and Dargemont, C. (2007). Coordination of Hpr1 and ubiquitin binding by the UBA domain of the mRNA export factor Mex67. *Molecular biology of the cell* 18, 2561.
- Husnjak, K., Elsasser, S., Zhang, N., Chen, X., Randles, L., Shi, Y., Hofmann, K., Walters, K., Finley, D., and Dikic, I. (2008). Proteasome subunit Rpn13 is a novel ubiquitin receptor. *Nature* 453, 481-488.
- Ikeda, F., and Dikic, I. (2008). Atypical ubiquitin chains: new molecular signals. *Protein Modifications: Beyond the Usual Suspects EMBO reports* 9, 536-542.
- Ishii, T., Funakoshi, M., and Kobayashi, H. (2006). Yeast Pth2 is a UBL domain-binding protein that participates in the ubiquitin-proteasome pathway. *The EMBO journal* 25, 5492-5503.
- Ivantsiv, Y., Kaplun, L., Tzirkin-Goldin, R., Shabek, N., and Raveh, D. (2006). Unique role for the Ubl-UbA protein Ddi1 in turnover of SCFUfo1 complexes. *Molecular and cellular biology* 26, 1579.
- Ju, D., Wang, L., Mao, X., and Xie, Y. (2004). Homeostatic regulation of the proteasome via an Rpn4-dependent feedback circuit. *Biochemical and biophysical research communications* 321, 51-57.
- Kajava, A. (2002). What Curves-Solenoids? *J Biol Chem* 277, 49791-49798.
- Kaneko, T., Hamazaki, J., Iemura, S., Sasaki, K., Furuyama, K., Natsume, T., Tanaka, K., and Murata, S. (2009). Assembly pathway of the Mammalian proteasome base subcomplex is mediated by multiple specific chaperones. *Cell* 137, 914-925.
- Kang, Y., Vossler, R., Diaz-Martinez, L., Winter, N., Clarke, D., and Walters, K. (2006). UBL/UBA ubiquitin receptor proteins bind a common tetraubiquitin chain. *Journal of molecular biology* 356, 1027-1035.
- Kaplun, L., Ivantsiv, Y., Kornitzer, D., and Raveh, D. (2000). Functions of the DNA damage response pathway target Ho endonuclease of yeast for degradation via the ubiquitin-26S proteasome system. *Proceedings of the National Academy of Sciences of the United States of America* 97, 10077.

- Kaplun, L., Tzirkin, R., Bakhrat, A., Shabek, N., Ivantsiv, Y., and Raveh, D. (2005). The DNA damage-inducible UbL-UbA protein Ddi1 participates in Mec1-mediated degradation of Ho endonuclease. *Molecular and cellular biology* *25*, 5355.
- Kim, I., Mi, K., and Rao, H. (2004). Multiple interactions of rad23 suggest a mechanism for ubiquitylated substrate delivery important in proteolysis. *Molecular biology of the cell* *15*, 3357.
- Kleijnen, M., Roelofs, J., Park, S., Hathaway, N., Glickman, M., King, R., and Finley, D. (2007). Stability of the proteasome can be regulated allosterically through engagement of its proteolytic active sites. *Nature structural & molecular biology* *14*, 1180-1188.
- Kobe, B., and Kajava, A. (2001). The leucine-rich repeat as a protein recognition motif. *Current opinion in structural biology* *11*, 725-732.
- Krylov, D.M., and Koonin, E.V. (2001). A novel family of predicted retroviral-like aspartyl proteases with a possible key role in eukaryotic cell cycle control. *Current biology: CB* *11*, R584.
- Lafaye, A., Junot, C., Pereira, Y., Lagniel, G., Tabet, J.C., Ezan, E., and Labarre, J. (2005). Combined proteome and metabolite-profiling analyses reveal surprising insights into yeast sulfur metabolism. *Journal of Biological Chemistry* *280*, 24723.
- Lam, Y.A., Lawson, T.G., Velayutham, M., Zweier, J.L., and Pickart, C.M. (2002). A proteasomal ATPase subunit recognizes the polyubiquitin degradation signal. *Nature* *416*, 763-767.
- Lambertson, D., Chen, L., and Madura, K. (1999). Pleiotropic defects caused by loss of the proteasome-interacting factors Rad23 and Rpn10 of *Saccharomyces cerevisiae*. *Genetics* *153*, 69.
- Lambertson, D., Chen, L., and Madura, K. (2003). Investigating the importance of proteasome-interaction for Rad23 function. *Current genetics* *42*, 199-208.
- Lawson, J., and Douglas, M.G. (1988). Separate genes encode functionally equivalent ADP/ATP carrier proteins in *Saccharomyces cerevisiae*. Isolation and analysis of AAC2. *Journal of Biological Chemistry* *263*, 14812.
- Lee, J., Sweredoski, M., Graham, R., Kolawa, N., Smith, G., Hess, S., and Deshaies, R. (2010). The steady-state repertoire of human SCF Ubiquitin ligase complexes does not require ongoing Nedd8 conjugation. *Molecular & Cellular Proteomics*.
- Leggett, D., Hanna, J., Borodovsky, A., Crosas, B., Schmidt, M., Baker, R., Walz, T., Ploegh, H., and Finley, D. (2002). Multiple associated proteins regulate proteasome structure and function. *Molecular cell* *10*, 495-507.

- Li, S., Armstrong, C., Bertin, N., Ge, H., Milstein, S., Boxem, M., Vidalain, P., Han, J., Chesneau, A., and Hao, T. (2004). A map of the interactome network of the metazoan *C. elegans*. *Science* *303*, 540.
- Liu, C., Van Dyk, D., Li, Y., Andrews, B., and Rao, H. (2009). A genome-wide synthetic dosage lethality screen reveals multiple pathways that require the functioning of ubiquitin-binding proteins Rad 23 and Dsk 2. *BMC biology* *7*, 75.
- Liu, Y., and Xiao, W. (1997). Bidirectional regulation of two DNA damage inducible genes, MAG1 and DDI1, from *Saccharomyces cerevisiae*. *Molecular microbiology* *23*, 777-789.
- Longtine, M., Mckenzie III, A., Demarini, D., Shah, N., Wach, A., Brachat, A., Philippsen, P., and Pringle, J. (1998). Additional modules for versatile and economical PCR-based gene deletion and modification in *Saccharomyces cerevisiae*. *Yeast* *14*, 953-961.
- Lowe, E.D., Hasan, N., Trempe, J.F., Fonso, L., Noble, M.E.M., Endicott, J.A., Johnson, L.N., and Brown, N.R. (2006). Structures of the Dsk2 UBL and UBA domains and their complex. *Acta Crystallographica Section D: Biological Crystallography* *62*, 177-188.
- Lupas, A., Baumeister, W., and Hofmann, K. (1997). A repetitive sequence in subunits of the 26S proteasome and 20S cyclosome (anaphase-promoting complex). *Trends in biochemical sciences* *22*, 195.
- Lustgarten, V., and Gerst, J.E. (1999). Yeast VSM1 encodes a v-SNARE binding protein that may act as a negative regulator of constitutive exocytosis. *Molecular and cellular biology* *19*, 4480.
- Matiuhin, Y., Kirkpatrick, D., Ziv, I., Kim, W., Dakshinamurthy, A., Kleifeld, O., Gygi, S., Reis, N., and Glickman, M. (2008a). Extraproteasomal Rpn10 restricts access of the polyubiquitin-binding protein Dsk2 to proteasome. *Molecular cell* *32*, 415-425.
- Matiuhin, Y., Kirkpatrick, D.S., Ziv, I., Kim, W., Dakshinamurthy, A., Kleifeld, O., Gygi, S.P., Reis, N., and Glickman, M.H. (2008b). Extraproteasomal Rpn10 restricts access of the polyubiquitin-binding protein Dsk2 to proteasome. *Molecular cell* *32*, 415-425.
- Mayor, T., Graumann, J., Bryan, J., MacCoss, M.J., and Deshaies, R.J. (2007). Quantitative profiling of ubiquitylated proteins reveals proteasome substrates and the substrate repertoire influenced by the Rpn10 receptor pathway. *Molecular & Cellular Proteomics* *6*, 1885.
- Medicherla, B., Kostova, Z., Schaefer, A., and Wolf, D. (2004). A genomic screen identifies Dsk2p and Rad23p as essential components of ER-associated degradation. *EMBO reports* *5*, 692-697.

- Miller, R.D., Prakash, L., and Prakash, S. (1982). Defective excision of pyrimidine dimers and interstrand DNA crosslinks in rad7 and rad23 mutants of *Saccharomyces cerevisiae*. *Molecular and General Genetics* *188*, 235-239.
- Mueller, T., and Feigon, J. (2003). Structural determinants for the binding of ubiquitin-like domains to the proteasome. *The EMBO journal* *22*, 4634-4645.
- Mueller, T.D., and Feigon, J. (2002). Solution structures of UBA domains reveal a conserved hydrophobic surface for protein-protein interactions. *Journal of molecular biology* *319*, 1243-1255.
- Mueller, T.D., Kamionka, M., and Feigon, J. (2004). Specificity of the interaction between ubiquitin-associated domains and ubiquitin. *Journal of Biological Chemistry* *279*, 11926.
- Nickell, S., Beck, F., Scheres, S., Korinek, A., Förster, F., Lasker, K., Mihalache, O., Sun, N., Nagy, I., and Sali, A. (2009a). Insights into the molecular architecture of the 26S proteasome. *Proceedings of the National Academy of Sciences* *106*, 11943.
- Nickell, S., Beck, F., Scheres, S., Korinek, A., Förster, F., Lasker, K., Mihalache, O., Sun, N., Nagy, I., and Sali, A. (2009b). Insights into the molecular architecture of the 26S proteasome. *Proceedings of the National Academy of Sciences* *106*, 11943.
- Ohno, A., Jee, J.G., Fujiwara, K., Tenno, T., Goda, N., Tochio, H., Kobayashi, H., Hiroaki, H., and Shirakawa, M. (2005). Structure of the UBA Domain of Dsk2p in Complex with Ubiquitin:: Molecular Determinants for Ubiquitin Recognition. *Structure* *13*, 521-532.
- Ortolan, T.G., Tongaonkar, P., Lambertson, D., Chen, L., Schaubert, C., and Madura, K. (2000). The DNA repair protein Rad23 is a negative regulator of multi-ubiquitin chain assembly. *Nature cell biology* *2*, 601-608.
- Pearce, M.J., Mintseris, J., Ferreyra, J., Gygi, S.P., and Darwin, K.H. (2008). Ubiquitin-like protein involved in the proteasome pathway of *Mycobacterium tuberculosis*. *Science* *322*, 1104.
- Peters, J., Franke, W., and Kleinschmidt, J. (1994). Distinct 19 S and 20 S subcomplexes of the 26 S proteasome and their distribution in the nucleus and the cytoplasm. *Journal of Biological Chemistry* *269*, 7709.
- Pickart, C., and Cohen, R. (2004). Proteasomes and their kin: proteases in the machine age. *Nature Reviews Molecular Cell Biology* *5*, 177-187.
- Pierce, N., Kleiger, G., Shan, S., and Deshaies, R. (2009). Detection of sequential polyubiquitylation on a millisecond timescale. *Nature* *462*, 615-619.

- Prakash, S., Inobe, T., Hatch, A.J., and Matouschek, A. (2008). Substrate selection by the proteasome during degradation of protein complexes. *Nature chemical biology* 5, 29-36.
- Qiu, X.B., Ouyang, S.Y., Li, C.J., Miao, S., Wang, L., and Goldberg, A.L. (2006). hRpn13/ADRM1/GP110 is a novel proteasome subunit that binds the deubiquitinating enzyme, UCH37. *The EMBO journal* 25, 5742-5753.
- Raasi, S., Varadan, R., Fushman, D., and Pickart, C.M. (2005). Diverse polyubiquitin interaction properties of ubiquitin-associated domains. *Nature structural & molecular biology* 12, 708-714.
- Rao, H., and Sastry, A. (2002). Recognition of specific ubiquitin conjugates is important for the proteolytic functions of the ubiquitin-associated domain proteins Dsk2 and Rad23. *Journal of Biological Chemistry* 277, 11691.
- Richardson, P.G., Sonneveld, P., Schuster, M.W., Irwin, D., Stadtmauer, E.A., Facon, T., Harousseau, J.L., Ben-Yehuda, D., Lonial, S., and Goldschmidt, H. (2005). Bortezomib or high-dose dexamethasone for relapsed multiple myeloma. *New England Journal of Medicine* 352, 2487.
- Richly, H., Rape, M., Braun, S., Rumpf, S., Hoege, C., and Jentsch, S. (2005). A series of ubiquitin binding factors connects CDC48/p97 to substrate multiubiquitylation and proteasomal targeting. *Cell* 120, 73-84.
- Rinaldi, T., Ricordy, R., Bolotin-Fukuhara, M., and Frontali, L. (2002). Mitochondrial effects of the pleiotropic proteasomal mutation mpr1/rpn11: uncoupling from cell cycle defects in extragenic revertants. *Gene* 286, 43-51.
- Rock, K.L., Gramm, C., Rothstein, L., Clark, K., Stein, R., Dick, L., Hwang, D., and Goldberg, A.L. (1994). Inhibitors of the proteasome block the degradation of most cell proteins and the generation of peptides presented on MHC class I molecules. *Cell* 78, 761-771.
- Roelofs, J., Park, S., Haas, W., Tian, G., McAllister, F.E., Huo, Y., Lee, B.H., Zhang, F., Shi, Y., and Gygi, S.P. (2009). Chaperone-mediated pathway of proteasome regulatory particle assembly. *Nature* 459, 861-865.
- Rosenzweig, R., Osmulski, P.A., Gaczynska, M., and Glickman, M.H. (2008). The central unit within the 19S regulatory particle of the proteasome. *Nature structural & molecular biology* 15, 573-580.
- Saeki, Y., Saitoh, A., Toh-e, A., and Yokosawa, H. (2002a). Ubiquitin-like proteins and Rpn10 play cooperative roles in ubiquitin-dependent proteolysis. *Biochemical and biophysical research communications* 293, 986-992.

- Saeki, Y., Sone, T., Toh-e, A., and Yokosawa, H. (2002b). Identification of ubiquitin-like protein-binding subunits of the 26S proteasome. *Biochemical and biophysical research communications* 296, 813-819.
- Saeki, Y., Toh-e, A., Kudo, T., Kawamura, H., and Tanaka, K. (2009). Multiple proteasome-interacting proteins assist the assembly of the yeast 19S regulatory particle. *Cell* 137, 900-913.
- Sanni, A., Hountondji, C., Blanquet, S., Ebel, J.P., Boulanger, Y., and Fasiolo, F. (1991). Interaction of the tRNA<sup>phe</sup> acceptor end with the synthetase involves a sequence common to yeast and *Escherichia coli* phenylalanyl-tRNA synthetases. *Biochemistry* 30, 2448-2453.
- Schauber, C., Chen, L., Tongaonkar, P., Vega, I., Lambertson, D., Potts, W., and Madura, K. (1998). Rad23 links DNA repair to the ubiquitin/proteasome pathway. *Nature* 391, 715-718.
- Schiller, D., Cheng, Y.C., Liu, Q., Walter, W., and Craig, E.A. (2008). Residues of Tim44 involved in both association with the translocon of the inner mitochondrial membrane and regulation of mitochondrial Hsp70 tethering. *Molecular and cellular biology* 28, 4424.
- Seeger, M., Hartmann-Petersen, R., Wilkinson, C., Wallace, M., Samejima, I., Taylor, M., and Gordon, C. (2003). Interaction of the anaphase-promoting complex/cyclosome and proteasome protein complexes with multiubiquitin chain-binding proteins. *Journal of Biological Chemistry* 278, 16791.
- Sherman, F., and Slonimski, P.P. (1964). Respiration-deficient mutants of yeast.: II. *Biochemistry. Biochimica et Biophysica Acta (BBA)-General Subjects* 90, 1-15.
- Sirkis, R., Gerst, J.E., and Fass, D. (2006). Ddi1, a eukaryotic protein with the retroviral protease fold. *Journal of molecular biology* 364, 376-387.
- Stone, M., Hartmann-Petersen, R., Seeger, M., Bech-Otschir, D., Wallace, M., and Gordon, C. (2004). Uch2/Uch37 is the major deubiquitinating enzyme associated with the 26 S proteasome in fission yeast. *Journal of molecular biology* 344, 697-706.
- Tagwerker, C., Flick, K., Cui, M., Guerrero, C., Dou, Y., Auer, B., Baldi, P., Huang, L., and Kaiser, P. (2006). A tandem affinity tag for two-step purification under fully denaturing conditions. *Molecular & Cellular Proteomics* 5, 737.
- Thrower, J., Hoffman, L., Rechsteiner, M., and Pickart, C. (2000). Recognition of the polyubiquitin proteolytic signal. *The EMBO journal* 19, 94-102.
- Tomko Jr, R.J., Funakoshi, M., Schneider, K., Wang, J., and Hochstrasser, M. (2010). Heterohexameric ring arrangement of the eukaryotic proteasomal ATPases: implications for proteasome structure and assembly. *Molecular cell* 38, 393-403.

- Tong, A.H.Y., Evangelista, M., Parsons, A.B., Xu, H., Bader, G.D., PagÈ, N., Robinson, M., Raghibizadeh, S., Hogue, C.W.V., and Bussey, H. (2001). Systematic genetic analysis with ordered arrays of yeast deletion mutants. *Science* 294, 2364.
- Trempe, J.F., Brown, N.R., Lowe, E.D., Gordon, C., Campbell, I.D., Noble, M.E.M., and Endicott, J.A. (2005). Mechanism of Lys48-linked polyubiquitin chain recognition by the Mud1 UBA domain. *The EMBO journal* 24, 3178-3189.
- van Nocker, S., Sadis, S., Rubin, D., Glickman, M., Fu, H., Coux, O., Wefes, I., Finley, D., and Vierstra, R. (1996). The multiubiquitin-chain-binding protein Mub1 is a component of the 26S proteasome in *Saccharomyces cerevisiae* and plays a nonessential, substrate-specific role in protein turnover. *Molecular and cellular biology* 16, 6020.
- Vembar, S., and Brodsky, J. (2008). One step at a time: endoplasmic reticulum-associated degradation. *Nature Reviews Molecular Cell Biology* 9, 944-957.
- Verma, R., Chen, S., Feldman, R., Schieltz, D., Yates, J., Dohmen, J., and Deshaies, R.J. (2000). Proteasomal proteomics: identification of nucleotide-sensitive proteasome-interacting proteins by mass spectrometric analysis of affinity-purified proteasomes. *Molecular biology of the cell* 11, 3425.
- Verma, R., and Deshaies, R. (2005). Assaying degradation and deubiquitination of a ubiquitinated substrate by purified 26S proteasomes. *Methods in enzymology* 398, 391-399.
- Verma, R., McDonald, H., Yates III, J.R., and Deshaies, R.J. (2001). Selective degradation of ubiquitinated Sic1 by purified 26S proteasome yields active S phase cyclin-Cdk. *Molecular cell* 8, 439-448.
- Verma, R., Oania, R., Fang, R., Smith, G.T., and Deshaies, R.J. (2011). Cdc48/p97 Mediates UV-Dependent Turnover of RNA Pol II. *Molecular cell* 41, 82-92.
- Verma, R., Oania, R., Graumann, J., and Deshaies, R. (2004). Multiubiquitin chain receptors define a layer of substrate selectivity in the ubiquitin-proteasome system. *Cell* 118, 99-110.
- Vögtle, F.N., Wortelkamp, S., Zahedi, R.P., Becker, D., Leidhold, C., Gevaert, K., Kellermann, J., Voos, W., Sickmann, A., and Pfanner, N. (2009). Global analysis of the mitochondrial N-proteome identifies a processing peptidase critical for protein stability. *Cell* 139, 428-439.
- Walters, K.J., Kleijnen, M.F., Goh, A.M., Wagner, G., and Howley, P.M. (2002). Structural Studies of the Interaction between Ubiquitin Family Proteins and Proteasome Subunit S5a. *Biochemistry* 41, 1767-1777.
- Wang, X., and Huang, L. (2008). Identifying dynamic interactors of protein complexes by quantitative mass spectrometry. *Molecular & Cellular Proteomics* 7, 46.

- Watkins, J., Sung, P., Prakash, L., and Prakash, S. (1993). The *Saccharomyces cerevisiae* DNA repair gene RAD23 encodes a nuclear protein containing a ubiquitin-like domain required for biological function. *Molecular and cellular biology* 13, 7757.
- Weber, E.R., Hanekamp, T., and Thorsness, P.E. (1996). Biochemical and functional analysis of the YME1 gene product, an ATP and zinc-dependent mitochondrial protease from *S. cerevisiae*. *Molecular biology of the cell* 7, 307.
- Wilkinson, C., Seeger, M., Hartmann-Petersen, R., Stone, M., Wallace, M., Semple, C., and Gordon, C. (2001). Proteins containing the UBA domain are able to bind to multi-ubiquitin chains. *Nature cell biology* 3, 939-943.
- Wisniewski, J., Zougman, A., and Mann, M. (2009). Combination of FASP and StageTip-based fractionation allows in-depth analysis of the hippocampal membrane proteome. *Journal of Proteome Research* 8, 5674-5678.
- Xie, Y., and Varshavsky, A. (2001). RPN4 is a ligand, substrate, and transcriptional regulator of the 26S proteasome: a negative feedback circuit. *Proceedings of the National Academy of Sciences of the United States of America* 98, 3056.
- Young, P., Deveraux, Q., Beal, R.E., Pickart, C.M., and Rechsteiner, M. (1998). Characterization of two polyubiquitin binding sites in the 26 S protease subunit 5a. *Journal of Biological Chemistry* 273, 5461.
- Zhang, D., Chen, T., Ziv, I., Rosenzweig, R., Matiuhin, Y., Bronner, V., Glickman, M.H., and Fushman, D. (2009). Together, Rpn10 and Dsk2 can serve as a polyubiquitin chain-length sensor. *Molecular cell* 36, 1018-1033.
- Zhu, X., Ménard, R., and Sulea, T. (2007). High incidence of ubiquitin like domains in human ubiquitin specific proteases. *Proteins: Structure, Function, and Bioinformatics* 69, 1-7.